e-Zine for meteor observers meteornews.net

MeteorNews

ISSN 2570-4745 VOL 7 / ISSUE 6 / NOVEMBER 2022

This notable bolide was spotted on 2022 September 3, at 3 h34m15.0 ± 0.1s UT by the Southwestern Europe Meteor Network. The maximum luminosity was equivalent to an absolute magnitude of –12.0 ± 1.0. T (Credit J.M. Madiedo).

- chi Cygnids (CCY#0757)
- tau Herculids
- CAMS reports
- Visual observing reports
- Radio meteor work
- Fireball reports

Contents

Affirming the α Coronæ Borealids as an established shower using Global Meteor Network meteor orbital data for 2022

John Greaves

United Kingdom

The alpha Coronae Borealids (ACB#00429) are currently flagged in the International Astronomical Union's Meteor Data Center Working List as a shower "to be established". Here meteor orbit data solely for the 2022 shower appearance as taken from the Global Meteor Network are used in order to establish the shower.

1 Introduction

The α Coronæ Borealids were presented as a candidate shower (Greaves, 2012) and subsequently included in the Working List of the IAU MDC as ACB #00429 under the same name[1]. During late January 2022, in a period of only a few days, the Global Meteor Network (GMN)[2] detected 48 meteoroids from this shower, as revealed via the Jopek (1993) variation of D criterion testing, henceforth D_J.

2 Results

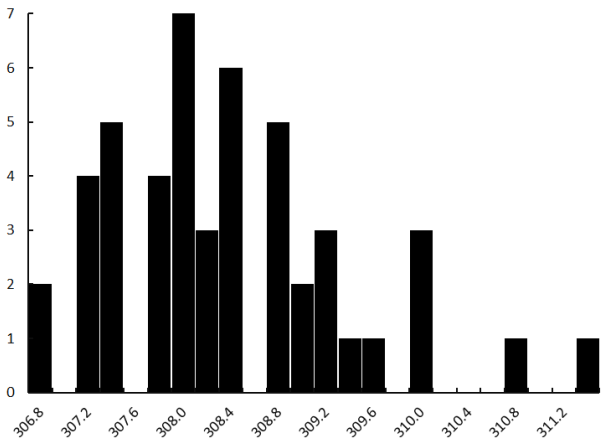

Figure 1 – Histogram showing the number of meteors per 0.2 degree Solar Longitude period for the GMN 2022 α Coronæ Borealids.

The mean particulars for the 2022 appearance of the shower as revealed by 48 meteor orbits in the GMN data are presented in *Table 1* whilst the frequency of meteors for every 0.2 degrees of Solar Longitude, $\lambda_\odot$, (roughly five hours) is demonstrated in *Figure 1*.

Of the 48 meteor orbits with D_J of 0.100 or less, 37 have D_J of 0.080 or less, 24 have D_J of 0.070 or less and 12 have D_J of 0.060 or less. Further, *Figure 1* demonstrates that between Solar Longitude 307.6 and 309.0 degrees (each bar is labelled with the end value for that bin of data) a total of 25 meteors appeared in just under 34 hours, with the gap at 308.6° occurring during daylight hours for most of Europe, where most GMN cameras are concentrated. If the end point is taken as 308.4 degrees instead it is shown that in fact a full 20 of those meteors appeared during roughly 19 hours of coverage.

3 Conclusion

Based upon a set of 48 GMN meteors detected as α Coronæ Borealids via D_J criterion testing during a very short interval in 2022 affirmation of them being an established shower is given. With respect to 2022 at least this appears to be a short-lived shower with the majority of the meteors appearing within the space of a day and thus prone to most of the selection effects dogging meteor detection (e.g., longitude coverage, weather, lunar phase, number and density of cameras per longitude strip). The recent dramatic increase in meteor coverage by various networks alongside the GMN policy of immediate data release allows for the shower to be established.

Table 1 – The mean particulars for the 2022 appearance of the α Coronoæ Borealids as revealed by GMN meteor orbit data. q is in Astronomical Units (AU), e is dimensionless and the rest of the columns are in degrees.

RA	Dec	$\lambda_\odot$	v_g	q	e	i	ω	Ω	β	$\lambda - \lambda_\odot$
232.06	27.26	308.283	58	0.983	0.972	105.5	175.7	308.3	44.4	271.9

[1] https://www.ta3.sk/IAUC22DB/MDC2022/Roje/roje_lista.php?corobic_roje=0&sort_roje=0

[2] https://globalmeteornetwork.org/data/

Acknowledgements

This analysis relied upon the publicly available data from the GMN group under license[3].

Reference

Greaves J. (2012). “Four Meteor Showers from the SonotaCo Network Japan”. *WGN, Journal of the International Meteor Organization*, **40**, 16–23.

Jopek T. J. (1993). “Remarks on the meteor orbital similarity D-criterion”. *Icarus*, **106**, 603–607.

[3] https://creativecommons.org/licenses/by/4.0/

Global Meteor Network: Outburst produced by dust from 73P/Schwassmann-Wachmann3

Masahiro Koseki

The Nippon Meteor Society, 4-3-5 Annaka Annaka-shi, Gunma-ken, 379-0116 Japan
geh04301@nifty.ne.jp

The Global Meteor Network completely covered the outburst of the meteor shower related to 73P/Schwassmann-Wachmann 3. The peak activity was recorded by camera operators in Western America when the radiant was at its culmination. The analysis of the observations shows a very important fact; the meteoroids are very porous. We can confirm the meteoroids are spread centered at the perihelion of the comet and along with the orbital plane of the comet.
The faint meteor shower observed in 1930 moved southward but we confirmed the radiant of this event moved northward. TAH (#0061) in the meteor shower database (SD) of the IAU meteor data center is very dispersed and these meteoroids are thought to be rather solid ones. It seems appropriate to give a new name to this meteor shower.

1 Introduction

73P/Schwassmann-Wachmann3 broke into pieces in 1995 and many investigators predicted the released dust would encounter the Earth in 2022. The Global Meteor Network covered this opportunity very successfully and we have valuable data on the outburst. Details about the methodology used by GMN have been published before (Vida et al., 2019; 2020; 2021). This is the first-time detailed observations of the debris from 73P/Schwassmann-Wachmann3 have been obtained because we have poor information on meteors produced by dust from this comet.

2 History

2.1 Japanese observation in 1930

The first and only witness is Nakamura's faint meteor shower in 1930 (Nakamura, 1930). Japanese researchers scheduled the observational program for observations immediately after the discovery of 73P/Schwassmann-Wachmann3. Nakamura started observations from May 24 before the expected maximum and witnessed many very faint meteors during the program till June 19. He wrote, "*When a specially limited area of the heavens (some five degrees square) is watched with the utmost caution, considerable numbers of faint meteors would be suspected*" and "*The observation of faint meteors usually causes considerable fatigue of the eyes; the author, therefore, works, mostly for 30 minutes, or at most, 60 minutes*". He noticed the radiant southward drift though there were discussions then whether a meteor shower radiant drifted or not. Many others were not able to detect such faint meteors except one amateur.

Komaki could not detect any meteors from 73P/Schwassmann-Wachmann3 in 1935 (Komaki, 1935) and we have no certain witness about any activity till photographic research became available.

2.2 Photographic τ-Herculids

The name of tau-Herculids given in the IAU Meteor Data Center Shower Database (SD) seems curious because the listed radiant point locates in Boötes according to the reference (Lindblad, 1971). Southworth and Hawkins named an activity detected by their statistical methods as τ-Herculids (Southworth and Hawkins, 1963), and Lindblad thought his No.168 stream can be identified with their τ-Herculids. Two types of research were based on different meteor databases; Southworth and Hawkins use the 'short trail method' and Lindblad uses the 'graphical reduction'. Koseki confirmed that both kinds of research are identical; the underlined numbers or marked in italics in *Table 1 to 3* are common meteors. He analyzed all types of photographic databases including former Soviet data and found a cluster MK-49 (Koseki, 1982). τ-Herculids have only two meteors in the first report but 18 meteors in the third are sufficient in number to confirm there is some meteor shower activity.

Table 1 – First report of τ-Herculids by Southworth and Hawkins (1963).

Time	a (AU)	e	i (°)	Ω (°)	π (°)	α (°)	δ (°)	v_∞ (km/s)	
53 June 20.35000	2.07	0.521	28.9	88.7	291	258.6	+50.4	21.2	H2-7920
54 June 25.24461	2.81	0.642	21.3	93.1	286.2	237.8	+46.4	18.8	H2-12711
Mean values	2.44	0.582	25.1	90.9	288.6	248.2	+48.4	20	

Table 2 – Second report of τ-Herculids by Lindblad (1971). Identification: Southworth-Hawkins, Comet 1930VI.

Duration	α_R (°)	δ_R (°)	v_g (km/s)	q (AU)	a (AU)	e	i (°)	ω (°)	Ω (°)	π (°)
May19 – June14	228	+40	18	0.97	2.695	0.633	18.6	204.2	71.9	276.1

Harvard serial no.: 3335, 4103, 4106, 4108, 4112, 7692, 7820, 12142, 12161, 12355, 12378, 12398, 12470, 12513.

Table 3 – Third report of τ-Herculids by Koseki (1982).

No.	α_R (°)	δ_R (°)	$\lambda-\lambda_\odot$ (°)	β (°)	v_g (km/s)	q (AU)	e	i (°)	ω (°)	Ω (°)	N
MK-49	228.7	+40.7	130.4	+55.2	14.8	0.979	0.625	19	201.3	75.9	18

Members: H1-7692, H1-3335, H1-12142, H1-12161, H1-12355, H1-12378, H1-12398, H1-12513, H1-4106, H1-4108, H1-4112, H2-*12711*, H3-4103, H3-12399, H3-7820, H6-40379A, D2-570212, K1-39.

Table 4 – Radiant density along with the distance from the converged center.

r (°)	1	2	3	4	5	6	7	8	9	10
N	583	487	208	95	29	24	7	18	10	13
Density	185.6	51.7	13.2	4.3	1	0.7	0.2	0.4	0.2	0.2

A meteor shower search using the D-criterion (D_{SH}; Southworth and Hawkins, 1963) finds sometimes a 'shower' beyond our common sense. In *Figure 1* crosses are video meteor radiants, circles are photographic radiants, circles filled with red are members of MK-49, and red squares are June Bootids (JBO, #0161). Although MK-49 is limited by $D_{SH} < 0.15$, member radiants are spread all over the chart. Interestingly, several candidates of JBO #0161 are shown in this plot as a compact group.

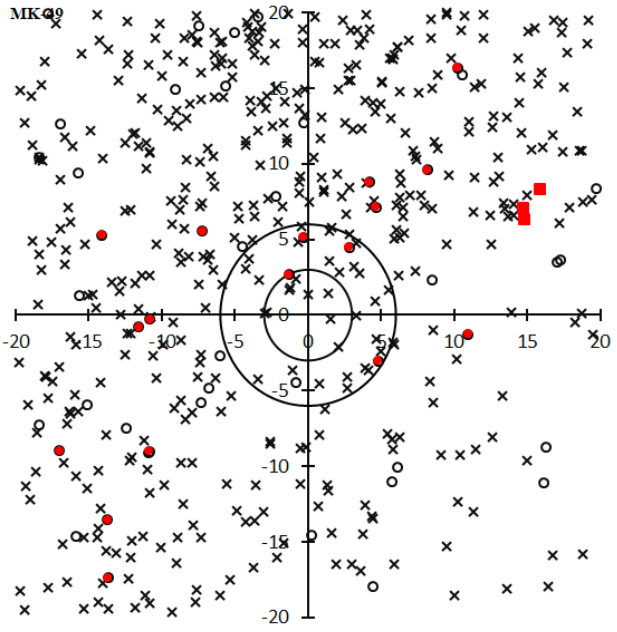

Figure 1 – The radiant distribution around TAH; red circles are members of MK-49 (compatible with TAH in the SD), black circles are photographic radiants not member of MK-49, crosses are video radiants (SonotaCo net 2007–2021)[4], red squares correspond to JBO (#0161) of the SD.

3 GMN observations in 2022

3.1 Data selection method

As we discussed in the former section, meteoroids of this meteor shower are spread widely, but the tau Herculids we investigate here is a young and very compact component. It seems not appropriate to adopt $D_{SH} < 0.15$ to select TAH members in the GMN database or even worse to identify using the radiant distribution for instance with a distance from the center less than 20 degrees.

There are two ways to select members of a meteoroid stream. One is the radiant-based method, and another is the orbit-based method. We get meteor data in a 4th-dimensional space: radiant point (α, δ), time of observation ($\lambda_\odot$), and geocentric velocity (v_g). We can use these data and convert them to orbital elements: eccentricity (e), distance of perihelion (q), inclination (i), argument of perihelion (ω), and node (Ω). These two sets of data are convertible to each other, and we can select any set to analyse τ-Herculids. The author chooses the radiant-based method because the orbit-based method seems superior in the case of asteroid and comet positions which are determined precisely with errors less than a few arc seconds.

We start with the initial data set: $63° < \lambda_\odot < 73°$, $(\lambda-\lambda_\odot, \beta) = (125°, +32°)$. *Figure 2 (left)* gives the initial radiant distribution. A tailpole-like figure is made by the radiant drift and we estimate it using the regression analysis. We plot the data in ($\lambda_\odot$, x), ($\lambda_\odot$, y), and ($\lambda_\odot$, v_g) and analyze them by linear regression. We select meteors within 10 degrees distance from the center estimated by intermediate results and repeat this process until it converges. An example of the final converged results of ($\lambda_\odot$, y) is shown in

[4] "SonotaCo Network Simultaneously Observed Meteor Data Sets", http://sonotaco.jp/doc/SNM/

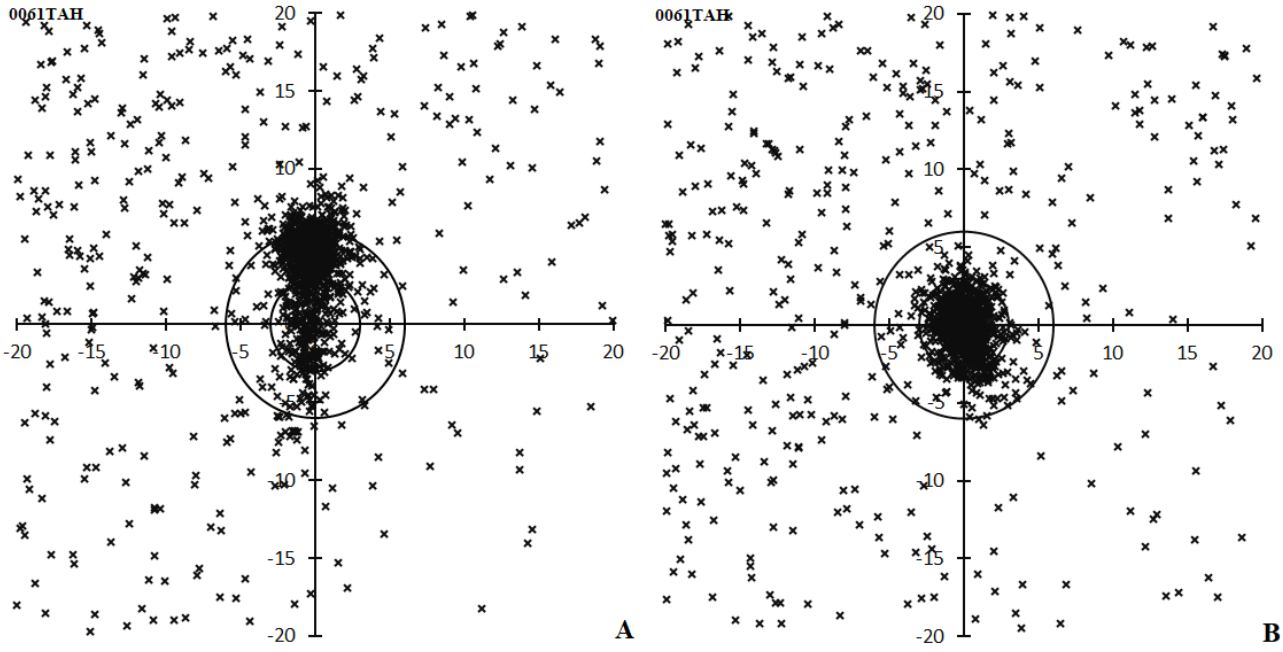

Figure 2 – Radiant distribution of video meteors (GMN) centered at (λ–$\lambda_\odot$, β) = (125°, +32°) between 63° < $\lambda_\odot$ < 73°. (A, left); initial distribution, (B, right); the result after that the iterative process converged.

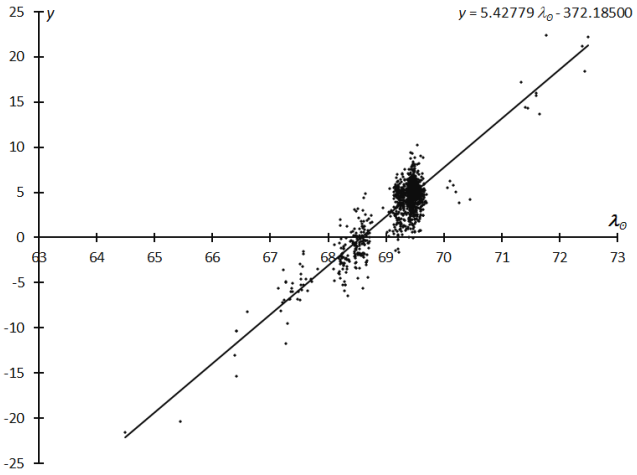

Figure 3 – Example of the linear regression analysis. The final converged results of ($\lambda_\odot$, y) after 9 steps of the iteration. The largest group of the data indicates the maximum and the preceding groups suggest the shower activity starts 2 days before the maximum, May 29, at the latest.

Figure 3. The radiant distribution of TAH resulted in *Figure 2B* and we realize that the tau Herculid radiant is compact (see *Table 4*). Five observations of 2021 are included in this table. We select 1278 radiants within 3 degrees from the center as τ-Herculids members and use them in the following analyses.

3.2 Radiant distribution

We note the final radiant distribution (*Figure 2B, right*) shows the elongated shape yet although the iteration converged. It is necessary to check whether the regression analysis is insufficient, or if the elongated shape is real. *Figure 4* compares the radiant distributions for three periods: 63.0° < $\lambda_\odot$ < 69.0° (left), 69.0° < $\lambda_\odot$ < 69.5° (middle) and 69.5° < $\lambda_\odot$ < 73.0° (right). The radiant distribution around the maximum (*Figure 4B, middle*) proves the elongated distribution is real because the period of this figure is short enough to avoid the radiant drift; the regression analysis is properly done. The elongated distribution is peculiar for this meteor shower (see section 3.6 Extent of meteoroid stream).

3.3 Activity profile

The distribution of the observations in *Figure 3* is intermittent and indicates GMN could not catch the activity profile of τ-Herculids continuously, but *Figure 5* shows GMN members in Europe and North America covered the activity around the maximum successfully. *Figure 6* gives the detail of the activity profile of the tau Herculid maximum; we estimate the number of meteors per time bin of one solar longitude using the period of 30 meteors, smoothed by the sliding average. The τ-Herculids reached their maximum at $\lambda_\odot$ = 69.417° (May 31, 04^h14^m UTC) with 13580 meteors per solar longitude: HR = 565 or about 10 τ-Herculid meteors per minute. The maximum is very short, and the HR decreased to 200 after 2 hours.

The depression around $\lambda_\odot$ = 69.3°~69.4° seems to be caused by the scarce number of observations between Europe and Western America. The ephemeris for the τ-Herculid outburst was confirmed by observers in Western America as expected.

3.4 Observational restriction

3.4.1 Observational location and elevation angle

GMN camera operators pursued the tau Herculid activity but the elevation angle altered as *Figure 7* shows; we perceive several peaks, indicating that several observational groups exist. The radiant of the τ-Herculids was descending under 30 degrees and the morning dawn hindered European observers before the maximum ($\lambda_\odot$ = 69.417°). Such conditions cause an apparent decrease in τ-Herculid rates.

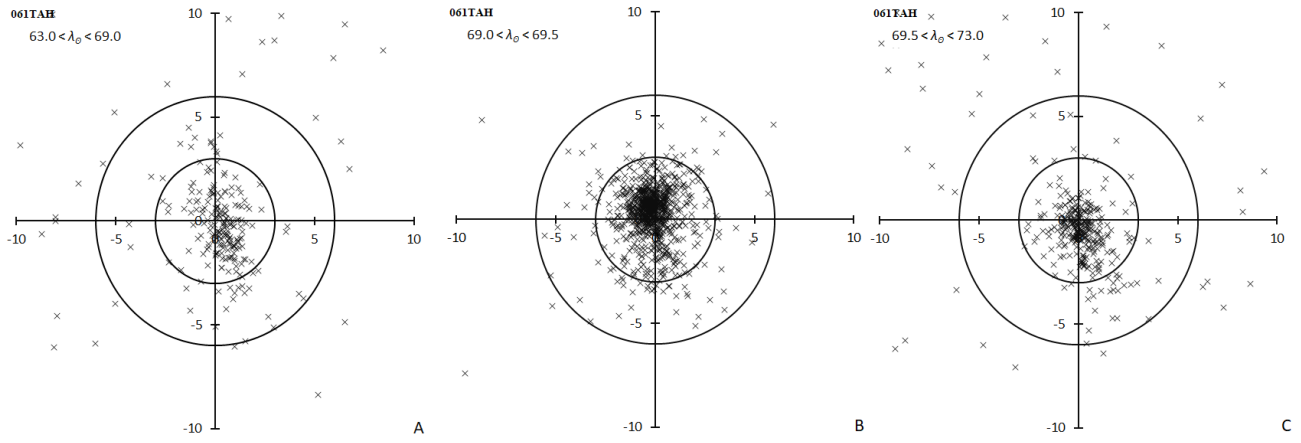

Figure 4 – Radiant distribution of video meteors (GMN) centered at (λ–$\lambda_\odot$, β) = (125°, +32°). (A); 63.0° < $\lambda_\odot$ < 69.0°, (B); 69.0° < $\lambda_\odot$ < 69.5°, (C); 69.5° < $\lambda_\odot$ < 73.0°.

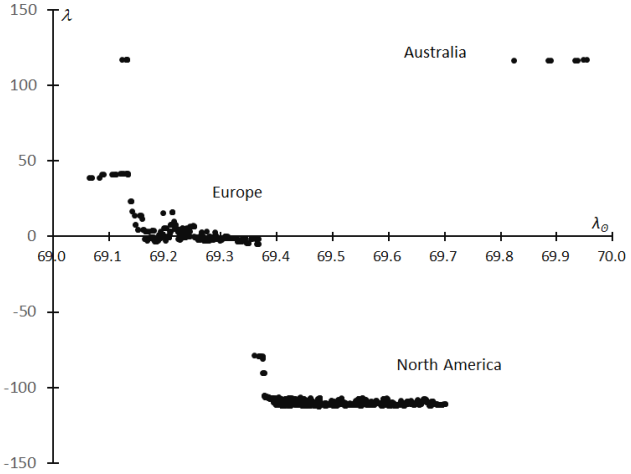

Figure 5 – Moving median of the geographic longitude λ of the begin point of the meteor paths in bins by 10 in function of time ($\lambda_\odot$). Observations around the maximum are linked from Europe to Canada and America.

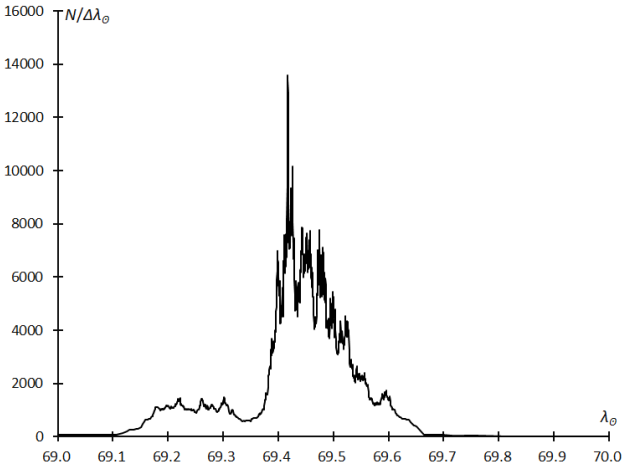

Figure 6 – Profile of the outburst obtained by the GMN. The ordinate is the estimated number of meteors per one solar longitude from the time span of 30 video meteors.

On the other hand, evening twilight ends, and the radiant of the τ-Herculids rises to its culmination for observers in North America. But, after $\lambda_\odot$ = 69.7°, the radiant goes down, and the morning dawn hindered observations from Europe. The activity profile of the τ-Herculids after $\lambda_\odot$ = 69.7° is lower than the reality.

It is worthwhile to note that the zenith attraction for the τ-Herculids is larger than for the usual meteor showers we observe. *Figure 8* shows the difference between the apparent radiant and the geocentric radiant during

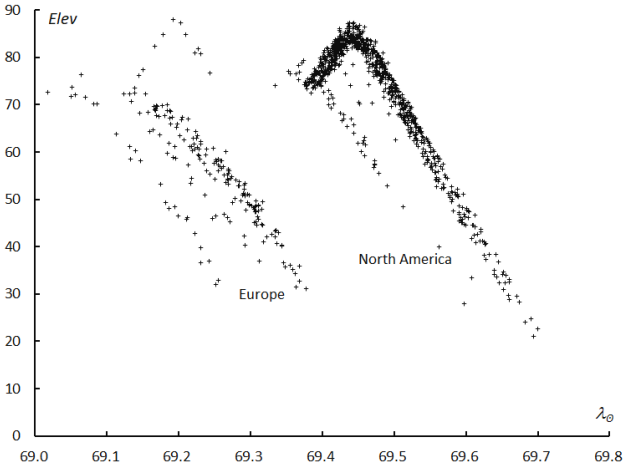

Figure 7 – Elevation angle of meteors of the outburst. Observations continued from Europe to Canada, Midwestern of USA, and Western USA.

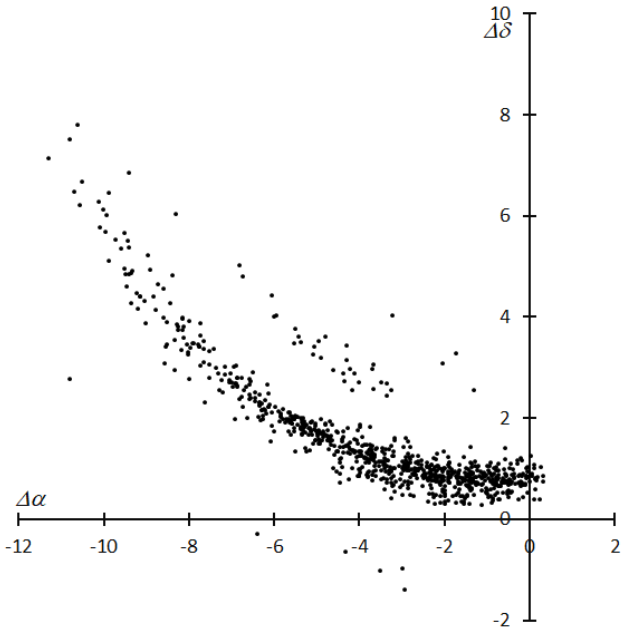

Figure 8 – Difference between the apparent radiant and the geocentric radiant. Left is east and top is north. When the geocentric radiant goes down, the apparent radiant seems to remain.

Table 5a – The positional error distributions of the classified τ-Herculids.

$\alpha \pm$	0	0.1	0.2	0.3	0.4	0.5	0.6	0.7	0.8	0.9	1	1.1	1.2	1.3	1.4	1.5	1.5<
N	0	39	140	166	175	134	111	101	77	57	52	55	35	31	33	15	57
$\delta \pm$	0	0.1	0.2	0.3	0.4	0.5	0.6	0.7	0.8	0.9	1	1.1	1.2	1.3	1.4	1.5	1.5<
N	0	42	150	169	179	142	107	96	71	66	61	42	27	31	29	16	50

Table 5b – The velocity error distributions of the classified τ-Herculids.

$v_g \pm$	0	0.1	0.2	0.3	0.4	0.5	0.6	0.7	0.8	0.9	1	1.1	1.2	1.3	1.4	1.5
N	6	313	364	225	131	87	62	23	21	24	13	5	3	1	0	0

λ_O = 69.4°~69.7°, which is for observations from North America. The difference is minimum at the radiant culmination and it becomes larger as the radiant goes down. The difference widens more than 10 degrees when the elevation of the radiant becomes lower than 40 degrees; visual observers encounter difficulties in such cases, to classify a meteor whether sporadic or not without careful observations.

3.4.2 Observational errors and the spread of meteoroids

We get the corrected radiant distribution for the tau Herculids from the regression analysis (see *Figure 2B*), *Table 4* gives the radiant density per square degree. It is clear that the radiant distribution from about 6 degrees away from the center becomes diffuse enough to merge with the sporadic background. It is necessary to confirm whether this distribution exhibit the real spread of meteoroids or is mainly influenced by observational errors.

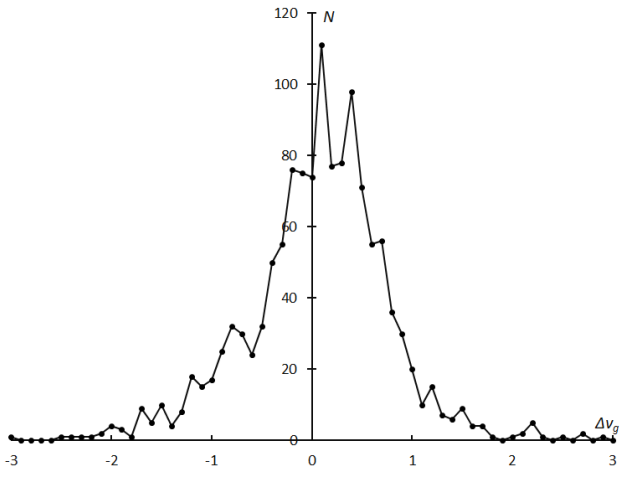

Figure 9 – Residual distribution of geocentric velocity after the regression analysis.

Table 5a shows the errors for α and δ given in the GMN database. Observational errors are estimated to be less than 1 degree in both α and δ. The radiant distribution in *Table 4* is much larger than in *Table 5a*. It could be suggested that *Table 4* represents the spread of the meteoroids themselves and not observational errors. It could be partially the case (see section 3.6 Extent of meteoroid stream). The activity profile (*Figure 6*) is so sharp that meteoroids are distributed tightly because they are very young. It is suggested that the radiant distribution (*Figure 5A*) is caused mainly by errors, what means that the error estimation of the GMN might be too small.

For the velocity determination, we can suggest a similar conjecture that the error estimates on the geocentric velocity might be too small. *Figure 9* displays the residual distribution of the geocentric velocity after the regression analysis and suggests a wider spread than the error estimations given by GMN (*Table 5b*).

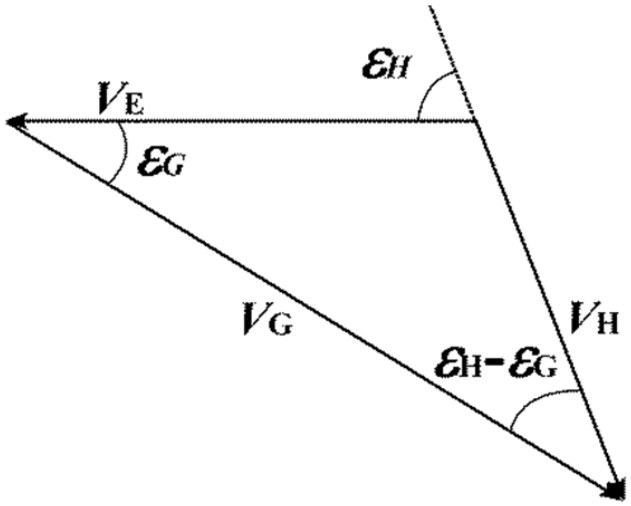

Figure 10 – Scheme of the meteoroid motion (v_h), Earth's motion (v_e), and the motion of the meteor viewed from Earth (v_g).

But the tau Herculids are very special as we see in *Figure 8*. The tau Herculid meteor shower is very slow because its meteoroids collide with Earth from behind. *Figure 10* displays the ordinary relation of the meteoroid motion (v_h), Earth's motion (v_e), and the motion of the meteor viewed from Earth (v_g). Their relations can be expressed in the following formula:

$$\frac{v_h}{\sin \varepsilon_g} = \frac{v_e}{\sin(\varepsilon_h - \varepsilon_g)} = \frac{v_g}{\sin(180 - \varepsilon_h)} = \frac{v_g}{\sin \varepsilon_h}$$

This formula indicates that when v_h changed linearly, v_g would not change linearly. We can estimate the apparent radiant spread of the tau Herculids as about 2.5 times larger than the apex source meteor showers by this formula. If we considered this influence, the error estimates of GMN would be exact.

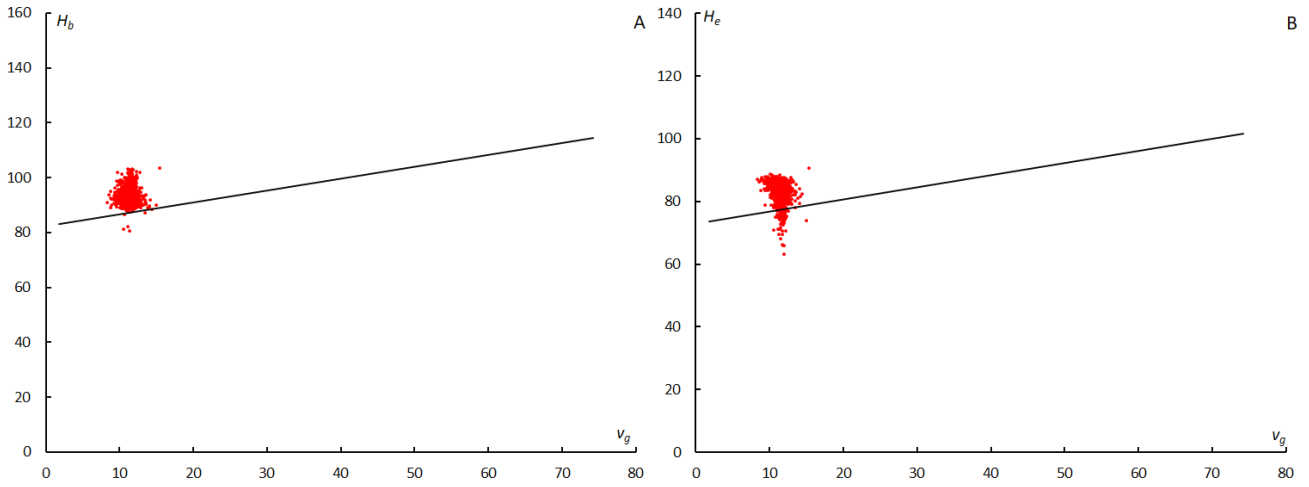

Figure 11 – Beginning height H_b of the tau Herculids (graph A, left) and end height H_e (graph B, right). Black lines are the approximate velocity of other meteors that appeared during the survey (63° < $\lambda_\odot$ < 73°).

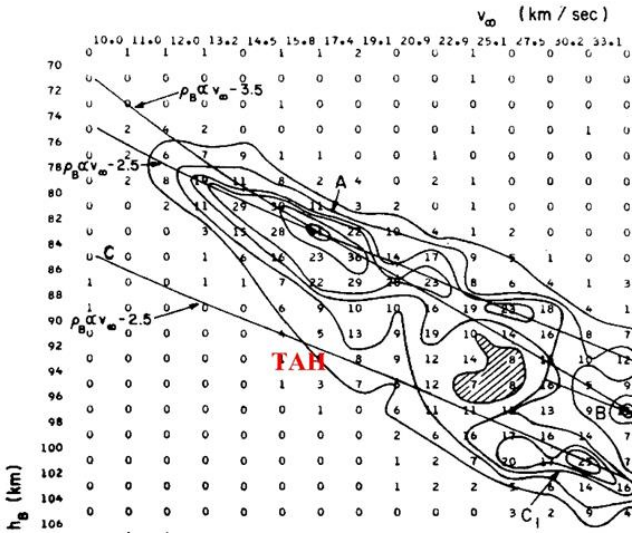

Figure 12 – Relation of beginning height to velocity outside the atmosphere (Ceplecha, 1968). TAH in red indicates the results of this research.

3.5 Distinctive nature of τ-Herculids meteoroids

3.5.1. Beginning height and velocity

τ-Herculid meteoroids start to radiate and fade away at higher elevations than other meteoroids (*Figure 11A and 11B*). We know that slower meteors ablate lower, but τ-Herculid meteors ablate higher than others with the same velocity. Ceplecha (1968) investigated the relation of beginning height to velocity outside the atmosphere and found three ridges of maximum density of points (*Figure 12*). Cook (1973) considered τ-Herculids in Ceplecha's class as 'A or lower'; it is necessary to note the ordinate of Ceplecha's figure (*Figure 12*) is inverse, and the lower height is displayed at the top in the figure. The beginning height of τ-Herculids expressed in *Figure 11A* is indicated as 'TAH' in red in *Figure 12*. It could be described as 'above C' according to the style of Cook. Other showers which Cook classified as 'above C' are the October Draconids, Leonids and Monocerotids. Cook (1973) wrote: "*association of Ceplecha's Class C with the residue of the ice-impregnated surface of a cometary nucleus after sublimation of the ices, and of Ceplecha's Class A with the core of a cometary nucleus*'. Omission. '*Furthermore, the density of Class A meteoroids (1.2 g cm^{-3}) is so close to that of Type I carbonaceous chondrites (2 g cm^{-3}).*' Omission. '*The recovery of Comet 1930 VI, Schwassmann-Wachmann 3, at its return in 1979 is urged since it is the only available comet producing a shower (τ Herculids) of Class A*". It is clear that the 2022 outburst of the τ Herculids is formed from new cometary particles but the photographic, formerly recorded τ Herculids could be from another asteroidal body or ancient cometary nuclei. We find a new question on the origin of the former τ Herculids (fTAH).

Cook classified Geminids as class B. We will compare the new τ Herculids (nTAH) with the Geminids in the following sections.

3.5.2. Beginning height and elevation

We notice that nTAH shows different heights compared to other ordinary meteor showers, for example, the Geminids (*Figure 13A and 13B*). It is common that the beginning height is higher for a lower elevation angle as shown in *Figure 13B* because meteors move oblique in the atmosphere when the elevation angle is low. But the beginning height of the nTAH meteors increases to the culmination elevation angle (*Figure 13A*).

3.5.3. Beginning height and maximum

We compare nTAH with the Geminids in *Figures 14A and 14B*. The beginning height of the Geminids shows periodic change with time ($\lambda_\odot$) because the culmination of the Geminids occurs per day. Meanwhile, the beginning height of nTAH increases towards the maximum. It is noticeable that the beginning height shows a small hillock around $\lambda_\odot$ =68.5° and at the maximum ($\lambda_\odot$ =69.4°) and this hillock coincide with the radiant culmination for observers of Western America.

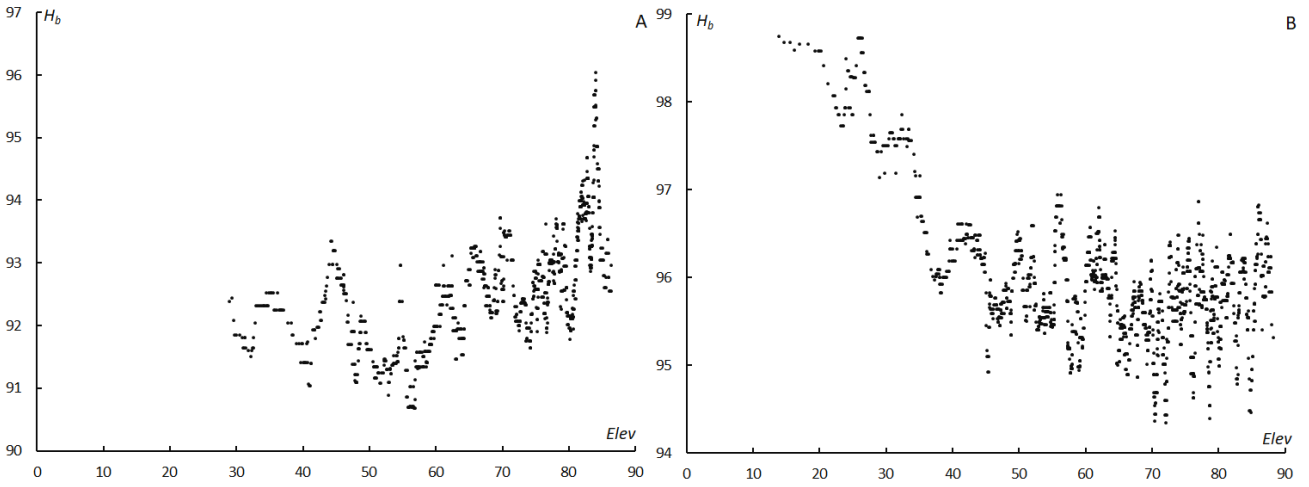

Figure 13 – Beginning height and elevation angle. (A); τ Herculids, (B); Geminids.

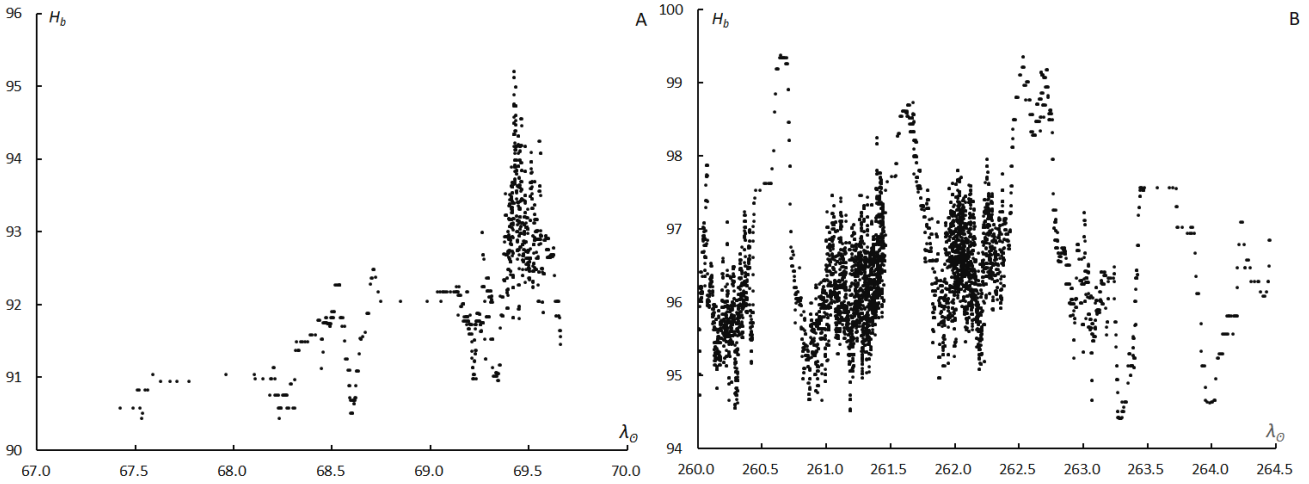

Figure 14 – Beginning height with time around the maximum. (A); τ Herculids, (B); Geminids.

3.5.4. Absolute magnitude

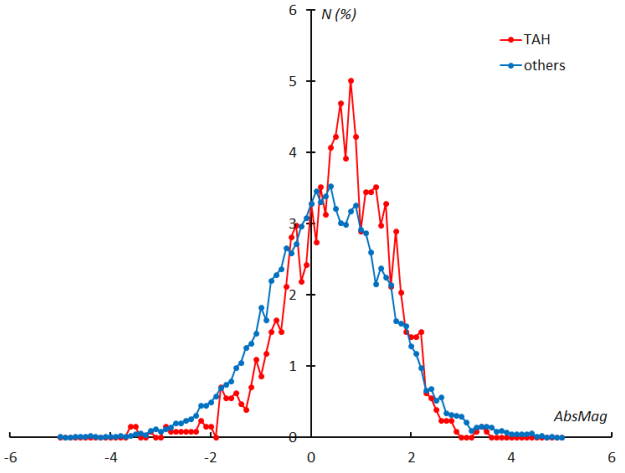

Figure 15 – Frequency distribution of the absolute magnitude of the τ Herculids compared to the distribution of other meteors that appeared during the survey ($63° < \lambda_\odot < 73°$).

We realize that meteoroids of nTAH are unique and we suppose that their absolute magnitude distribution might be also unique. *Figure 15* compares the frequency distributions of the nTAH with other meteors that appeared in the same time period. It is clear that the nTAH meteors are fainter than other meteors, but this does not mean meteoroids of nTAH are smaller than others. The luminous efficiency changes a lot with meteoroid velocity and the velocity of the nTAH is much lower than that of other meteors.

It is suggested that the absolute magnitude might change with the elevation as the beginning height changes. *Figure 16A* shows that the absolute magnitude of the nTAH decreases with the elevation in contrast to the Geminids case (*Figure 16B*). But we should be careful to conclude this because the absolute magnitude reaches the minimum at the maximum activity (*Figure 16A*). Camera operators of GMN in Western America met the activity maximum at the radiant culmination (see 3.3 Activity profile).

We observe brighter meteors around the shower maximum as in the case of Geminids (*Figure 17B*). The minimum of the absolute magnitude occurs just after the activity maximum in the Geminids but just at the activity maximum in the case of the nTAH (*Figure 17A*). nTAH meteoroids are so unique that both the beginning height and the absolute magnitude reach their extremes at the activity maximum ($\lambda_\odot = 69.4°$). Cook (1973) estimated 'Class C' as the residue of the surface of a cometary nucleus, which are, very porous and fragile particles. The meteoroids at the maximum of the nTAH can be considered as the most

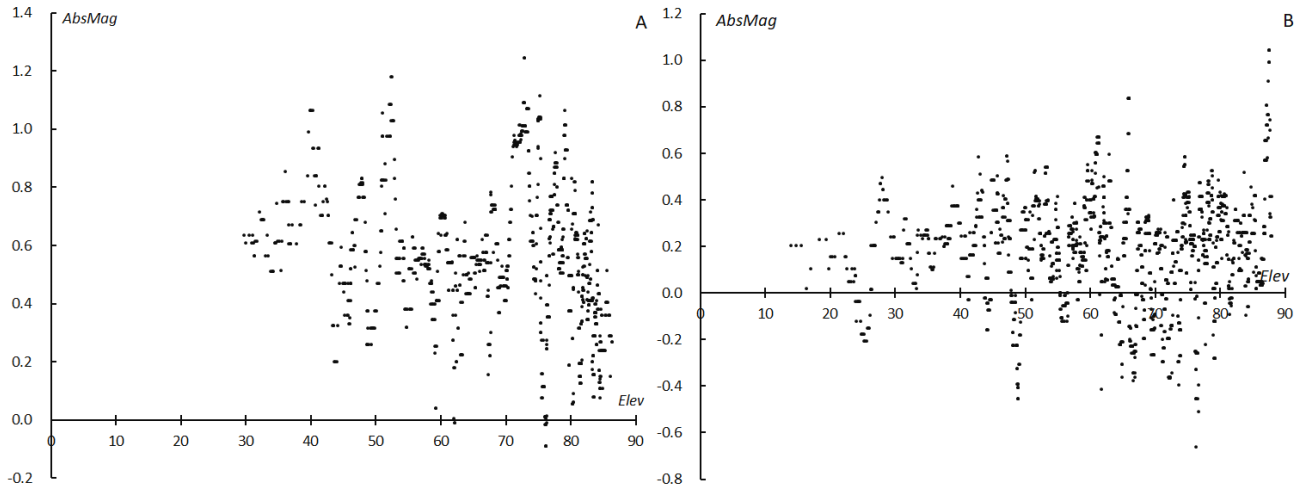

Figure 16 – Absolute magnitude and elevation angle. (A); τ Herculids, (B); Geminids.

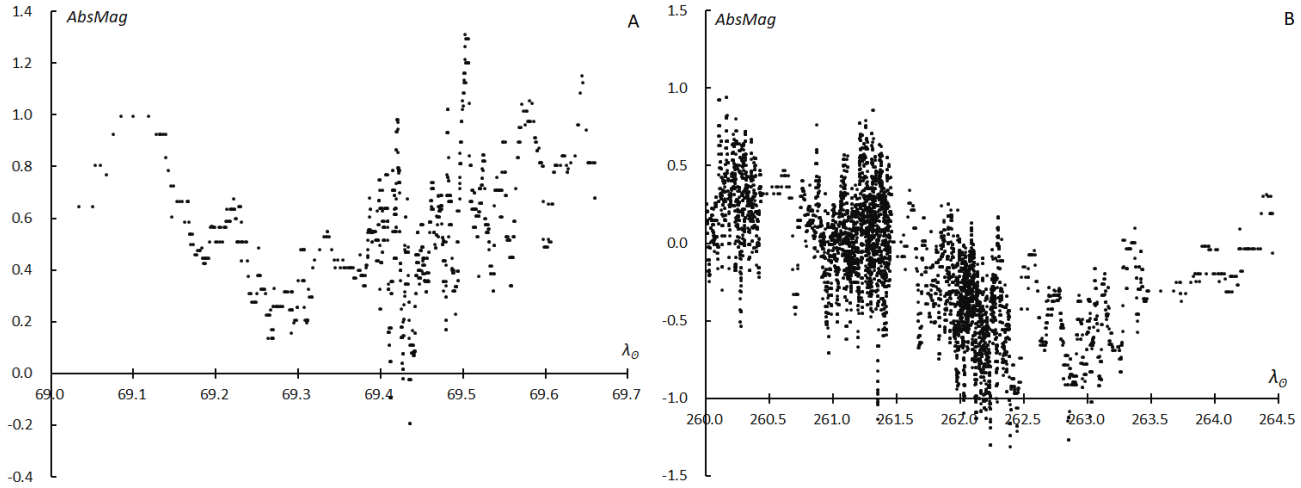

Figure 17 – Absolute magnitude with time around the maximum. (A); τ Herculids, (B); Geminids.

porous and fragile. Hawkins and Southworth give the following formula (Hawkins and Southworth, 1958). The intensity of light is inversely proportional to the 2/3 power of the density of the meteoroid. It is clear that the meteoroids at the nTAH maximum are more porous than those of the outskirts.

$$I = \frac{\Lambda A m^{2/3}}{4\zeta \rho_m^{2/3}} \tau \rho v^5$$

Where I is the intensity of light, Λ is the efficiency of the energy exchange, A is the shape factor, m and ρ_m are the mass and the density of the meteoroid, ζ is the energy required to ablate one gram of the meteoroid, τ is the fraction of the kinetic energy converted into light, ρ is the density of the atmosphere, v is the velocity of the meteoroid.

3.6 Extent of meteoroid stream

We realize that the elongated shape of the nTAH radiant distribution is peculiar (*Figure 4A~C*). *Figure 18* shows the perihelion distribution corresponding to the radiant distribution of *Figure 4B* ($69.0° < \lambda_\odot < 69.5°$). It is clear the radiant distribution is caused by nTAH meteoroids distributed along with the orbital plane of the comet 73P/Schwassmann-Wachmann3. We witnessed a meteor shower of a newly formed meteoroid stream which has not yet dispersed widely.

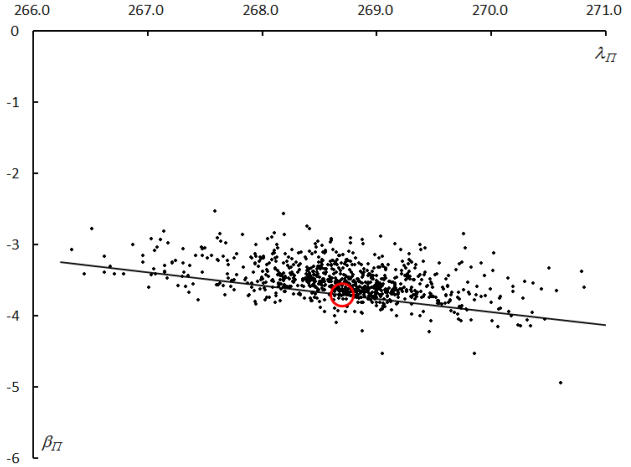

Figure 18 – Perihelion distribution of the τ Herculid meteoroids corresponding to *Figure 4B* ($69.0° < \lambda_\odot < 69.5°$). The black line shows the orbital plane of 73P/Schwassmann-Wachmann3 and the red circle indicates the position at its perihelion.

It seems to be appropriate that we do not call this meteor shower outburst of 2022 by the name of the τ Herculids

(TAH). It is better to call this shower the 73P/Schwassmann-Wachmann 3ids or SW3ids; suffix -ids means 'descendants of' or 'children of'. This shower does not represent the children of Hercules.

Acknowledgment

We appreciate the daily efforts by all camera operators of the Global Meteor Network. This analysis owes to their work. If GMN would be a bit idle and publish data too slowly, we would not reach the important view for this invaluable event. This analysis relied upon the publicly available data from the GMN group under license[5] (Vida et al., 2019; 2020; 2021).

References

Ceplecha Z. (1968). "Discrete Levels of Meteor Beginning Height". *Smithsonian Astrophysical Observatory Special Report*, **279**, 54 pages.

Cook A. F. (1973). "Discrete Levels of Beginning Height of Meteors in Streams". *Smithsonian Contributions to Astrophysics*, **14**, 1–10.

Hawkins G. S. and Southworth R. B. (1958). "The statistics of meteors in the Earth's atmosphere". *Smithsonian Contributions to Astrophysics*, **2**, 349–364.

Komaki K. (1935). "On the meteoric shower associated with comet 1930VI (Schwassmann-Wachmann)". *Astronomische Nachrichten*, **256**, 233–234.

Koseki M. (1982). "Meteor Shower Research on Photographic Meteors by Cluster analysis". 23rd Japanese Meteor Conference. (In Japanese).

Lindblad B. A. (1971). "A Computerized Stream Search among 2401 Photographic Meteor Orbits". *Smithsonian Contributions to Astrophysics*, **12**, 14–24.

Nakamura K. (1930). "On the Observation of Faint Meteors, as experienced in the case of those from the orbit of comet Schwassmann-Wachmann, 1930c". *Monthly Notices of the Royal Astronomical Society*, **91**, 204–209.

SonotaCo (2009). "A meteor shower catalog based on video observations in 2007–2008". *WGN, Journal of the IMO*, **37**, 55–62.

Southworth R. B. and Hawkins G. S. (1963). "Statistics of meteor streams". *Smithsonian Contributions to Astrophysics*, **7**, 261–285.

Vida D., Gural P., Brown P., Campbell-Brown M., Wiegert P. (2019). "Estimating trajectories of meteors: an observational Monte Carlo approach - I. Theory". *Monthly Notices of the Royal Astronomical Society*, **491**, 2688–2705.

Vida D., Gural P., Brown P., Campbell-Brown M., Wiegert P. (2020). "Estimating trajectories of meteors: an observational Monte Carlo approach - II. Results". *Monthly Notices of the Royal Astronomical Society*, **491**, 3996–4011.

Vida D., Šegon D., Gural P. S., Brown P. G., McIntyre M. J. M., Dijkema T. J., Pavletić L., Kukić P., Mazur M. J., Eschman P., Roggemans P., Merlak A., Zubrović D. (2021). "The Global Meteor Network – Methodology and first results". *Monthly Notices of the Royal Astronomical Society*, **506**, 5046–5074.

[5] https://creativecommons.org/licenses/by/4.0/

Appendix

Estimated elements of TAH resulting from the regression analysis.

$\lambda_\odot$ (°)	$\lambda - \lambda_\odot$ (°)	β (°)	α (°)	δ (°)	v_g (km/s)	e	q (AU)	i (°)	ω (°)	Ω (°)	λ_Π (°)	β_Π (°)	a (AU)
65	128.8	12.6	197.6	6.1	9.8	0.607	0.982	3.3	203.3	65	268.2	–1.3	2.5
66	128.1	18	200	11	10.2	0.624	0.983	4.9	202.6	66	268.6	–1.9	2.62
67	127.3	23.5	202.4	15.9	10.5	0.636	0.985	6.4	201.9	67	268.8	–2.4	2.71
68	126.5	28.9	204.9	20.8	10.9	0.643	0.987	8.1	201	68	268.8	–2.9	2.76
69	125.7	34.3	207.5	25.7	11.2	0.643	0.99	9.7	200	69	268.7	–3.3	2.77
69.1	125.6	34.9	207.8	26.2	11.3	0.643	0.99	9.9	199.9	69.1	268.7	–3.3	2.77
69.2	125.5	35.4	208	26.7	11.3	0.642	0.99	10.1	199.7	69.2	268.7	–3.4	2.77
69.3	125.4	36	208.3	27.2	11.3	0.642	0.991	10.2	199.6	69.3	268.6	–3.4	2.77
69.4	125.3	36.5	208.6	27.7	11.4	0.642	0.991	10.4	199.5	69.4	268.6	–3.5	2.77
69.5	125.2	37	208.8	28.2	11.4	0.641	0.991	10.6	199.4	69.5	268.6	–3.5	2.76
69.6	125.1	37.6	209.1	28.7	11.4	0.641	0.992	10.7	199.3	69.6	268.6	–3.5	2.76
69.7	125	38.1	209.4	29.2	11.5	0.64	0.992	10.9	199.2	69.7	268.5	–3.6	2.75
69.8	124.9	38.7	209.7	29.6	11.5	0.639	0.992	11.1	199	69.8	268.5	–3.6	2.75
69.9	124.8	39.2	209.9	30.1	11.5	0.638	0.993	11.2	198.9	69.9	268.5	–3.6	2.75
70	124.7	39.8	210.2	30.6	11.6	0.638	0.993	11.4	198.8	70	268.4	–3.7	2.74
71	123.5	45.2	213.1	35.5	11.9	0.626	0.996	13.1	197.4	71	268	–3.9	2.66
72	122.1	50.6	216.1	40.3	12.3	0.608	1	14.8	195.8	72	267.3	–4	2.55
73	120.4	56	219.5	45.2	12.7	0.583	1.003	16.5	194	73	266.4	–3.9	2.41
74	118.1	61.3	223.2	49.9	13	0.552	1.007	18.1	191.8	74	265.2	–3.7	2.25
75	114.8	66.6	227.5	54.6	13.4	0.515	1.01	19.8	189.2	75	263.7	–3.1	2.08

Will C/2022 R2 Atlas lead to meteors leaping from Lepus in late November?

John Greaves

United Kingdom

C/2022 R2 is a recently discovered comet with a preliminary orbit that passes within 0.05 AU of Earth's orbit. D criterion assessment suggests that this comet has the potential to lead to an annual radiant in the heart of Lepus around November 22nd to 24th.

1 Introduction

On 2022 September 20 the Central Bureau for Astronomical Telegrams[6] released a discovery notice inclusive of orbital elements for the newly discovered comet designated C/2022 R2 Atlas (Nakano, 2022). On the same day MPEC S87 was released containing astrometry from several sources (see MPC Staff[7]) covering a roughly 5-day arc of this long period comet's orbit.

2 Discussion

The current orbit is still somewhat preliminary but given no major changes going forwards this small Halley Type comet with a highly eccentric orbit will pass closest to Earth at roughly 1 Astronomical Unit (AU) on its way to a 0.628 AU perihelion on October 25th 2022 for the first time in around 220 years. The orbit is such that the comet's ascending node lies within roughly 0.05 AU of the Earth's orbit, and the comet was already at that point during its September 14th 2022 discovery. The Earth itself will later pass the projection of this point around the 20th to 25th of November 2022. Given the current preliminary nature of the orbit all values are being expressed somewhat roughly.

A potential shower radiant's particulars will be in the heart of Lepus near Right Ascension 84 degrees and Declination –20 degrees, the radiant should be active centered around Solar Longitude 240.2 degrees, or 19 hours on November 22nd 2022 UT, with the meteors being of medium speed with geocentric velocity of around 38 km/s.

However, as said, this comet is on a return to the inner Solar System for the first time in at least two centuries or so and although the comet did pass near Earth's orbit before Earth itself it was still 1 AU from the Sun at that time and around five to six weeks prior to perihelion. In which case any particles ejected from the comet will not really have had enough time to cross the Earth orbit's path. The same date in 2023 would give an extra year for such to occur.

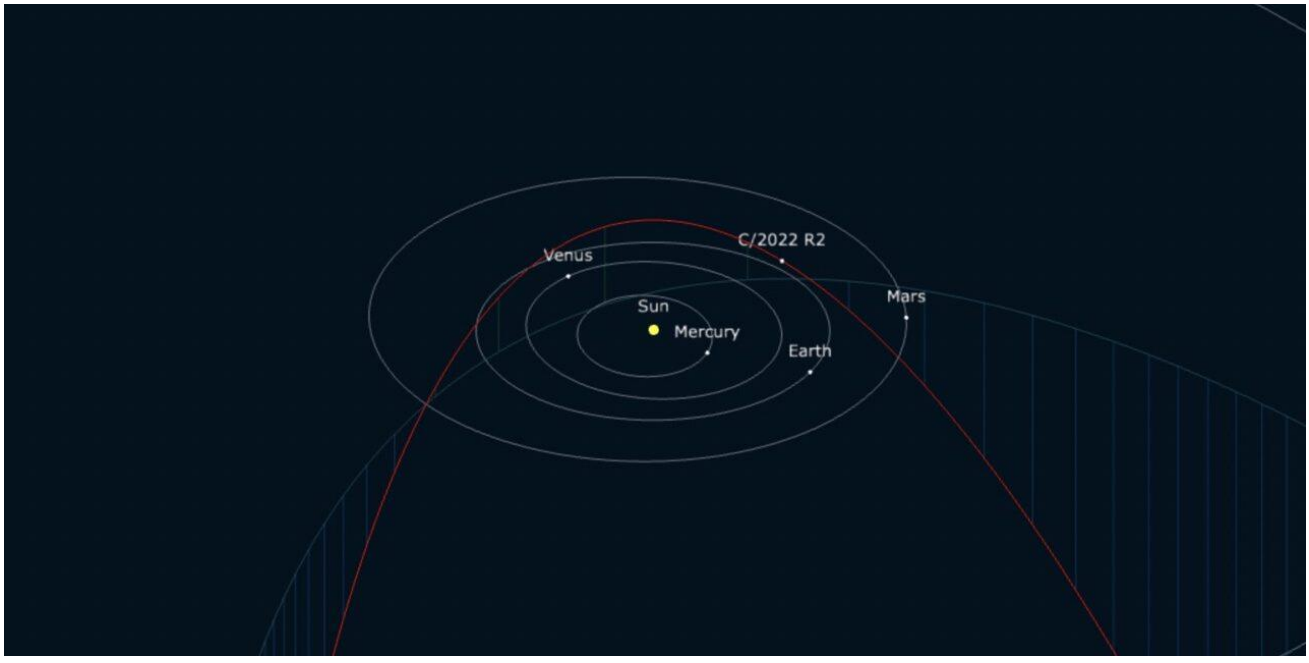

Figure 1 – The orbit of C/2022 R2 relative to the inner planets.

[6] http://www.cbat.eps.harvard.edu

[7] http://www.cbat.eps.harvard.edu/iau/cbet/005100/CBET005171.txt

Indeed, there are often predictions based on cometary orbits in the current era that do not come to pass and it may take many years for any meteoroids from this comet, if any at all, to hit the Earth's atmosphere. On the other hand, the Southworth and Hawkins (1963) D criterion value for an Earth crossing shower is around 0.04 which in itself is promising given there being any actual meteoroids to be presented.

Examination of a collection of nearly two million meteor orbits of various derivation, both published and in the public domain, revealed only 7 candidates when seeded with the comet's preliminary orbit for a period spanning from 2008 to 2021 inclusive, with none before then, some years providing none during that span, some years providing one, and, only 2021 providing 2 candidates. All of these could therefore be simply coincidental sporadics. Although given this is likely a small and indistinct comet, as it will never be much brighter than magnitude 15 at its best (barring any outbursts which would be occurring after the nodal passage thus therefore not likely to lead to any meteor activity before 2023 at the very earliest, with none guaranteed even then) it is possible that any meteoroids derivable from its last apparition are already long dispersed.

Meanwhile any potential 2022 activity at least has the rare decency to coincide with a virtually New Moon.

3 Conclusion

In the modern era potential meteor showers either freshly occurring due to or enhanced by comet passages can often be predicted. Whether they occur or not is another matter. C/2022 R2 has a preliminary 5-day arc orbit pointing to a potential of an annual meteor radiant with Solar Longitude 240.2 degrees emanating from the constellation of Lepus near 84 degrees Right Ascension and –20 degrees Declination, with a geocentric velocity of around 38 km/s.

Although the comet has already passed the point in its orbit closest to the Earth's orbit both roughly five to six weeks prior to its perihelion and roughly nine to ten weeks before the Earth reaches that point in its own orbit, there is a chance for enhanced meteor activity in Lepus around November 22nd to 23rd (add one to each date for leap years) from 2022 onwards. Current meteor orbit datasets suggest that there is currently no real activity in the heart of this constellation at around that time.

Any activity would be likely to be picked up during current multi-station meteor surveys as a matter of routine, given sufficient brightness.

Acknowledgment

This research has made use of data and/or services provided by the International Astronomical Union's Minor Planet Center.

References

Jopek T. J. (1993). "Remarks on the meteor orbital similarity D-criterion". *Icarus*, **106**, 603–607.

Nakano S. (2022). "Comet C/2022 R2 (Atlas)". CBET 5171, published 2022, September 20. Ed.: D. W. E. Green. Cambridge: Central Bureau for Astronomical Telegrams.

Southworth R. B. and Hawkins G. S. (1963). "Statistics of meteor streams". *Smithsonian Contributions to Astrophysics*, **7**, 261–285.

SonotaCo net vs CAMS vs EDMOND vs GMN in the case of the chi Cygnids (CCY#0757)

Masahiro Koseki

The Nippon Meteor Society, 4-3-5 Annaka Annaka-shi, Gunma-ken, 379-0116 Japan
geh04301@nifty.ne.jp

We confirmed the 5-year periodicity of the χ-Cygnids (CCY#0757) and find an increasing trend in the activity; the next return might be expected in 2025. The chi Cygnid meteor shower displays activity mainly in the photographic range; very similar as in the case of the tau Herculids (TAH) and the outburst of meteors from 73P/Schwassmann-Wachmann3. The chi Cygnid activity in photographic meteors might be related to 2020RF as suggested by Jenniskens (2020).
We have four video meteor databases and compare them in this study of the chi Cygnids. Each dataset has its unique characteristics, and we use them carefully in accordance with their properties. The SonotaCo net database is the longest database in the time, and we can estimate the long-term changes in activities. CAMS and EDMOND stopped publishing their data after 2016, although that their data for each year became larger than that of SonotaCo net. GMN is developing and, therefore, it is necessary to compare the changes in meteor activity; we can get a most reliable activity profile of a meteor shower for a single year because the data is stable and abundant.

1 Introduction

The chi Cygnids (CCY#0757) were first observed unexpectedly (Jenniskens, 2015) but their periodicity was soon established from the former apparition (Shiba, 2015). Jenniskens used data from CAMS and Shiba from SonotaCo net. Adding to these two datasets, the detailed report from EDMOND confirmed its apparition in 2010 and its 5-year periodicity. Unfortunately, EDMOND ceased its observations after 2016 and also CAMS has not published new data after 2016. The expected return of the chi Cygnids was observed well by SonotaCo net, GMN, and CAMS, but raw data have been only published by SonotaCo net and GMN, but not by CAMS. Now, we have observational evidence for three returns of the chi Cygnids, in 2010, 2015, and 2020 from 4 different data sources. It seems a nice case to study the differences in the observational situations of the shower in these 4 datasets.

2 Data analysis

We analyze data using the same method given in our latest work (Koseki, 2022). For example, we present the raw data and the final results for the period of ($161.33° < \lambda_{\odot} < 181.33°$) in the case of SonotaCo net data (*Figure 1*). The chi Cygnids have a long elongated radiant

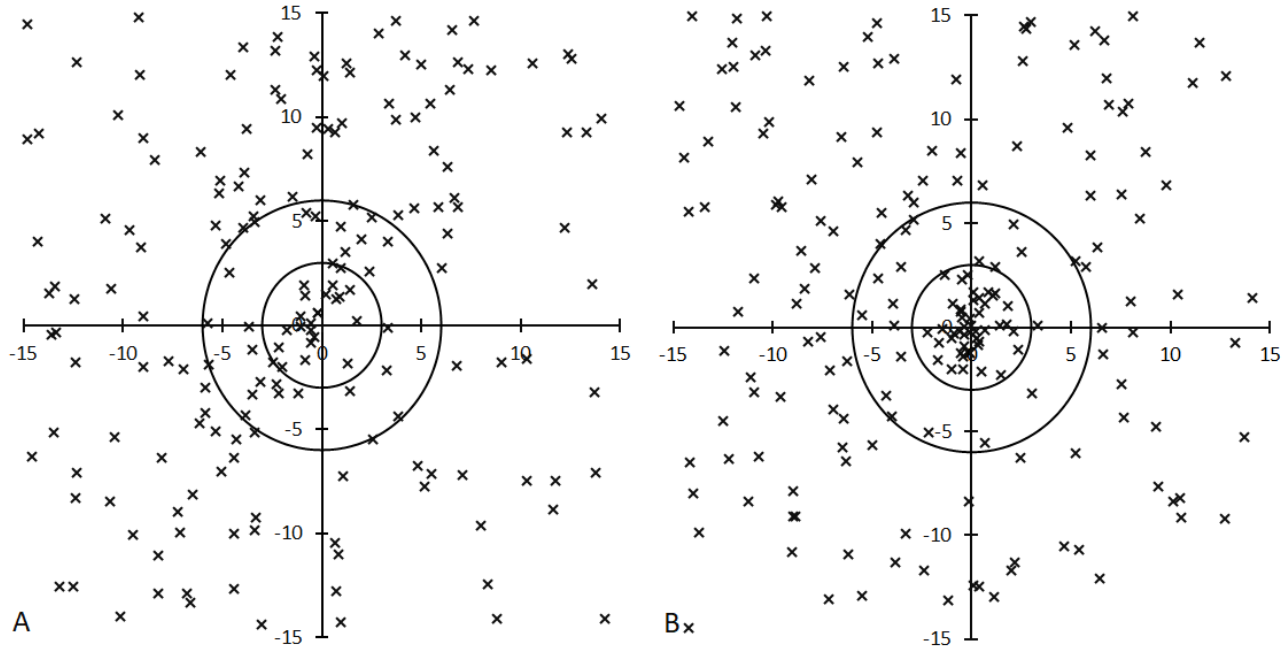

Figure 1 – Radiant distributions centered at CCY01 ($\lambda - \lambda_{\odot}$, β) = (141.3°, 50.2°) around $\lambda_{\odot}$ = 161.33° with 10 degrees width. A (left): raw distribution, B (right): converged distribution after regression analysis.

Table 1 – Observational periods of each dataset. N_{CCY} is the number of CCY members defined in this study as the distance from the estimated radiant center is less than 3 degrees. N_{all} is the total number of meteors within the analyzed period ($161.33° < \lambda_\odot < 181.33°$). P_{CCY} is the proportion of CCY within the total number of observed meteors. Years in bold are the years with enhanced activity.

SonotaCo																
Year	2007	2008	2009	**2010**	2011	2012	2013	2014	**2015**	2016	2017	2018	2019	**2020**	2021	Total
N_{CCY}	0	0	2	11	0	0	1	0	7	0	0	0	1	23	2	47
N_{all}	804	899	1473	1157	1708	1301	1239	795	539	292	666	375	1401	1078	1295	15022
P_{CCY}	0	0	0.14	0.95	0	0	0.08	0	1.3	0	0	0	0.07	2.13	0.15	0.31

CAMS								
Year	2010	2011	2012	2013	2014	**2015**	2016	Total
N_{CCY}	0	1	3	2	6	132	2	146
N_{all}	0	2672	2715	4794	5875	7349	5763	29168
P_{CCY}	-	0.04	0.11	0.04	0.1	1.8	0.03	0.5

EDMOND														
Year	2004	2005	2006	2007	2008	2009	**2010**	2011	2012	2013	2014	**2015**	2016	Total
N_{CCY}	0	0	0	0	0	0	19	2	0	0	2	53	0	76
N_{all}	0	0	17	178	175	472	1236	2182	2341	3228	2389	8549	672	21439
P_{CCY}	-	-	0	0	0	0	1.54	0.09	0	0	0.08	0.62	0	0.35

GMN						
Year	2018	2019	**2020**	2021	2022	Total
N_{CCY}	0	5	318	16	16	355
N_{all}	0	3529	11498	15669	17913	48609
P_{CCY}	-	0.14	2.77	0.1	0.09	0.77

distribution visible in raw data (*Figure 1A*), but they converge into a narrow radiant within only 3 degrees diameter after the regression analysis (*Figure 1B*). We analyzed the three other datasets and get similar results. We will compare the results in the next section.

3 Comparison between four datasets

We have four datasets to study the chi Cygnids but each of them has different characteristics (Koseki, 2018; 2019). It seems that the difference in the observational period is very important for the chi Cygnids studies (see *Table 1*). And more, the periodicity of the chi Cygnids affects the apparent activity profile because the observing conditions during the year with enhanced activity are very different (see *Figures 3 and 6*).

3.1. Radiant drift

Figure 2 shows the radiant drift estimated from the four datasets and it is clear that they are consistent with each other. The radiant moves fast northward across Cygnus. The elongated radiant distribution in *Figure 1A* is caused by this fast radiant drift. Of course, the difference in position becomes larger apart from the maximum ($\lambda_\odot$ ~173°). The estimated radiants for CAMS and GMN almost overlap because they got a large amount of chi Cygnid meteors.

3.2. Activity profile

We compare the activity profiles by the daily number of chi Cygnid meteors (*Nr* < =3) and by the moving mean of the 3-day bin of radiant density ratio (*DR20*) in *Figure 3*; *DR20* expresses the ratio of the radiant density within 3 degrees from the center to one between 15 degrees and 20 degrees from the center.

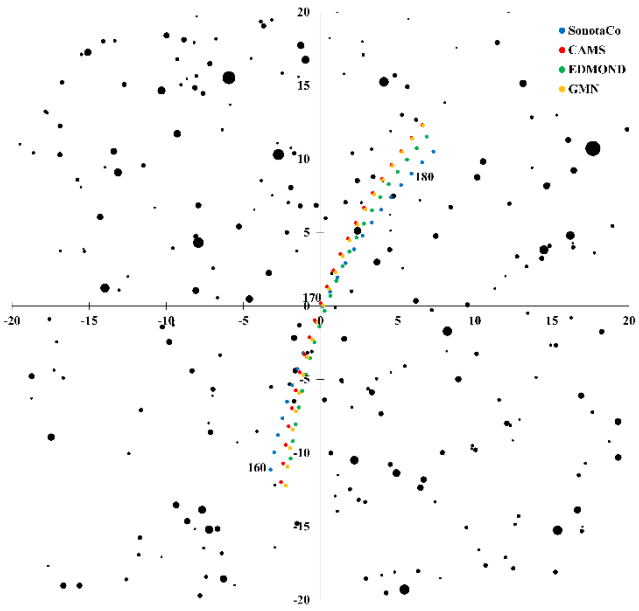

Figure 2 – Comparison of estimated radiant drift of the chi Cygnids between $160° < \lambda_\odot < 182°$ centered at (α, δ) = (302°, +30°). The radiant moves from the lower center upward crossing Cygnus.

September is a rainy season in Japan and, therefore, SonotaCo net got the lowest number of chi Cygnid meteors, and the profile is undulating. The maximum lies around $\lambda_\odot$ = 172° and the raw meteor number reaches 8; suggesting

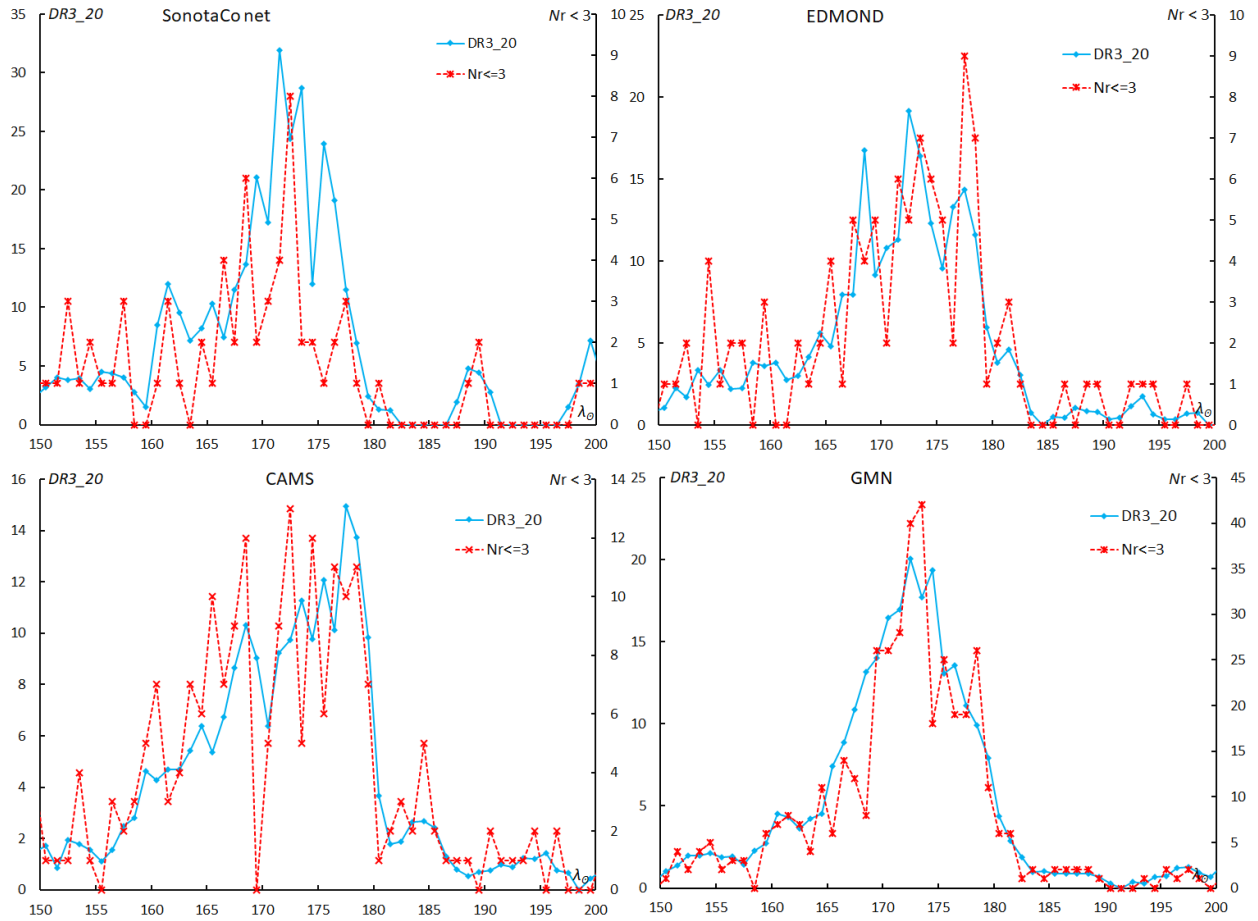

Figure 3 – Activity profiles by daily number of chi Cygnid meteors (*Nr* <= 3) and by the radiant density ratio (*DR20*); *DR20* is the ratio of the radiant density within 3 degrees from the center to one between 15 degrees and 20 degrees from the center.

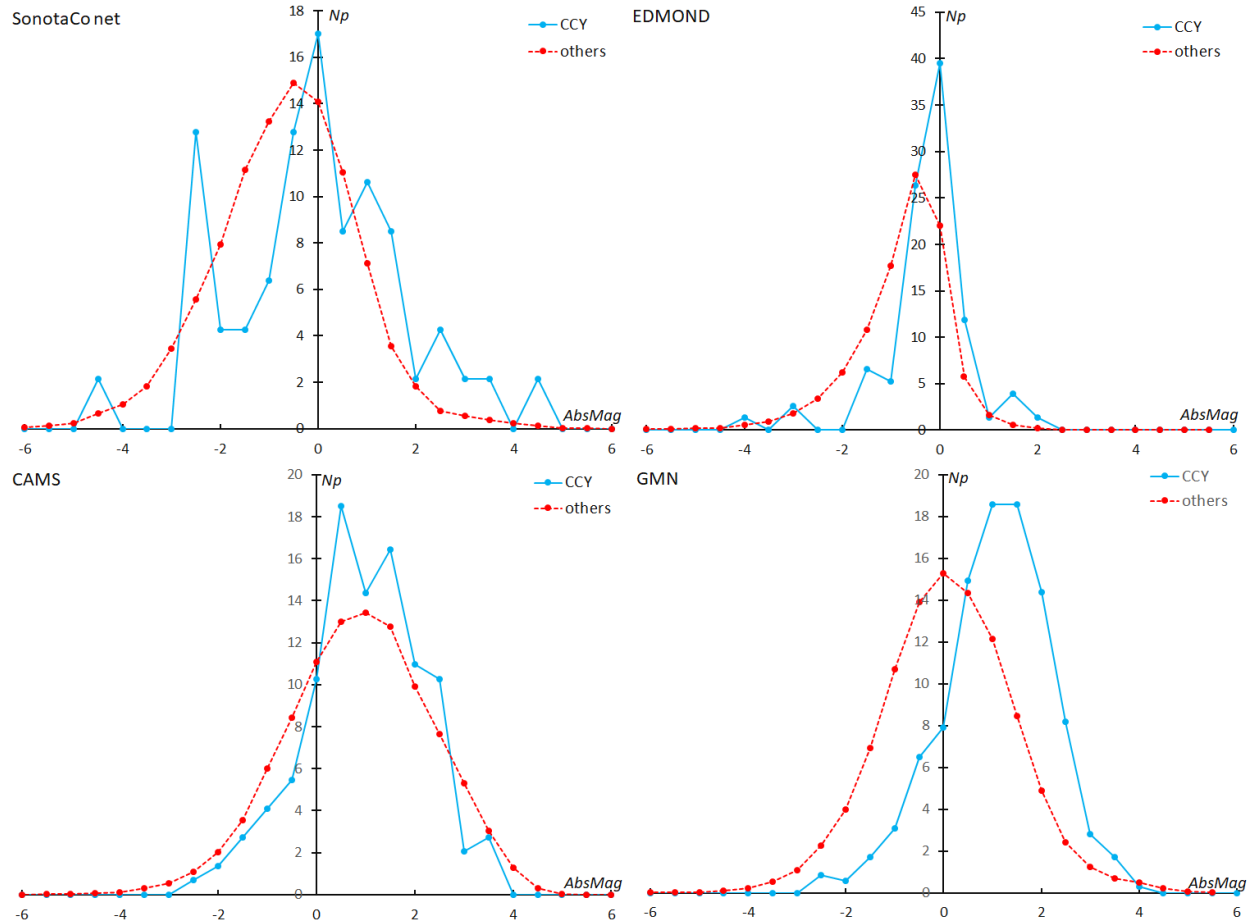

Figure 4 – Absolute magnitude distribution of chi Cygnid meteors compared with other meteors. The ordinate represents the portion in each group.

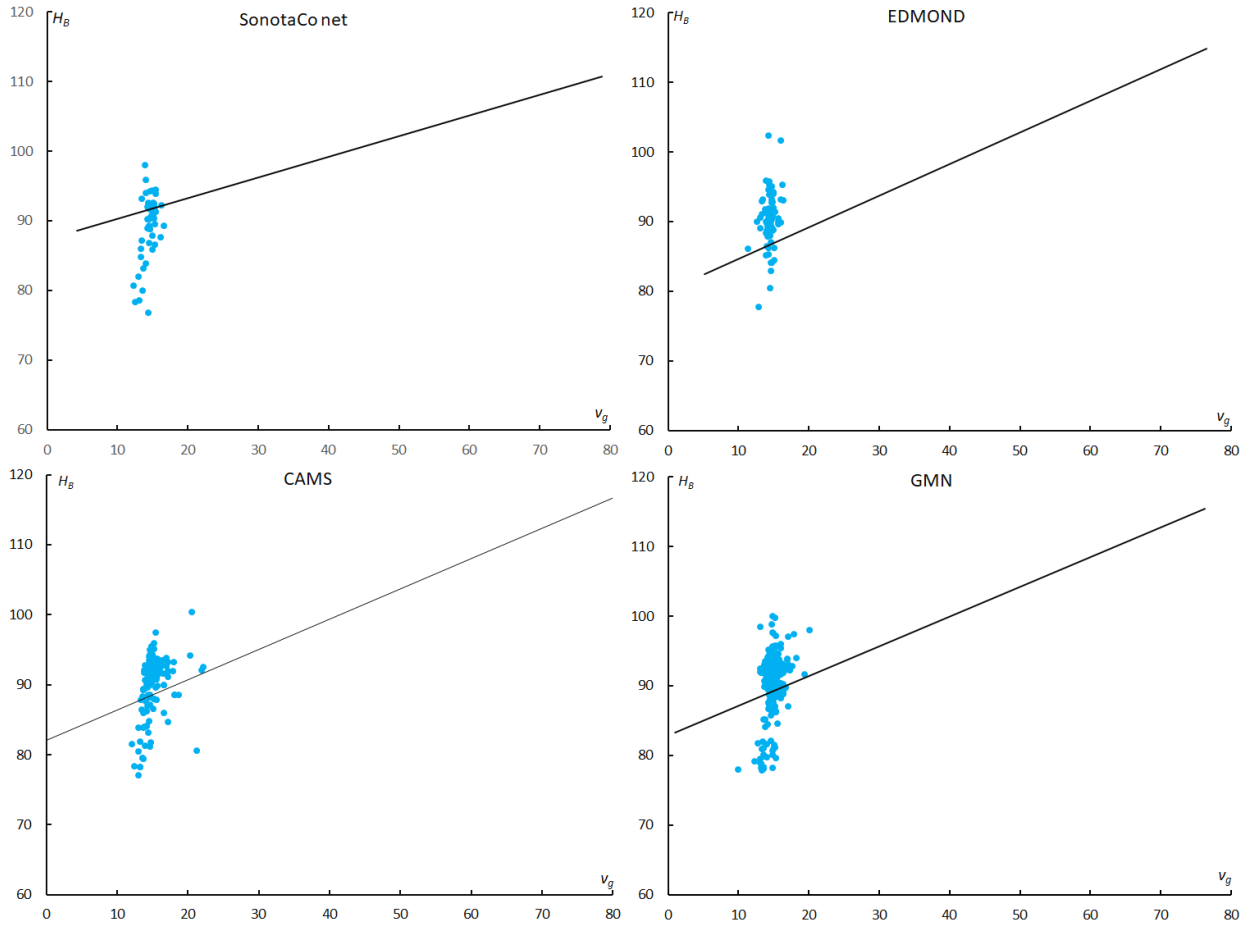

Figure 5 – Distribution of beginning height H_B of chi Cygnid meteors; the bold line is the mean height of other meteors.

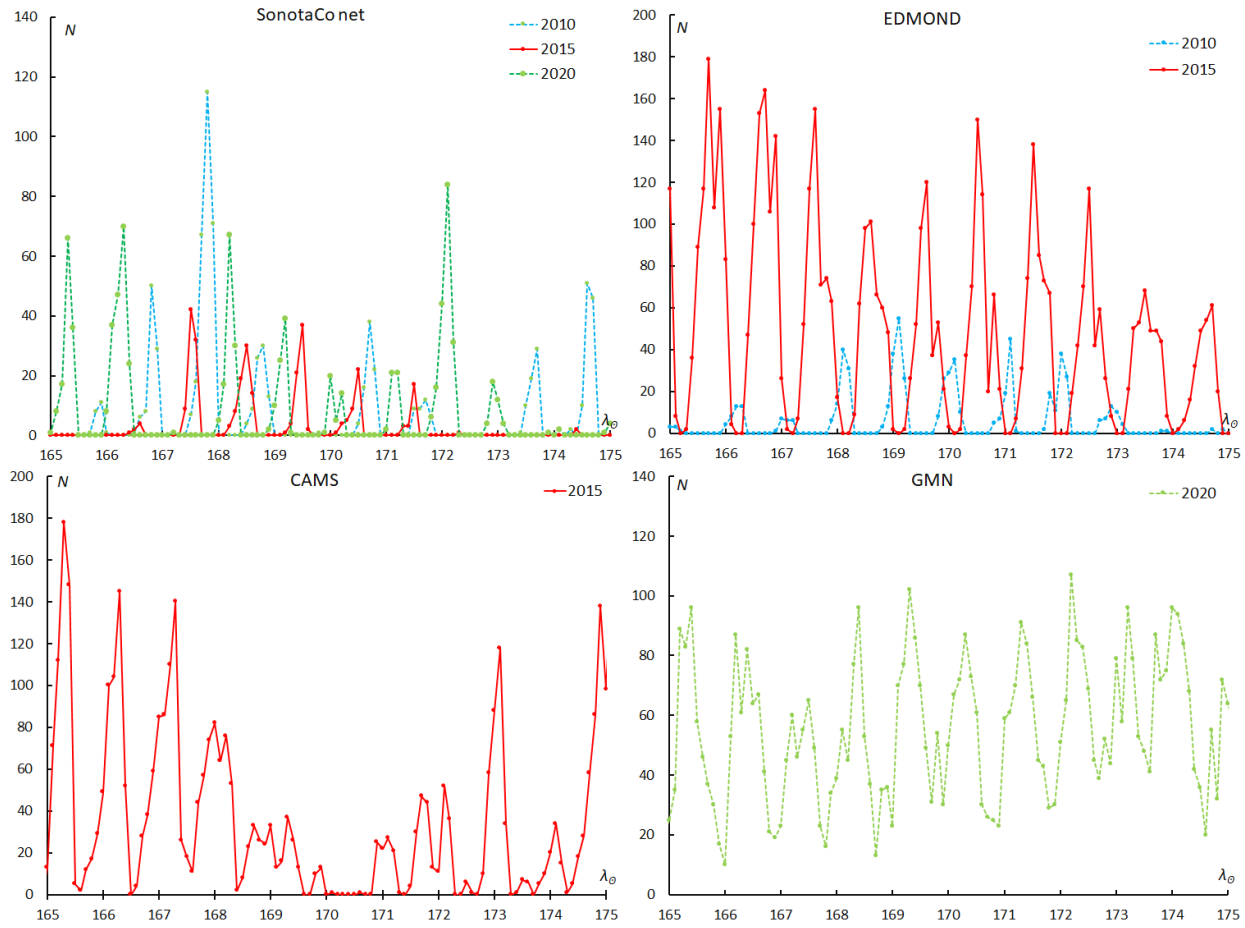

Figure 6 – All numbers of observed meteor totals in a 0.1-degree bin of $\lambda_\odot$ around the maximum ($165° < \lambda_\odot < 175°$); given for enhanced years only.

that the visual hourly meteor rates (*HR*) would be less than 1 at the most. SonotaCo net caught the enhanced activity of the chi Cygnids three times, but the weather conditions obstructed the observations around the maximum except for 2020 (see *Figure 6*).

The activity profile obtained for CAMS depends on 2015 observations only and the result is affected by observational conditions (see *Figure 6*). The deep gap before the maximum is caused by the absence of observations. Raw data suggests that the maximum is located around $\lambda_{\odot}$ = 172° but after $\lambda_{\odot}$ > 175° from the radiant density ratio (*DR20*). The raw number at the maximum is larger than that for SonotaCo net but the *DR20* is smaller.

EDMOND was organized in 2004 but the possible apparition of CCY in 2005 was missed by the scarce observations. EDMOND developed observations rapidly and, therefore, the number of the obtained CCY meteors is of course larger in 2015 than in 2010. The activity profile by EDMOND depends on 2015 observations mainly and the raw data fluctuate largely. Contrary to the results of CAMS, the supposed maximum by EDMOND locates around $\lambda_{\odot}$ = 173° in *DR20* but after $\lambda_{\odot}$ = 175° in the raw data.

GMN observed the chi Cygnids only in 2020 but both raw and *DR20* profiles are in good agreement. The two profiles reveal that the chi Cygnid maximum lies around $\lambda_{\odot}$ = 173°. GMN got the most chi Cygnids of all four datasets and, therefore, the maximum raw data is of course the highest among them. The *DR20* maximum reaches about 20 at the maximum and seems moderate in all four networks. This ratio means that the chi Cygnid shower is a typical minor meteor shower but not weak at its apparition.

3.3. Tendency of activity level change

We know that the first report of the chi Cygnids was made by observations of CAMS in 2015 (Jenniskens, 2015) and the detection of the apparition in 2010 was soon pointed out based on Japanese video observations (Shiba, 2015); followed by the report of the observations of EDMOND (Koukal et al., 2016). It is supposed that the shower became active in 2015 compared to 2010 because both SonotaCo net and EDMOND did not notice the apparition in 2010. We can expect that the chi Cygnid activity will be more and more active thenceforth. Unfortunately, EDMOND stopped its activity after 2016 and CAMS has not shared any results after 2016.

It may be useful to compare the different data sources using the records of the total number of obtained meteors in the period of the survey (161.33° < $\lambda_{\odot}$ < 181.33°) as the reference. *Table 1* gives the number of the chi Cygnid meteors classified in this study, the total number of meteors in the same period, and the ratio of the former to the latter.

We can assume that the activity of the chi Cygnids might become stronger based on SonotaCo net observations, though EDMOND suggests the apparition in 2015 might be weakened. This uncertainty comes from the small amount of data in both data sources in 2010 and in 2015. It is interesting that the proportion of the chi Cygnids observed by CAMS is about three times larger than that of EDMOND; CAMS started its observations after the chi Cygnid activity in 2010. If we take the observational conditions into consideration, the proportion could become larger because observations by CAMS around the maximum are scarce (*Figure 6*).

A comparison of the two apparitions in 2015 and in 2020 seems easier than the above case and the apparition in 2020 is stronger than in 2015. SonotaCo net data indicate an increase of chi Cygnid meteors. CAMS and GMN are missing the data for one of both apparitions, but both have sufficient amount of data. Even if we considered the observational condition for CAMS in 2015, its proportion (1.80) might not exceed that of GMN in 2020 (2.77). It seems clear that the apparition of 2020 was stronger than that of 2015.

We may conclude that the activity of the chi Cygnids is increasing with some uncertainty before 2015. If so, we can expect a more active chi Cygnid meteor shower in 2025.

3.4. Magnitude distribution

Four observation systems use different devices and a different data management. SonotaCo net and EDMOND use small CCD cameras that have a wide field of view and analyze meteor trails using SonotaCo software. CAMS and GMN use CCD cameras that have larger lenses and a rather narrow view and analyze data by their own software. *Figure 4* compares the absolute magnitude distribution of chi Cygnid meteors compared with other meteors, excluding chi Cygnid meteors. The ordinate represents the portion in the groups; for example, 0 absolute magnitude meteors occupy about 40% of the chi Cygnids and 22% of the other meteors in the case of EDMOND. The magnitude distribution of other meteors shows the difference in the four systems.

It is clear that CAMS and GMN can catch about 1 magnitude fainter meteors than SonotaCo net and EDMOND. Both magnitude distributions in EDMOND seem curiously narrow. Photometry of meteor figures on CCD chips is difficult and its result differs by more than 1 magnitude case by case even for the same meteors. We should be careful to study the magnitude distribution of EDMOND.

We know SonotaCo net system catches fast meteors mainly but misses slower meteors compared to CAMS (Koseki, 2018). Therefore, the magnitude distribution of other meteors in *Figure 4* for SonotaCo net shows mainly fast meteors. The magnitude distributions of CAMS represent the chi Cygnid apparition in 2015 and those of GMN the return in 2020.

We should be careful to draw a conclusion from *Figure 4*, but the peaks of the magnitude distributions suggest the chi Cygnid meteors might be fainter than the sporadic background; the GMN distribution which has the largest

number of chi Cygnid meteors among the four datasets indicates this tendency strongly.

3.5. Beginning height

Meteors produced by comet 73P/Schwassmann-Wachmann3 tend to ablate higher in the atmosphere than sporadic meteors (Koseki, 2022). It is interesting to study the chi Cygnid shower which has a recurrent nature with a 5-year period. Bold lines in *Figure 5* show the mean height of the beginning heights of other meteors excluding the chi Cygnid shower members.

The beginning heights of the chi Cygnid meteors in the larger part are above the bold line except for the SonotaCo net data. This exception might be caused by a tendency in SonotaCo net data, as there are less slow meteors in it.

Chi Cygnid meteors are classified as C-type by Ceplecha's (1968) graph, though SW3 meteors are above C (Koseki, 2022). The type C meteors seem to be cometary particles and not asteroidal ones.

It is noteworthy to mention that faster meteors in the chi Cygnid shower tend to ablate higher; dots in *Figure 5* distribute lower left to the upper right. The meteoroid density of the chi Cygnid meteors has been dispersed wider compared to 73P/Schwassmann-Wachmann3 meteoroids. It might be suggested that the chi Cygnid meteoroids are a mixture of young and old particles released from the parent body over a long period.

3.6. Conditions of observations

We cannot compare these four datasets as they are, because their devices and analyzing software are different as described above. There are additional reasons why we must be careful; observational periods in different years and its tendency, weather and technical problems which cause interruptions of observations.

Figure 6 compares the observed meteor number in a 0.1-degree bin of $\lambda_{\odot}$ around the maximum ($165° < \lambda_{\odot} < 175°$). Graphs look like saw blades; observational stations are not deployed in the world evenly. The peaks of meteor numbers also change day by day as well as year to year. These changes are caused not only by natural fluctuations but also by observational conditions, such as the weather.

Figure 6 (SonotaCo net) reveals how Japanese weather conditions in September hinder optical meteor observations; the graph for 2015 is lower than in other years and this makes the chi Cygnid meteors in 2015 less numerous than in 2010 (*Table 1*). *Figure 6* (CAMS) shows that the observed meteor number drops around the maximum and this explains the deep gap before the maximum in *Figure 2* (CAMS).

Figure 6 (EDMOND) shows that the number of observations increased more in 2015 than in 2010. The observations in 2010 were limited around the maximum and, therefore, the calculated proportion of the chi Cygnids in 2010 by EDMOND in *Table 1* might be exaggerated.

Figure 6 (GMN) shows stable observational conditions and the activity profile of the chi Cygnids in 2020 could be best reproduced using GMN observations (*Figure 2*).

4 Photographic observations of the chi Cygnids

There is no meteor shower related to the chi Cygnids in the published meteor shower catalogs though MK-92 might correspond to the chi Cygnids; the author searched meteor showers among photographic meteor orbits using the centroid method of cluster analysis D_{SH} (Southworth and Hawkins, 1963) as a scale (Koseki, 1982); *Figure 7* shows the radiant distribution of photographic meteors; the positions are compensated, the radiant drift has been estimated from GMN observations and the radii are inversely proportional to D_{SH} calculated relative to the orbit estimated for $\lambda_{\odot} = 173°$ by GMN data.

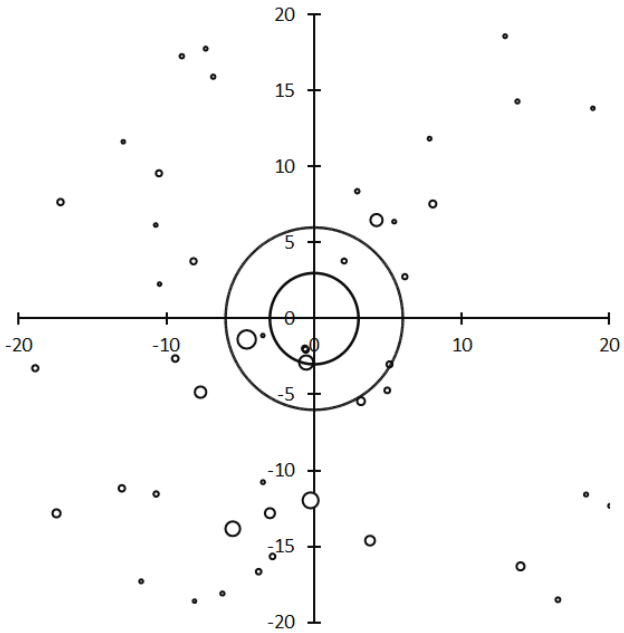

Figure 7 – The photographic radiant distribution. Centered at the estimated chi Cygnid radiant by GMN observations, the radii of the circles are inversely proportional to D_{SH} calculated to the estimated chi Cygnids orbit at $\lambda_{\odot} = 173°$ by GMN data.

We can find 16 photographic meteors within $D_{SH} < 0.20$ from the estimated orbital elements from GMN at $\lambda_{\odot} = 173°$ (*Table 2*); the 7 meteors in *Table 2* in bold italic are members of MK-92, though H1-4335 has $D_{SH} > 0.20$. We add K2-104 at the end of *Table 2*. The radiant point of K2-104 is near the estimated center (x, y) = (–6.0, 0.7), though its geocentric velocity is extremely high (v_g = 35.0 km/s) and, therefore, its orbit is very different from the chi Cygnids (D_{SH} = 1.346). Its geocentric velocity might be in error; the measurement or treatment of the data was mistaken, unfortunately, this happened sometimes in former Soviet data.

If we include two candidates, H1-4335 and K2-104, there would be enough meteors to certify a meteor shower activity. Some meteor activity related to the chi Cygnids is confirmed by photographic observations, though the

Table 2 – Possible members of the chi Cygnids among photographic meteors. Selected for $D_{SH} < 0.20$ using the estimated orbit data from GMN at $\lambda_\odot = 173°$. H1-4335 is included although it has $D_{SH} > 0.20$ because it is a member of MK-92; MK-92 has been found by Koseki (1982) and seems to relate to the chi Cygnids. Members of MK-92 are shown in bold italic.

Code	Year	$\lambda_\odot$ (°)	$\lambda - \lambda_\odot$ (°)	β (°)	v_g (km/s)	e	q (AU)	i (°)	ω (°)	Ω (°)	D_{SH}	x	y
CCY	Ref.	173	140.6	52.3		0.659	0.956	18.4	208.7	173			
H4-10849	1957	171.7	148.7	51.3	16.3	0.685	0.935	20	214.3	171.7	0.068	–4.6	–1.4
H4-10877	1957	174.6	138.2	44.3	13	0.634	0.955	14.3	209.3	174.6	0.08	–0.2	–12
O4-424	1965	181	135.7	49.1	14.4	0.69	0.96	16.7	206.5	181	0.088	–5.5	–13.8
O4-425	1965	183	124	62.5	14.3	0.607	0.986	19.9	196.9	183	0.09	–0.5	–2.9
H2-4304	1952	169.9	135.6	57	15.8	0.701	0.97	20.4	204	169.9	0.108	4.2	6.5
H1-4307	1952	170.7	153.6	46.3	16.1	0.66	0.91	19	220	170.7	0.116	–7.7	–4.8
H6-39766	1967	189.7	108.3	57.8	12.1	0.58	0.995	15.9	190.4	189.7	0.133	–3	–12.8
H1-4286	1952	167.7	141	33.3	12.1	0.62	0.94	11	213	167.7	0.138	3.8	–14.6
H6-42312	1974	179.7	140.8	40	13.9	0.69	0.94	13.7	212.3	179.7	0.151	–8.6	–21.4
H6-39755A	1967	178.7	112.7	42.7	11.3	0.66	0.992	11.6	193.7	178.7	0.167	14	–16.3
H6-39764C	1967	187.7	139	52.5	14.9	0.67	0.956	18.1	207.4	187.7	0.167	–17.4	–12.8
O3-426	1965	183	116.7	59.7	16.3	0.795	0.99	20.8	193.6	183	0.173	3.2	–5.4
H3-4313	1952	171.1	132.4	27.6	11.1	0.643	0.961	7.9	207.6	171.1	0.187	8.8	–24.1
H6-42341	1974	207.7	78.4	57.2	12.1	0.6	0.995	15.6	176.5	207.7	0.194	–23.3	–0.3
H1-3802	1952	152.7	145.9	36.2	14.3	0.7	0.93	13	217	152.7	0.195	8	7.6
H3-4964	1952	208.4	79.4	47.3	11.8	0.693	0.994	13	176.4	208.4	0.195	–31.3	–6.1
H1-4335	1952	171.7	158.4	40.2	16.4	0.67	0.88	17	227	171.7	0.213	–13	–11.2
Average		179.4	128.8	47.4	13.9	0.665	0.958	15.7	203.9	179.4			
K2-104	1964	172.6	150.6	54.3	35	1.97	0.912	35.6	210.8	172.6	1.346	–6	0.7

radiants are much more dispersed than video observations (*Figure 1B*). This situation is very similar to the tau Herculids; the traditional tau Herculid radiants are wider dispersed than the radiant distribution of the outburst in 2022 (Koseki, 2022).

5 Discussions

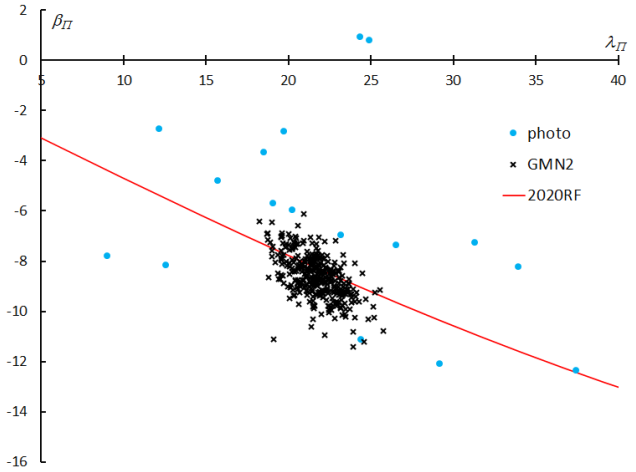

Figure 8 – Perihelion distribution of the perihelia of video and photographic meteors with the orbital plane of 2020RF. λ_Π and β_Π are the ecliptic coordinates.

Jenniskens (2020) indicates 2020RF might be the parent body of the chi Cygnids. *Figure 8* shows the perihelion distribution of chi Cygnid meteors for GMN data with the orbital plane of 2020RF and the above-mentioned photographic meteors, except for K2-104. The perihelion distribution of photographic meteors appears to be along the orbital plane of 2020RF and might suggest that these photographic meteors are descendants of asteroid 2020RF.

However, whether the chi Cygnid activity observed by video is related to it is uncertain. The video chi Cygnid meteors might be too fragile (see 3.5. Beginning height) for an asteroidal origin and their perihelion distribution appears inclined to the orbital plane of 2020RF (*Figure 8*).

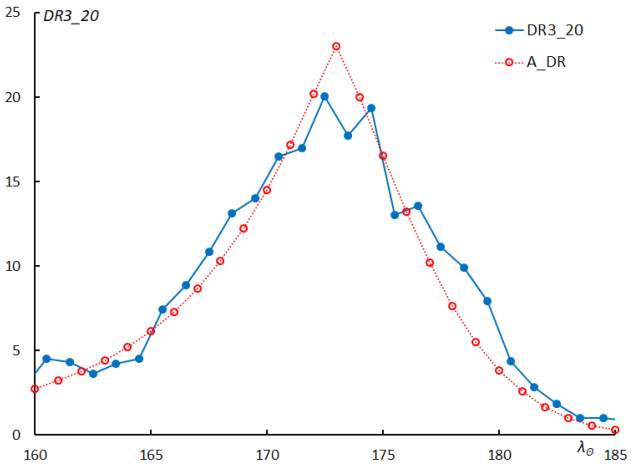

Figure 9 – Comparison of chi Cygnid activity (DR20 for GMN) and the estimated activity profile assuming a stationary perihelion (A_DR).

Four video chi Cygnid datasets indicate that the perihelion of the chi Cygnid orbit is stable and does not rotate (*Figure 8* and Appendix). We estimate the activity profile of the chi Cygnids assuming a stationary perihelion and we compare DR20 obtained from GMN (*Figure 9*). The two graphs are in very good agreement and suggest that the chi Cygnids are under strong perturbation from Jupiter; the exact periodicity of 5 years supports this hypothesis.

Acknowledgment

We appreciate the daily efforts by all camera operators of the SonotaCo net[8], EDMOND, CAMS[9] and the Global Meteor Network[10]. This analysis owes to their work. This analysis relied upon the publicly available data from the GMN group under license[11] (Vida et al., 2019; 2020; 2021).

References

Ceplecha Z. (1968). "Discrete Levels of Meteor Beginning Height". *Smithsonian Astrophysical Observatory Special Report*, **279**, 54 pages.

Jenniskens P. (2015). "New Chi Cygnids meteor shower". CBET 4144. IAU Central Bureau for Astronomical Telegrams. D.W.E. Green (ed.).

Jenniskens P., Baggaley J., Crumpton I., Aldous P., Pokorny P., Janches D., Gural P. S., Samuels D., Albers J., Howell A., Johannink C., Breukers M., Odeh M., Moskovitz N., Collison J., Ganju S. (2018). "A survey of southern hemisphere meteor showers". *Planetary Space Science*, **154**, 21–29.

Jenniskens P. (2020). "The 2020 chi-Cygnids", *WGN, Journal of the IMO*, **48**, 146–149.

Kornoš L., Koukal J., Piffl R., and Tóth J. (2014a). "EDMOND Meteor Database". In Proceedings of the International Meteor Conference, Poznań, Poland, Aug. 22-25, 2013, Eds.: Gyssens M., Roggemans P., Zoladek, P. International Meteor Organization, pages 23–25.

Kornoš L., Matlovič P., Rudawska R., Tóth J., Hajduková M. Jr., Koukal J., and Piffl R. (2014b). "Confirmation and characterization of IAU temporary meteor showers in EDMOND database". In Proceedings of the Meteoroids 2013 Conference, A.M. University, Poznań, Poland, Aug. 26-30, 2013, Eds.: Jopek T.J., Rietmeijer F.J.M., Watanabe J., Williams I.P. Pages 225–233.

Koseki M. (1982). "Meteor Shower Research on Photographic Meteors by Cluster analysis". 23rd Japanese Meteor Conference. (In Japanese).

Koseki M. (2018). "Different definitions make a meteor shower distorted. The views from SonotaCo net and CAMS". *WGN, Journal of the International Meteor Organization*, **46**, 119–135.

Koseki M. (2019). "EDMOND and SonotaCo net". *eMetN*, **4**, 220–224.

Koseki M. (2022). "Global Meteor Network: Outburst produced by dust from 73P/Schwassmann-Wachmann3". *eMetN*, **7**, 369–378.

Koukal J., Srba J., Toth J. (2016). "Confirmation of the chi Cygnids (CCY, IAU#757)". *WGN, Journal of the IMO*, **44**, 5–9.

Shiba Y. (2015). "χ Cygnids observation in Japan". *WGN, the Journal of the IMO*, **43**, 179–180.

SonotaCo (2009). "A meteor shower catalog based on video observations in 2007–2008". *WGN, Journal of the IMO*, **37**, 55–62.

SonotaCo, Uehara S., Sekiguchi T., Fujiwara Y., Maeda K., and Ueda M. (2021). "J14: A Meteor Shower and Cluster Catalog". *WGN, Journal of the IMO*, **49**, 76–97.

Southworth R. B. and Hawkins G. S. (1963). "Statistics of meteor streams". *Smithsonian Contributions to Astrophysics*, **7**, 261–285.

Vida D., Gural P., Brown P., Campbell-Brown M., Wiegert P. (2019). "Estimating trajectories of meteors: an observational Monte Carlo approach - I. Theory". *Monthly Notices of the Royal Astronomical Society*, **491**, 2688–2705.

Vida D., Gural P., Brown P., Campbell-Brown M., Wiegert P. (2020). "Estimating trajectories of meteors: an observational Monte Carlo approach - II. Results". *Monthly Notices of the Royal Astronomical Society*, **491**, 3996–4011.

Vida D., Šegon D., Gural P. S., Brown P. G., McIntyre M. J. M., Dijkema T. J., Pavletić L., Kukić P., Mazur M. J., Eschman P., Roggemans P., Merlak A., Zubrović D. (2021). "The Global Meteor Network – Methodology and first results". *Monthly Notices of the Royal Astronomical Society*, **506**, 5046–5074.

[8] See also "SonotaCo Network Simultaneously Observed Meteor Data Sets", http://sonotaco.jp/doc/SNM/.
[9] http://cams.seti.org/
[10] https://globalmeteornetwork.org/data/
[11] https://creativecommons.org/licenses/by/4.0/

Appendix

Estimated radiant and orbital elements of the chi Cygnids based on GMN observations.

$\lambda_\odot$ (°)	$\lambda - \lambda_\odot$ (°)	β (°)	α (°)	δ (°)	v_g (km/s)	e	q (AU)	i (°)	ω (°)	Ω (°)	λ_Π (°)	β_Π (°)	a (AU)
160	151.9	36.3	304.4	17.8	14.7	0.661	0.904	13.9	222.4	160	21.6	–9.3	2.66
161	151.2	37.6	304.2	19	14.7	0.662	0.908	14.3	221.4	161	21.5	–9.4	2.68
162	150.5	38.9	304.1	20.3	14.7	0.662	0.913	14.7	220.4	162	21.5	–9.5	2.7
163	149.7	40.1	303.9	21.6	14.7	0.663	0.917	15.1	219.4	163	21.4	–9.5	2.72
164	149	41.4	303.7	22.8	14.7	0.663	0.921	15.4	218.4	164	21.4	–9.5	2.74
165	148.2	42.6	303.5	24.1	14.7	0.664	0.925	15.8	217.3	165	21.3	–9.5	2.75
166	147.4	43.9	303.2	25.3	14.8	0.664	0.929	16.1	216.3	166	21.2	–9.5	2.76
167	146.6	45.1	302.9	26.5	14.8	0.664	0.933	16.5	215.2	167	21.1	–9.4	2.78
168	145.7	46.3	302.6	27.7	14.8	0.663	0.937	16.8	214.2	168	21	–9.4	2.78
169	144.8	47.5	302.2	28.9	14.8	0.663	0.941	17.2	213.1	169	20.9	–9.3	2.79
170	143.8	48.8	301.8	30	14.8	0.662	0.945	17.5	212	170	20.8	–9.2	2.8
171	142.8	50	301.3	31.2	14.8	0.661	0.949	17.8	210.9	171	20.7	–9	2.8
172	141.7	51.2	300.8	32.3	14.8	0.66	0.953	18.1	209.8	172	20.6	–8.9	2.8
173	140.6	52.3	300.3	33.4	14.9	0.659	0.956	18.4	208.7	173	20.5	–8.7	2.81
174	139.4	53.5	299.7	34.5	14.9	0.658	0.96	18.7	207.6	174	20.3	–8.5	2.8
175	138.2	54.7	299.1	35.5	14.9	0.656	0.963	19	206.5	175	20.2	–8.3	2.8
176	136.8	55.8	298.4	36.5	14.9	0.654	0.966	19.2	205.3	176	20.1	–8.1	2.8
177	135.4	57	297.6	37.5	14.9	0.652	0.97	19.5	204.2	177	19.9	–7.8	2.79
178	133.9	58.1	296.8	38.5	14.9	0.65	0.973	19.7	203	178	19.8	–7.6	2.78
179	132.4	59.2	296	39.4	15	0.648	0.976	20	201.8	179	19.6	–7.3	2.77
180	130.7	60.3	295.1	40.3	15	0.645	0.978	20.2	200.6	180	19.4	–7	2.76
181	128.9	61.3	294.1	41.2	15	0.642	0.981	20.4	199.4	181	19.3	–6.7	2.74
182	126.9	62.3	293.1	42	15	0.639	0.983	20.7	198.2	182	19.1	–6.3	2.73

On the question of an unexpected meteor shower June 21, 1937

Alexandra Terentjeva[1] **and Ilya Kurenya**[2]

[1] **Institute of Astronomy of the Russian Academy of Sciences, Moscow, Russia**
ater@inasan.ru

[2] **Institute for the Humanities and IT, Moscow, Russia**
luisito@inbox.ru

The unexpected abundant meteor shower of June 21, 1937, described by I. S. Astapovich (1940), was caused by the Scorpionids, long known from visual observations. According to photographic data we found that the Scorpionids are part of the ecliptic complex meteoroid Ophiuchi-Scorpionid stream (No. 93, Terentjeva, 1966). The observed phenomenon indicates the presence of significant local concentrations in the stream, which, if the stream encounters Earth under favorable conditions, can cause abundant meteor showers.

1 Introduction

I. S. Astapovich (1940), giving the observation data collected by A. A. Shreider, V. I. Belyaev, and K. I. Yermolaeva in the Sarykamysh Depression, wrote about this phenomenon: *"... the hourly number of meteors, despite the full Moon (stars weaker than +3 magnitude were not visible), reached 90 after 16^h UT; meteors poured "in bunches" from the radiant α = 239°, δ = –23° (1880.0), lying 5° from the Moon. At 21^h UT, the phenomenon ended. The meteors were bluish, all of them brighter than +3 magnitude. Here lies the radiant of the famous Scorpionid cosmic shower, active permanently for almost 100 years. The observed phenomenon indicates the presence of significant local concentrations in the cosmic streams, which was not known until now*."

In 1949, while making meteor observations on June 22, I. S. Astapovich (1949) turned his attention to the unusual abundance of meteors from the radiant α = 249°, δ = –19° (1900.0), located on the boundary of the constellations of Scorpius and Ophiuchus. During the previous two weeks, the shower was incessantly active but weak (2–3 meteors per hour). Observations on June 22 gave the hourly number of meteors of 24. Radiant dispersion covered an area of 4°. I. S. Astapovich wrote further (1949): "*It was giving the impression that the intensity of the shower was decreasing and that its maximum had been a few hours before the beginning of observations in Ashkhabad, when it was still light.*" In his visual observation system, I. S. Astapovich estimated the geocentric velocity of the shower at about 30 km/s. He also believed it possible that the shower should have the period of 12 years according to its previous maximum of 1937.

2 Research results

First of all, it should be noted that the period of 12 years for the Scorpionid shower is no longer to be assumed. The intensity of the shower in 1949 was almost four times lower. Second, it is not known whether its maximum took place a few hours before the beginning of observations in Ashkhabad (when it was still light) or not. In 1949 Earth may have encountered another "concentration" in the stream on the orbit with a different period. But most importantly, by now, in a period of 12 years, the "concentration" of 1937 should have returned to Earth exactly seven times. So why have these maxima of activity not been registered? It is possible, of course, that, as a result of planetary perturbations, the orbit of the stream has ceased to approach the Earth's orbit, or this "concentration" has dissipated, like the Andromedids did once before the eyes of astronomers of one generation.

What do modern photographic observations of the Scorpionid shower show? According to them, there is a meteoroid stream of the Ophiuchi-Scorpionids (No. 93, Terentjeva, 1966). It is a highly disturbed ecliptic stream with a very wide range of radiants active from June 22 to 30. Obviously, the stream has N and S branches (possibly an ecliptic Q branch, too). The Scorpionid stream is included in this stream as its part. The Ophiuchi-Scorpionid stream includes six photographic orbits. Two orbits with radiants close to those of 1937 and 1949 are listed here. (See *Table 1*).

Table 1 – The orbital elements for the Scorpionids, eq. 1950.0 (No. 93, Terentjeva, 1966).

Date (UT)	α_g (°)	δ_g (°)	v_∞ km/s	a AU	e	q AU	Q AU	ω (°)	Ω (°)	i (°)	π (°)
54 VI 25.22	240	–25	18.2	3.50	0.75	0.89	6.1	45	273	1	318
54 VI 30.35	249	–16	16.7	2.45	0.64	0.90	4.0	226	98	2	324

Figure 1 – Prof. I. S. Astapovich with the scientists of the Ashkhabad Astrophysical Laboratory (AAL) and students (from the personal archive of A. Terentjeva).

These are the Scorpionids themselves as part of the wide stream of the Ophiuchi-Scorpionids. These are short-period orbits with periods P = 6.5 and 3.8 years. An orbit with an aphelion of 6.1 AU at an inclination of 1° should experience significant perturbations from Jupiter at close encounter with it. This may have been the reason for the alteration of the orbit of the Scorpionids after 1937.

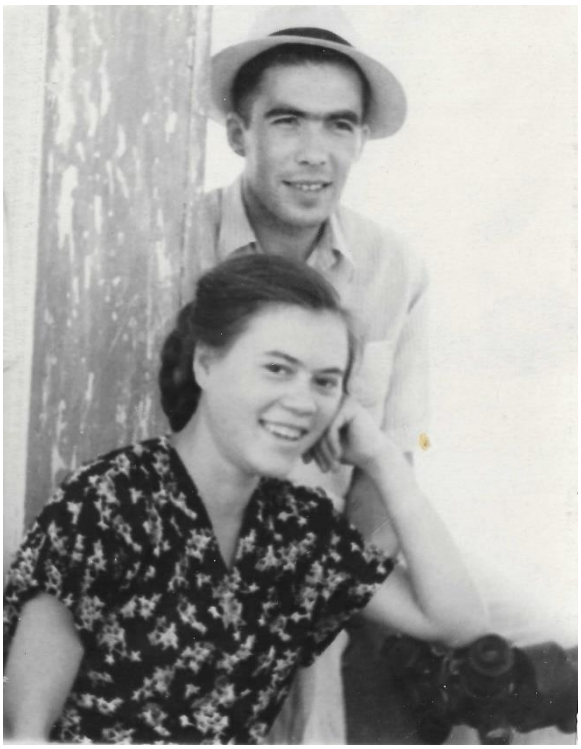

Figure 2 – A. K. Terentjeva and Y. L. Trutce during their probation period with Prof. I. S. Astapovich at the AAL, the mid-1950s (from the personal archive of A. Terentjeva).

In conclusion, it is interesting to cite an extract from an article by I. S. Astapovich (1954): "*According to our interpretation, the stone meteorite of May 19–29(?), 1419 in Velikiy Novgorod, described in Russian annals, may belong to the shower of the Scorpionids. The ancient Greek myth of Phaethon was deciphered by us as the flight and fall of a large meteorite from the same constellation at the beginning of the first millennium BC. If that's true, the Scorpionids have been active for three thousand years.*"

3 Conclusion

In the meteoroid stream of the Ophiuchi-Scorpionids, there are local concentrations which, if the stream encounters Earth under favorable conditions, can cause abundant meteor showers. Who knows, maybe this "legendary" shower will surprise us with its unexpected action – a fall of a meteorite.

Acknowledgment

This paper was translated into English by *I. Kurenya*.

The authors thank *Paul Roggemans* for his efforts enabling the preparation and publication of this paper.

References

Astapovich I. S. (1940). "The unexpected meteor shower on June 21, 1937". *Nature*, No. 7, 105. (In Russian).

Astapovich I. S. (1949). "The maximum of the Scorpionids on June 22, 1949". *Astron. Tsirk. AN SSSR*, No. 89, 3–4. (In Russian).

Astapovich I. S. (1954). "On some patterns in small body systems". *Trudy Stalinabad. Astron. Obs. AN Tajik SSR*, **20**, 78–105. (In Russian).

Terentjeva A. K. (1966). "Minor meteor streams". Results of researches of international geophysical projects: Meteor Investigations. No. 1. Publishing House "Nauka", Moscow, pages 62–132. (In Russian). See also *eMetN* (2017), **2**, 95.

August 2022 in Ermelo, The Netherlands: a very successful Perseids campaign

Koen Miskotte

Dutch Meteor Society, the Netherlands
k.miskotte@upcmail.nl

August 2022 became a splendid month for meteor observing. Never before the author could observe so often from the Netherlands: 18 nights (54.10 hours), 869 meteors counted. It was a successful campaign taking into account the fact that observations were made from the Netherlands and also despite the fact that there was a Full Moon around the Perseid maximum. Hopefully next year observing will take place again from a really dark location.

1 Introduction

After the observations in Northern France at the end of May and early June, the visual observations temporarily stopped. The author had to undergo a major surgery on July 6th. Recovery at home would take 2 months. In this case, a wisdom from the famous Dutch footballer Johan Cruijff applies: *elk nadeel heeft zijn voordeel* (translated: every disadvantage has its advantage)! In my case the advantage was that I had all the time to observe the Perseids. The weather during this period was very sunny and this resulted in quite a few clear nights, especially in August. Unfortunately, the Full Moon was a bummer around the Perseid maximum. Nevertheless, the author was able to observe during a record number of hours in August. The author has never observed so many hours in August from the Netherlands since 1980! Most observations were done on the Groevenbeekse Heide (a heath south of Ermelo).

2 Observations

After the Full Moon on July 14, observation activities could resume. Soon a clear night presented itself:

2022 July 19–20

A short session because of the rapidly rising waning Moon. This 1.5-hour session yielded the first Perseids and Capricornids. A blue-green 0 Capricornid was the most beautiful meteor during this session. After a period with many nights that were cloudy or partly clear (cirrus), it was possible to observe again in the night:

2022 July 29–30

The start of this session was great with a crystal-clear sky and high transparency. Scorpius was visible in the southwest, Saturn shone nice in the southeast, and Jupiter appeared above the horizon a little later. And a little later, the Pleiades with Mars nearby were visible again. A single tuft of cirrus was visible here and there, but these disappeared quickly. The southern wind blew very weakly and initially kept the fog away. The temperature also dropped quickly at ground level to 6 degrees Celsius. Later in the night it became increasingly foggy causing varying limiting magnitudes between 6.0 and 6.4. There was a funny incident when I observed an SDA and recorded the data on my dictaphone: a bird flew right past my face: I got slapped by the wing in my face! It happened so fast I had no idea what kind of bird it was! Observing exactly 4 hours resulted in 56 meteors, of which 9 Perseids, 8 Southern delta Aquariids and 4 Capricornids. The most beautiful meteors were a –1 Southern delta Aquariid and a 0 Perseid and a 0 sporadic meteor (SPO). After a few more or less cloudy nights, the night 2–3 August was clear again:

2022 August 2–3

The Moon had now become an evening apparition, but that is no problem in August, as it set at 21^h00^m UT. A quiet night, only the sound of an owl in the woods can be heard. The observations started at 21^h40^m UT: it was beautifully clear weather with a Milky Way visible from Cassiopeia to above Sagittarius. SQM 20.50, which is a good value for Ermelo standards. Limiting magnitude rose to over 6.4. Thanks to the dry air there was no problem with fog, unfortunately some thin cirrus floated in after 01^h10^m UT. The temperature dropped to 13 degrees Celsius, which is quite high at the beginning of August.

4.1 hours of observation yielded 82 meteors, of which 19 Perseids, 10 Southern delta Aquariids, 5 Capricornids and 5 Antihelions. The SDAs were remarkably active between 23^h and 01^h UT with 4 meteors every hour. They were also striking in brightness, for example, a beautiful blue-white SDA of magnitude –2 was visible at 23^h56^m UT, and a minute later another +1 SDA appeared.

The Perseids were also active with hourly counts increasing from 2 to 7. At 23^h36^m UT a nice –1 Perseid was seen and at 00^h25^m UT another one of –2. All in all, it was a fun night!

This day, it was also clear that we were heading for a heatwave in the period around the Perseid maximum. Fortunately, the nights until August 14 were still relatively cool and the air was also very dry.

2022 August 5–6

This was also a beautiful clear night. It was striking that the Weather&Radar app predicted some clouds just northeast of Ermelo. Indeed, it did, and for most of the night cloud

cover remained visible in low northeasterly direction moving in the southeasterly direction. Also, the clouds eventually moved a little higher in the sky during the period 00^h43^m and 01^h44^m UT.

The SQM values were slightly lower than the previous clear night, but the limiting magnitude topped again at 6.4. Thanks to the combination of dry air and no wind, it cooled down very quickly. From 5 degrees Celsius at the start to 0 degrees Celsius at the end of the session! In the end, however, low sharply defined ground fog was formed, a beautiful sight and, thanks to the slightly higher location of the author, it remained below the field of view. Observations were done between 21^h40^m to 02^h05^m UT. The moon soon disappears at 22^h15^m UT. In total, 79 meteors were counted during 4.35 hours effectively.

The SDA were now clearly less active with 7 meteors and hourly counts of up to 2. The Perseids were comparable to the previous night: up to 9 Perseids per hour. A total of 28 Perseids, 5 Antihelions, 3 Capricornids and 1 kappa Cygnid completed the list. Two Perseids were the most beautiful meteors: at 22^h38^m UT a nice –3 in Perseus with 3 seconds of persistent train, and at 00^h32^m UT a 0 Perseid with a persistent train of 2 seconds. The following nights remained clear and this session turned into a real observation marathon.

2022 August 6–7

Unfortunately, the author overslept. Just after 1^h UT I woke up. So, I quickly decided to observe on the meteor roof at home. For example, an hour could be observed between 01^h21^m and 02^h22^m UT. That was definitely worth it with 21 meteors of which 12 Perseids, 1 SDA and 2 ANT. Two Perseids of –2 were the highlights at 01^h28^m and 01^h56^m UT.

Figure 1 – Perseid fireball magnitude –6 in the Big Dipper on August 6, 2022 at 22^h56^m UT. EN908, Canon 6D with Sigma 8mm F3.5 fish-eye lens. Shutter: 50/50, 16 breaks per second.

2022 August 7–8

This night went differently than expected. For starters, the sky background was quite light and there was fog. The limiting magnitude decreased from 6.3 to 6.0. The western parts of the sky were completely filled with cirrus moving from northwest to south, but these seemed to miss Ermelo at first. I signed on at 22^h29^m UT, the Moon set at 23^h10^m UT. However, after 00^h17^m the fog and cirrus increased rapidly and I had to stop this session. For 1.72 hours 28 meteors were counted of which 12 Perseids, 1 Southern delta Aquariid, 1 Capricornid and 1 kappa Cygnid. Best meteors were: two Perseids of magnitude 0 and –1, but a bright green slow-moving –2 Capricornid was the absolute highlight of this session. A pair of meteors appeared in quick succession at 23^h03^m UT (–1, fast in Cassiopeia) and at 23^h14^m UT (+1 in Pegasus). I classified the first as a Perseid but immediately there was doubt, the track was quite long. The second meteor appeared in the square of Pegasus with a direction from Algol (beta Persei). So: were these beta Perseids? Unfortunately, nothing more appeared and even afterwards looking in CAMS data of that night there was little to see in that area.

2022 August 8–9

More and more moonlight was present, moonset around 0^h UT, but luckily it disappears behind the trees at 23^h UT. That did yield some gains in terms of limiting magnitude. The limiting magnitude rose from 6.0 to 6.4 before falling again. At the beginning of the session, I thought back to the possible beta Perseids from the previous night. But oups, something is wrong with the constellation Perseus: Algol is noticeably weaker than normal. That's right, the star was at a minimum around 22^h UT. Thanks to the transparency, quite a few meteors were still counted: 62 in total in 3.37 hours of effective observation time. 38 Perseids, 2 Southern delta Aquariids, 1 Capricornid, 1 kappa Cygnid and 2 Antihelions. A –2 Perseid and –1 sporadic meteor were the highlights of this session.

2022 August 9–10

Wow, it was clear again... Session started at 23^h09^m UT. In the meantime, the Moon was already a very disturbing light source and set around 1^h05^m UT. Fortunately, she disappeared behind the trees around 00^h05^m UT. The sky was very transparent. The limiting magnitude was a bit disappointing despite the transparency. Limiting magnitude increased from 5.8 to 6.3.

In 3.28 effective hours, 66 meteors were counted. The Perseids were doing well with 34 meteors with the highest hourly count of 15 meteors. Furthermore, 2 Southern delta Aquariids, 1 Capricornid, 1 kappa Cygnid and 1 Antihelion were counted. A Perseid of –2 and a 0 Capricornid were the most beautiful appearances.

2022 August 10–11

This was the first session with moonlight all night long. Limiting magnitude increased from 5.4 to 5.8. The author has no dislike of observing meteors with moonlight, it gives the observation something special. During 2.60 hours 49 meteors were still counted, most of them Perseids (37). The maximum 30-minute count was 11. Three beautiful meteors were seen, the first a yellow-green –2 Capricornid passing just below Jupiter. A quick sporadic meteor of 0 left a 2 second glowing train and the very last meteor of this session was a sporadic beauty of –3, moving from Aries to the Pleiades.

Table 1 – Overview of the visual observations made in Ermelo (5.4 east, 52.2 north in the Netherlands) by the author.

Date	Start UT	End UT	$T_{eff.}$ Hr.	Lm	PER	SDA	CAP	GDR	KCG	AUR	ANT	SPO	TOT	Location	Remarks & fireballs
19–20/7	21^h44^m	23^h16^m	1.50	6.22	2	0	3	1	~	~	1	9	16	Heath	
29–30/7	21^h25^m	1^h30^m	4.00	6.22	9	8	4	0	~	~	~	35	56	Heath	Foggy
02–03/8	21^h40^m	1^h41^m	4.10	6.36	19	10	5	~	1	~	5	42	82	Heath	
05–06/8	21^h40^m	2^h05^m	4.35	6.35	28	7	3	~	1	~	5	35	79	Heath	Last hour fog, –3 PER
06–07/8	1^h21^m	2^h22^m	1	6.13	12	1	0	~	0	~	2	6	21	Home	Hazy sky
07–08/8	22^h29^m	0^h17^m	1.72	6.24	12	1	1	~	1	~	0	13	28	Heath	Increasing fog/cirrus
08–09/8	22^h50^m	2^h16^m	3.37	6.25	38	2	1	~	1	~	2	18	62	Heath	Moon until 0^h UT
09–10/8	23^h09^m	2^h30^m	3.28	6.09	34	2	1	~	1	~	1	27	66	Heath	Moon until 1^h UT
10–11/8	23^h45^m	2^h21^m	2.6	5.58	37	0	1	~	0	~	0	11	49	Heath	Moonlight
11–12/8	23^h36^m	2^h06^m	2.5	5.58	36	1	0	~	0	~	1	5	43	Heath	Full Moon
12–13/8	21^h45^m	2^h30^m	4.65	5.68	89	3	0	~	0	~	0	15	107	Home	Full Moon, –5 PER, –4 SPO
13–14/8	1^h00^m	2^h51^m	1.83	5.7	25	1	0	~	1	~	1	10	38	Home	Moon, –3 PER
18–19/8	20^h40^m	22^h13^m	1.5	6.21	2	~	~	~	0	~	2	10	14	Heath	Moon after 21^h20^m UT
20–21/8	20^h29^m	23^h31^m	3	6.3	4	~	~	~	1	0	6	24	35	Heath	Moon after 22^h15^m UT
24–25/8	23^h00^m	2^h18^m	2.52	6.25	2	~	~	~	0	1	5	26	34	Heath	Cloud fields
27–28/8	22^h25^m	2^h35^m	4.1	6.34	4	~	~	~	1	1	7	34	47	Heath	Last hour fog, –3 SPO
29–30/8	23^h20^m	3^h06^m	3	6.25	~	~	~	~	0	3	4	30	37	Heath	Cloud fields
31–01/8	21^h51^m	3^h05^m	5.08	6.34	~	~	~	~	2	9	7	37	55	Heath	
18 sessions			54.1		353	36	19	1	10	14	49	387	869	2 loc.	

2022 August 11–12

This one became a bit a strange night. Observations were again done on the Groevenbeekse Heide. But somehow there was little contrast in the sky. Perhaps caused by damp or dust, because the evening before I saw faint yellowish bands in the sky. The Moon was shielded by a bag. With the Moon above the horizon all night, a short session was held. The session started at 23^h36^m and ended at 02^h06^m UT. During these 2.50 hours effective I counted 43 meteors. Maximum 30-minute count was 10. A Perseid of –2 low in the southeast was the most beautiful meteor.

2022 August 12–13

Figure 2 – Perseid of magnitude –5 in the Big Dipper on 2022 August 13, 00^h47^m UT. Camera: EN908, Canon 6D with Sigma 8mm F 3.5 fish-eye lens. Shutter: 50/50, 16 breaks per second.

Figure 3 – The brightest Perseid fireball of 2022 August 12–13, at 01^h19^m UT low in the southwest. Camera: EN908, Canon 6D with Sigma 8mm F 3.5 fish-eye lens. Shutter: 50/50, 16 breaks per second.

Due to the low contrast the night before, I decided to observe this and the following night on the meteor roof at home. There, the Moon stays nicely behind the eaves. Indeed, the contrast and transparency were a lot better than the previous night. Observations started at 23^h36^m UT. The limiting magnitude was 5.8 at the start, then decreased to 5.4 and rose again to 5.7 at the end of the night. This session took place between 21^h45^m and 02^h30^m UT.

Immediately at the start two bright Perseids: a +1 and a –2. Activity was decent considering the almost Full Moon. 30-minute counts increased from 5 to 15 over the course of the night. A total of 107 meteors were seen. Two fireballs: at 00^h37^m UT a short sporadic meteor with flare –3 a –4 low west and at 00^h47^m UT a nice –5 Perseid in the Big Dipper, with a persistent train for 8 seconds. The bright fireball captured with my all-sky camera EN908 at 01^h19^m UT was not seen, but it was captured by the all-sky. From the author's point of view, the fireball appeared behind the neighbor's chimney. In addition to the many Perseids of –1 and –2, a beautiful SDA was also seen. This yellow meteor reached a maximum magnitude of 0 and showed fragmentation at the end in the form of a glitter wake 1 to 2 degrees long.

2022 August 13–14

In the evening some clouds appeared over Ermelo. This, the fatigue of the many nights without too much sleep and a party that evening made the author decide not to observe this night. Turns out the clouds disappeared soon. When I saw that the sky was cloudless at 00^h45^m UT I quickly went up the meteor roof. Good transparency and contrast! A quick session between 01^h00^m and 02^h51^m UT resulted in 38 meteors. A beautiful –3 Perseid was the highlight.

Figure 4 – Perseid fireball magnitude –4 in Pegasus on August 13, 20^h32^m UT. EN908, Canon 6D with Sigma 8mm F3.5 fish-eye lens. Shutter: 50/50, 16 breaks Perseid's second.

2022 August 18–19

A short session from the moors. The Moon rose quickly, this short session yielded 14 more meteors of which 2 Perseids and 2 Antihelions.

2022 August 20–21

A 3.00-hour session with moonlight during the last hour. A total of 35 meteors are counted amongst them 4 Perseids, 1 kappa Cygnid and 6 Antihelion. The most beautiful is a +1 sporadic meteor.

2022 August 24–25

A long session, but hampered with passing clouds. In terms of conditions a moderate night, a light sky background and twice observations had to be stopped for a long time due to slowly passing cloud fields. A beautiful blue-white magnitude 0 sporadic meteor moved parallel to the northeast horizon through the constellation of Gemini. In total, 2.52 hours of observations yielded 34 meteors, of which 2 Perseids, 5 Antihelions and 1 Aurigid.

2022 August 27–28

A long period of observations of 4.10 hours yields 47 meteors of which 4 Perseids, 1 Aurigid, 1 kappa Cygnid and 7 Antihelions. Three sporadic meteors of magnitude 0, –1 and –3 were the highlights of this session.

2022 August 29–30

A nice session which was interrupted for 45 minutes after the first hour by a passing cloud field. 37 meteors were seen, of which 3 Aurigids and 4 sporadic meteors. A beautiful blue-yellow Aurigid of magnitude 0 was the most beautiful meteor. At 02^h36^m UT I observed an elongated string of "Mosquitoes" that appeared in the constellation Taurus: The Starlink Satellites of Space X. I watched the scene with mixed feelings. On the one hand it was a beautiful sight, on the other hand launching many thousands of satellites is also very, very controversial

2022 August 31–1 September: The Aurigid maximum

In anticipation of an expected small outburst of the Aurigids on September 1, 00^h55^m UT (see IMO Meteor Calendar 2022), observations were done between 21^h51^m and 03^h05^m UT (5.08 effective hours). Visually no extra activity was seen around the time mentioned. Aurigid activity remained at a normal level with hourly counts between 1 and 3. Few bright meteors, a nice +1 Antihelion and a +1 sporadic meteor were the best events. A total of 55 meteors were seen of which 9 Aurigids, 2 kappa Cygnids and 7 Antihelions.

Perseids from Brokerudhagan, Norway

Kai Gaarder

Søndre Ålsvegen 698A, N-2740 Roa, Norway
kai.gaarder@gmail.com

A summary is presented of the series visual observations carried out by the author during the Perseid maximum, at Brokerudhagan, Norway.

1 2022 August 11–12

After returning from a successful Southern delta Aquariid campaign under very dark skies in Crete, it was a bit of a downturn to return to Full Moon observations under a still bright summer sky in Norway. A good weather forecast still inspired me to try to observe the pre-maximum night of the Perseids. The sky was bright towards the horizon in all directions, leaving only a small part of the sky towards the zenith reasonable dark, with a *lm* of 5.26 at the start of the observation. The Full Moon was low in the southern sky, but behind my back and field of view.

After 4 minutes of observation, I became aware of a slow moving, yellow/red sporadic meteor of mag +1 that glided through Ursa Major, leaving multiple fragments in its path. After 10 minutes the first Perseid was seen, a beautiful, yellow, –2 mag in Cepheus. Two more bright Perseids of mag +0 were seen during the first hour, and the total count came in at 8.

In the next hour the *lm* in zenith improved slightly to 5.36. Perseid rates kept steady and came in at 10, with a –1 and a +0-magnitude meteor as the brightest events.

In the third hour morning twilight was already approaching, but still a *lm* of 5.26 could be obtained in the zenith. 9 Perseids could be seen this hour, with a –1 and a +0-magnitude meteor as highlights.

Despite the bright sky conditions, it proved worth to sacrifice a night of good sleep to observe the pre-maximum night of the Perseids. Some really nice meteors were seen, and it was a special feeling to lay out in the field observing meteors in the bright moonlight.

A total of 35 meteors were seen during 3 hours of observation. Of these were: 27 PER, 8 SPO, and 0 KCG.

Observed showers:

- Perseids (007 PER)
- Kappa Cygnids (012 KCG)

21^h50^m – 22^h50^m. T_{eff}: 1.00, *F*: 1.00, *lm*: 5.26, RA: 330, DEC: +75

- PER: 8 meteors. –2, +0(2), +1, +2, +3, +4, +5
- SPO: 2 meteors. +1(2)
- KCG: 0 meteors.

22^h50^m – 23^h50^m. T_{eff}: 1.00, *F*: 1.00, *lm*: 5.36, RA: 330, DEC: +75

- PER: 10 meteors. –1, +0, +1, +2, +3(4), +4(2)
- SPO: 3 meteors. +2, +3(2)
- KCG: 0 meteors.

23^h50^m – 00^h55^m. T_{eff}: 1.00 (5 minutes break), *F*: 1.00, *lm*: 5.26, RA: 330, DEC: +75

- PER: 9 meteors. –1, +0, +1(2), +2(2), +4, +5(2)
- SPO: 3 meteors. +3(2), +5
- KCG: 0 meteors.

2 2022 August 12–13

The observation of this year's Perseid maximum had to be delayed half an hour due to clouds. That left only 2.5 hours suitable for meteor observations before morning twilight. The Moon was higher in the sky than the night before, making the sky even brighter. I still wanted to give this year's Perseid maximum a chance, and started to make observations under a bright but cloudless sky at 22^h30^m UT. The count for this night is given in 30-minute periods.

The first half hour period gave Perseid rates of 5, close to the activity level from the night before. A brilliant –2 mag Perseid with a smoke train close to the radiant in Cassiopeia, was the highlight of the period.

In the next 30-minute period, activity level rose to 9 meteors, a clear step up in activity from the previous night. The brightest Perseid seen in this period was of magnitude +0.

In the third period activity was quite constant with 8 meteors seen. Most of the Perseids seen in this period were between mag –1 and +2. At 00^h03^m UT a brilliant, slow moving sporadic meteor with a final flare of mag –3 glided through Ursa Major. This meteor may have been an alpha Capricornid, but it was impossible to determine the radiant precisely because of the lack of visible stars in the brightly moonlit southern horizon.

The fourth period gave the best counts of the night, with 11 Perseids seen. Most of the meteors were between mag +0 and +3, with no really bright events.

The last 30-minute period the sky was becoming even brighter with a *lm* of 5.12. 7 Perseids were seen in this

period, with the brightest meteor being a –1 mag in Cassiopeia.

It is difficult to rate this Perseid maximum due to the bright observing conditions. Anyway, I have the impression of a modest activity level, with an almost total lack of meteors brighter than –1. Despite the bright moonlight, I got an impression of the strength of the maximum and gathered some memorable moments worth the sacrifice of a night sleep.

A total of 49 meteors were seen in 2.5 hours of observation. Of these were: 40 PER, 9 SPO, and 0 KCG.

Observed showers:

- Perseids (007 PER)
- Kappa Cygnids (012 KCG)

22^h30^m – 23^h00^m. T_{eff}: 0.500, *F*: 1.00, *lm*: 5.26, RA: 330, DEC: +75

- PER: 5 meteors. -2, +0, +1, +4(2)
- SPO: 2 meteors. +5(2)
- KCG: 0 meteors.

23^h00^m – 23^h30^m. T_{eff}: 0.500, *F*: 1.00, *lm*: 5.26, RA: 330, DEC: +75

- PER: 9 meteors. +0, +1(2), +2, +3(3), +4(2)
- SPO: 1 meteor. +2
- KCG: 0 meteors.

23^h30^m – 00^h05^m. T_{eff}: 0.500 (5 minutes break), *F*: 1.00, *lm*: 5.26, RA: 330, DEC: +75

- PER: 8 meteors. -1, +0(2), +1(3), +2, +5
- SPO: 4 meteors. -3, +1, +3(2)
- KCG: 0 meteors.

00^h05^m – 00^h35^m. T_{eff}: 0.500, *F*: 1.00, *lm*: 5.17, RA: 330, DEC: +75

- PER: 11 meteors. +0, +1(4), +2(2), +3(2), +4, +5
- SPO: 2 meteors. +0, +5
- KCG: 0 meteors.

00^h35^m – 01^h05^m. T_{eff}: 0.500, *F*: 1.00, *lm*: 5.12, RA: 330, DEC: +75

- PER: 7 meteors. -1, +0(2), +1(2), +3(2)
- SPO: 0 meteors
- KCG: 0 meteors.

Late Summer from Brokerudhagan, Norway

Kai Gaarder

Søndre Ålsvegen 698A, N-2740 Roa, Norway
kai.gaarder@gmail.com

A summary is presented of the series visual observations carried out by the author during late August and September, at Brokerudhagan, Norway.

1 2022 August 27–28

After observing the maximum of the Perseids under a bright moonlit sky, I was looking forward to observing the Aurigids under dark skies. My first chance came on August 27, and after some hours of early sleep, I went out to my observing field some 200 meters uphill from my house. The air was calm and humid, and the temperature was +14 degrees Celsius. After putting up my observation gear, I could enjoy a clear and transparent sky, with a weak Aurora Borealis in the north, too faint to cause any problems.

I started my observation 22^h00^m UT, and a +4-mag sporadic was instantly seen in the first minute of observation. After that a steady flow of faint sporadic meteors continued throughout the hour, ending at 11 meteors. An exception from the faint meteors came after 55 minutes, when a +1-mag sporadic with a smoke train appeared in Taurus. The highlight of the first hour was a red +0-mag ANT that started in Pegasus and glided slowly through Cepheus before ending its long path in Ursa Major. One possible AUR was seen the first hour at 22^h49^m UT, when a yellow meteor of mag +1 shot into Ursa Major.

The second hour started very slowly, and the first meteor was seen only after 17 minutes, when a brilliant, slow, white sporadic meteor of mag –1 glided through Draco. Considering its path, velocity, and length from the radiant, this meteor may have been a zeta Draconid (Robert Lunsford – Meteor Activity Outlook 27. August – September 2, 2022[12]). No Aurigids were seen this hour, and the sporadic count came in at 9 meteors.

The third and final hour yielded 8 sporadic meteors, among them a brilliant +0-mag with a smoke train in Taurus. Another swift, yellow, +1-mag meteor was also seen near the Pleiades. No Aurigids were seen this hour either, and I ended my observation at 01^h05^m UT. During the observation the temperature had dropped 4 degrees to +10, and my sleeping bag was dripping wet from the humid conditions as I walked downhill to my house for some hours of early morning sleep.

A total of 31 meteors were seen during 3 hours of observation. Among these were: 28 SPO, 2 ANT, and 1 AUR.

Observed showers:

- Aurigids (206 AUR)
- Antihelion source (ANT)

22^h00^m – 23^h00^m. T_{eff}: 1.00, F: 1.00, lm: 6.19, RA: 0.00, DEC: +60

- SPO: 11 meteors. +1, +3(2), +4(5), +5(3)
- AUR: 1 meteor. +1
- ANT: 1 meteor. +0

23^h00^m – 00^h00^m. T_{eff}: 1.00, F: 1.00, lm: 6.23, RA: 15, DEC: +60

- SPO: 9 meteors. –1, +2, +3(2), +4(3), +5(2)
- AUR: 0 meteors.
- ANT: 0 meteors.

00^h00^m – 01^h05^m. T_{eff}: 1.00 (5 minutes break), F: 1.00, lm: 6.23, RA: 30, DEC: +60

- SPO: 8 meteors. +0, +1, +2, +3(2), +4(2), +6
- AUR: 0 meteors.
- ANT: 1 meteor. +2

2 2022 August 29–30

This was the second night of Aurigid observations from my homeplace in Norway. The night arrived with a very transparent sky, and I hoped to observe an increase in the Aurigid rates from 2 nights ago. Some thin drifting clouds were present in the outskirts of my observing field the first hour, but not imposing a real problem.

After only 3 minutes, a beautiful, yellow/red, slow, –1-mag sporadic meteor glided through Cepheus. 13 minutes later there was time for another bright meteor, when a white, slow, –1-mag Antihelion appeared in Pisces. Only 6 minutes after this bright event, a red, medium speed, sporadic meteor of mag –1, streaked out from Cepheus towards Draco! The good observing conditions also

[12] https://www.meteornews.net/2022/08/26/16015/

allowed me to see the fainter meteors, and the sporadic rate the first hour came in at 10. 1 Aurigid of mag +4, and 2 Antihelions, were also seen this first hour.

The next hour the sky conditions improved further when the thin drifting clouds disappeared. The Aurigids stole the show the first minutes of the hour. After 2 minutes a +2 mag Aurigid shot through Aries. Only 4 minutes later a stunning, yellow, –2-mag Aurigid streaked from Andromeda into Pegasus, leaving a smoke train for 3 seconds. Another nice meteor appeared at 23^h38^m UT, when a +0-mag, yellow, fast moving sporadic, shot from Cassiopeia into Cygnus. A total of 12 sporadic meteors were seen this second hour, alongside with the 2 Aurigids mentioned.

The third hour started with a +1-mag Aurigid in Cassiopeia after only 4 minutes. This was the only Aurigid seen this hour. The sporadic rate climbed to 14, with a yellow, +0-mag meteor with a smoke train in Pegasus, as the brightest event. Also 1 meteor from the Antihelion source was seen this last hour. Altogether it had been an enjoyable night with good observing conditions, a good portion of bright meteors, and high sporadic rates!

A total of 43 meteors were seen during 3 hours of observation. Among these were: 36 SPO, 3 ANT, and 4 AUR.

Observed showers:

- Aurigids (206 AUR)
- Antihelion source (ANT)

21^h55^m – 22^h55^m. T_{eff}: 1.00, *F*: 1.00, *lm*: 6.19, RA: 0.00, DEC: +60

- SPO: 10 meteors. –1(2), +3(2), +4(4), +5, +6
- AUR: 1 meteor. +4
- ANT: 2 meteors. –1, +5

22^h55^m – 00^h00^m. T_{eff}: 1.00 (5 minutes break), *F*: 1.00, *lm*: 6.23, RA: 15, DEC: +60

- SPO: 12 meteors. +0, +1, +3(4), +4(3), +5(2), +6
- AUR: 2 meteors. –2, +2
- ANT: 0 meteors.

00^h00^m – 01^h00^m. T_{eff}: 1.00, *F*: 1.00, *lm*: 6.23, RA: 30, DEC: +60

- SPO: 14 meteors. +0, +1, +2, +3(2), +4(5), +5(3), +6
- AUR: 1 meteor. +1
- ANT: 1 meteor. +4

3 2022 August 31 – Sepember 1

The long-awaited maximum night of the Aurigids showed up with excellent weather. Some excitements were attached to whether the Aurigids would show a minor enhancement around 00^h55^mUT as predicted by Sato (2021). I had decided to do observations for 4 hours, starting at 21^h45^m UT. No Aurigids were seen the first hour with the radiant quite low in the sky, but a decent rate of 9 sporadic meteors were seen.

In the second hour 7 sporadic meteors were seen. The brightest of these meteors may in fact have been a late kappa Cygnid. It appeared at 23^h24^m UT, when a –2-mag, yellow/red, slow-moving meteor glided from Cygnus into Lacerta. The first Aurigid of the night appeared at 23^h30^m UT, with a white, fast meteor in Aries.

After a short break, the real excitement started in the third hour as we got closer to the time of the predicted enhancement. At 00^h03^m the first Aurigid of the hour appeared with a +2-mag, yellow meteor in Ursa Minor. At 00^h24^m UT a +0-mag, yellow Aurigid with a smoke train, streaked from Cepheus into Cygnus. 4 minutes before the time of the predicted enhancement, another +0-mag Aurigid flared up between Auriga and Gemini. I hoped this could be the start of an enhancement, but no more Aurigids were seen the next 15 minutes. Sporadic rates the third hour came in at 11.

The last hour Aurigid rates stayed at the same level as the previous hour, with 3 meteors seen. The Aurigids seen were still on the brighter side, with a –1 and a +1-mag meteor as highlights. The sporadic rate came in at 8, mostly with faint meteors. An exciting night had come to an end. No outburst was seen, but I had the joy to observe 43 meteors under good sky conditions, among them some bright events that will be remembered for some time!

A total of 43 meteors were seen during 4 hours of observation. Among these were: 35 SPO, 1 ANT, and 7 AUR.

Observed showers:

- Aurigids (206 AUR)
- Antihelion source (ANT)

21^h45^m – 22^h45^m. T_{eff}: 1.00, *F*: 1.00, *lm*: 6.23, RA: 0.00, DEC: +60

- SPO: 9 meteors. +1, +2, +3(3), +4, +5(2), +6
- AUR: 0 meteors.
- ANT: 0 meteors.

22^h45^m – 23^h45^m. T_{eff}: 1.00, *F*: 1.00, *lm*: 6.23, RA: 15, DEC: +60

- SPO: 7 meteors. –2, +3(2), +4(3), +5
- AUR: 1 meteor. +3
- ANT: 1 meteor. +2

23^h45^m – 00^h55^m. T_{eff}: 1.00 (10 minutes break), *F*: 1.00, *lm*: 6.23, RA: 30, DEC: +60

- SPO: 11 meteors. +0, +1, +3(3), +4(4), +5(2)
- AUR: 3 meteors. +0(2), +2
- ANT: 0 meteors.

00^h55^m -01^h55^m. T_{eff}: 1.00, *F*: 1.00, *lm*: 6.15, RA: 30, DEC: +60

- SPO: 8 meteors. +1, +3, +4(4), +5, +6
- AUR: 3 meteors. –1, +1, +4
- ANT: 0 meteors.

4 2022 September 5–6

The weather forecast for September 5–6 was excellent and provided a good opportunity to study the late Aurigids, the early September epsilon Perseids, and the mysterious chi Cygnids. The night came as promised with calm and clear weather, and temperatures around +10 degrees Celsius. As soon as I was ready to start my observations, the meteors started to flow. 5 meteors were seen during the first 7 minutes of the observation, among them a +2-mag, red, slow-moving chi Cygnid, moving from Cygnus towards Cassiopeia. 18 minutes later, another good candidate for this shower appeared with a +5-mag meteor in Cepheus. Also, the Aurigids showed activity the first hour, with a really nice +0-mag meteor that shot through Cassiopeia at 22^h34^m UT. My first September epsilon Perseid of the year came seconds later, with a +4-mag meteor in Perseus. Other highlights of the hour were a fast +2-mag Sporadic in Andromeda, and a long-pathed, red, +2-mag Antihelion meteor that crossed a great portion of the sky.

16 minutes into the second hour, a yellow, fast, +0-mag September epsilon Perseid, streaked from Auriga into Gemini. After some weaker Sporadic meteors, a fast, red, +1-mag Sporadic, flared up near the double cluster in Perseus. At 23^h35^m UT, a white, +2-mag Antihelion, glided into Perseus, making it the last meteor of the hour.

In the third hour, the steady Sporadic rates continued with 9 mostly faint meteors. Also, a +5-mag Aurigid, and a +5-mag September epsilon Perseid were seen. 2 meteors from the Antihelion region were also observed, among them a nice, white, slow moving meteor in Pegasus. With this, another night with good observing conditions and nice meteor activity had come to an end, and I could enjoy a couple of hours of sleep before going to work this Tuesday morning.

A total of 35 meteors were seen during 3 hours of observation. Among these were: 24 SPO, 4 ANT, 2 AUR, 3 SPE, and 2 CCY.

Observed showers:

- Aurigids (206 AUR)
- September epsilon Perseids (208 SPE)
- chi Cygnids (757 CCY)
- Antihelion source (ANT)

21^h45^m – 22^h45^m. T_{eff}: 1.00, *F*: 1.00, *lm*: 6.19. RA: 0.00, DEC: +60

- SPO: 8 meteors. +0, +2, +3(2), +4(3), +5
- SPE: 1 meteor. +4
- AUR: 1 meteor. +0
- CCY: 2 meteors. +2, +5
- ANT: 1 meteor. +2

22^h45^m – 23^h45^m. T_{eff}: 1.00, *F*: 1.00, *lm*: 6.23, RA: 15, DEC: +60

- SPO: 7 meteors. +1, +3, +4(2), +5(2), +6
- SPE: 1 meteor. +0
- AUR: 0 meteors.
- CCY: 0 meteors
- ANT: 1 meteor. +2

23^h45^m – 00^h55^m. T_{eff}: 1.00 (10 minutes break), *F*: 1.00, *lm*: 6.23, RA: 30, DEC: +60

- SPO: 9 meteors. +2, +3(2), +4(4), +5, +6
- SPE: 1 meteor. +5
- AUR: 1 meteor. +5
- CCY: 0 meteors.
- ANT: 2 meteors. +1, +4

UK radio meteor beacon project

John Berman

**Radio Astronomy Section of the British Astronomical Association (BAA),
Radio Society of Great Britain (RSGB) and The Mansfield and Sutton Astronomical Society**
Contact@ukmeteorbeacon.org

The following article describes the UK Radio Meteor Beacon Project current status and talks about Meteor Radio Basics, The Beacon and associated technical information and plans for the future of the project.

1 Introduction

The UK Meteor Beacon (call sign GB3MBA: 'Meteor Beacon for Astronomy') is a collaborative project between the UK amateur radio and radio astronomy communities, to facilitate the study of meteor events above the UK. Funding has been provided by the Radio Society of Great Britain (RSGB) Legacy Fund, while the Mansfield & Sutton Astronomical Society have kindly agreed to host the beacon at their Sherwood Observatory (*Figure 1*). Running costs will be supported by the radio astronomy community, and the beacon was built by amateur radio volunteers.

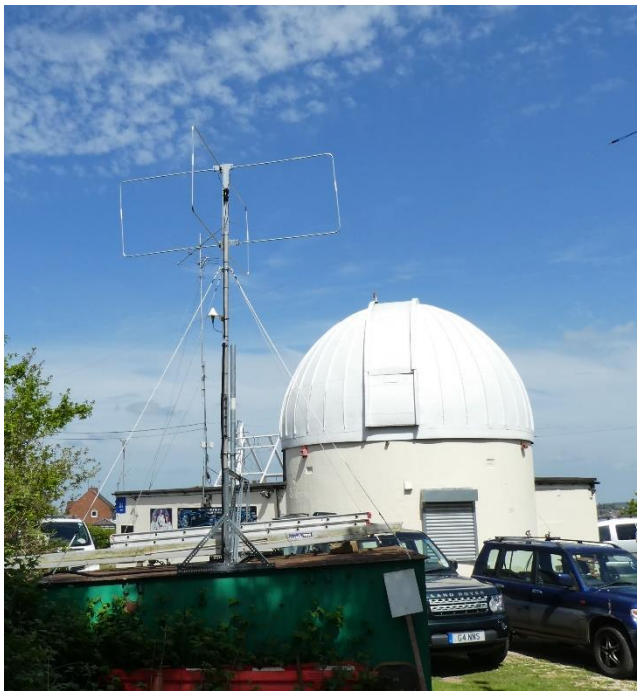

Figure 1 – The beacon installation at the Sherwood Observatory.

The beacon transmitter, operating on a frequency of 50.408MHz, is directed vertically upwards with a beam width sufficient to illuminate a region with a diameter of about 400km, centered above the observatory. This region is at an altitude of 90 to 100km, where meteors burn up due to friction with the atmosphere, briefly creating an ionized trail that is reflective to radio as they do so. Radio reflections from the ionized trails can be observed to a distance of about 1200km from the observatory. An advantage of making meteor observations by radio is that such observations are largely independent of weather conditions and can be made equally well by day and night. The operational status of the installation and further information can be found at the beacon website[13].

In addition to facilitating academic and citizen-science studies of meteors, a key aim of the project is to build on the widespread interest in space to develop STEM-related projects for schools, attracting young people into radio engineering and astronomy.

2 Meteor radio basics

My introduction to meteor observation by radio was through using reflections from the GRAVES radar in France[14]. Operating on 143.050MHz, just below the two-meter amateur band, I coupled my existing receiver with Spectran to provide a waterfall display and this sparked my interest in meteors[15]. Visitors to my radio room, seeing the echoes from meteors displayed on the computer screen, were also fascinated.

I then started to make observations using the BRAMS and VVS meteor beacons in Belgium[16], which operate on 49.970MHz and 49.990MHz, respectively. The observing experience at this longer wavelength (6m) was quite different to that using GRAVES, with a wavelength of 2m. This is in part due to differences in reflectivity with frequency/wavelength of the ionization created as meteors burn up, and partly due to geometry. But these systems provide few opportunities to observe meteor events above the UK, so the idea of creating our own UK beacon was born.

As meteors burn up, they briefly produce an ionized trail reflective to radio. This behaves like a wire following the

[13] http://ukmeteorbeacon.org/
[14] GRAVES: http://bit.ly/3BOzkLI
[15] Spectran V2: http://bit.ly/3RWMBaH
[16] BRAMS: http://bit.ly/3LngBdw

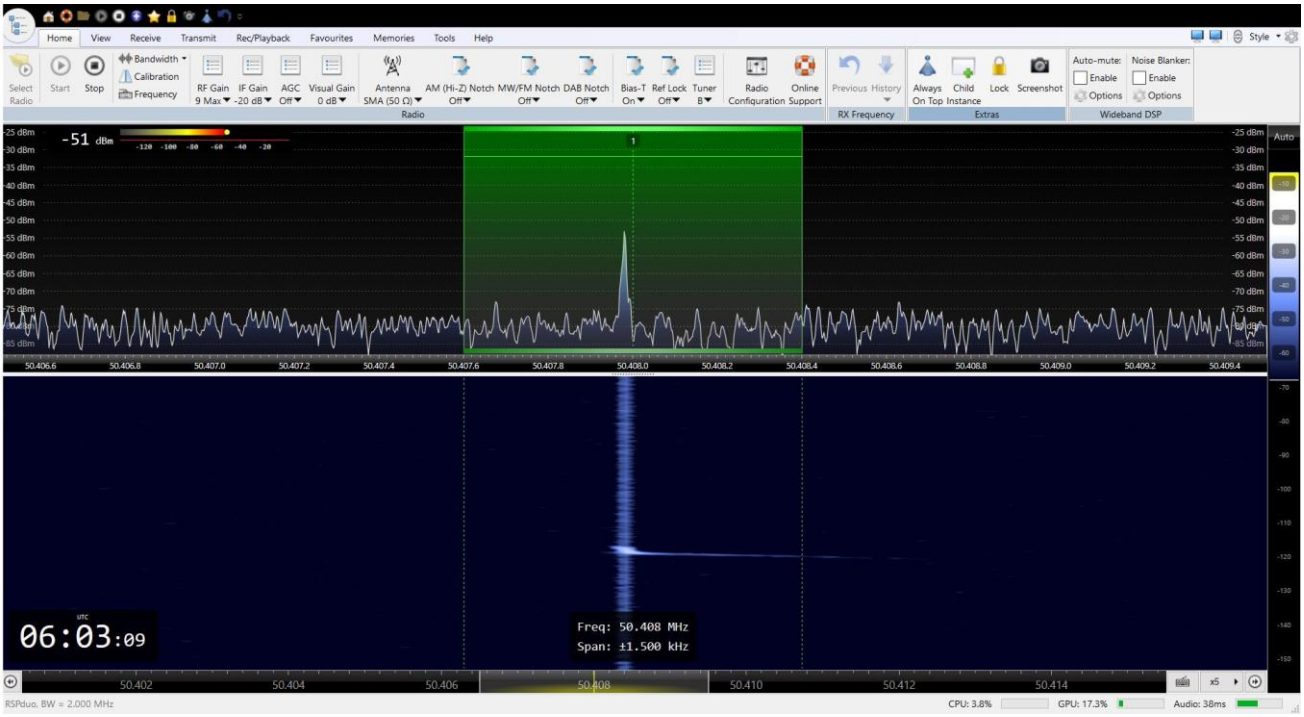

Figure 2 – A meteor head echo from GB3MBA, obtained with a direct signal from the beacon.

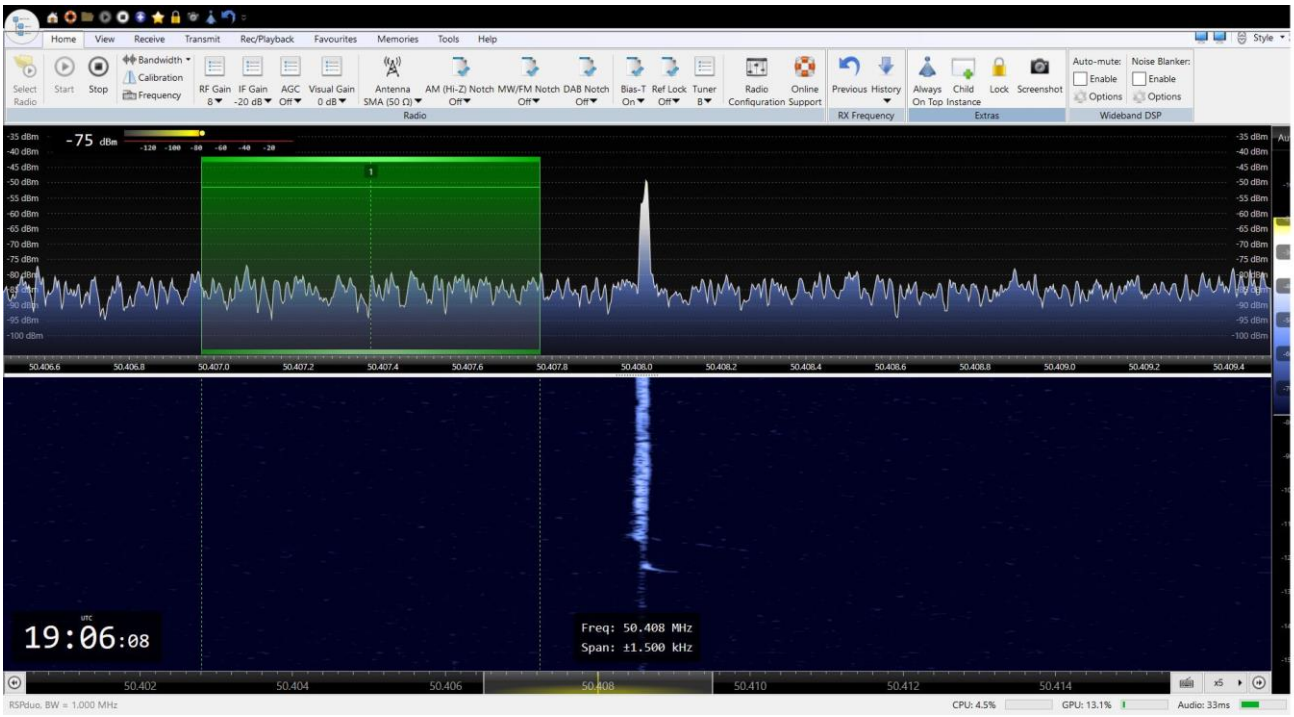

Figure 3 – A small head echo followed by a strong, long-lasting tail echo.

meteor and gives rise to reflections (echoes) known, slightly confusingly, as 'head echoes'. (See *Figure 2*). They are very brief – less than one second in duration – and exhibit rapid Doppler shift as the meteor is decelerated due to friction. Reflections from this thin trail of ionization are polarized and directional, so depending on the angle from which the trail is 'viewed', not all observers will see a head echo.

Passage of the meteor through this region of the ionosphere often triggers it to become sufficiently ionized, locally, to be reflective to radio for a longer period of time. Reflections from these regions are more or less isotropic, exhibit little Doppler shift and are known in astronomy circles as 'tail echoes'. (See *Figure 3*) It is reflections from these regions that are used by radio amateurs and others to extend the range of very-high-frequency (VHF) radio communications far beyond the horizon, a propagation mode known as meteor scatter (MS).

The head or fireball of most meteors has a radar cross-section too small to give echoes at this wavelength, while the reflective region giving rise to tail echoes has a larger volume, reflects more or less isotropically and may also have refractive properties. Reflections from different parts of the reflective volume give rise to some spectral spreading, as is the case with other scatter modes of radio

propagation. The small, relatively stable Doppler shift which is sometimes observed is due to wind.

Phase I of this project has been to build and deploy the beacon transmitter; this was accomplished on 2022 May 14. Phase II is to design and build a network of web-based receivers deployed to different locations, so that meteor events can be observed from multiple directions. Measurements of the Doppler shift of head echoes at a particular instant, observed from different directions, can then be used to calculate the location and trajectory of meteors. The amount of shift is a function of the rate at which the path from the transmit beacon to the meteor and onwards to the receiver is reducing, giving rise to a positive shift, or extending, giving a negative shift.

3 The beacon

The beacon (see *Figure 4*), which is licensed by Ofcom, transmits a continuous carrier with about 75W, identifying every 10 minutes or so by A1A keying (as required by its license). For its intended purpose any form of modulation is undesirable, as in Phase II of this project the carrier, which is generated by a precision GPS frequency reference, will be used to make precision Doppler measurements and modulation detracts from this.

Figure 4 – The beacon transmitter.

The output from the frequency reference passes through a filter and then drives the power amplifier (PA), which is rated for 100W continuous operation[17]. A four-port hybrid splits the power to two outputs with a 90-degree phase shift. This is required to generate circular polarization. Any imbalance between the antennas is fed to the fourth 'dump' port, which has a load monitored by a detector. If there is an antenna fault, the 'dump power' will increase, the transmitter will close down, and a fault condition will be reported. Circular polarization is used as the head echoes from meteors behave like a wire antenna and are polarized. It reduces the loss due to potential misalignment of polarization.

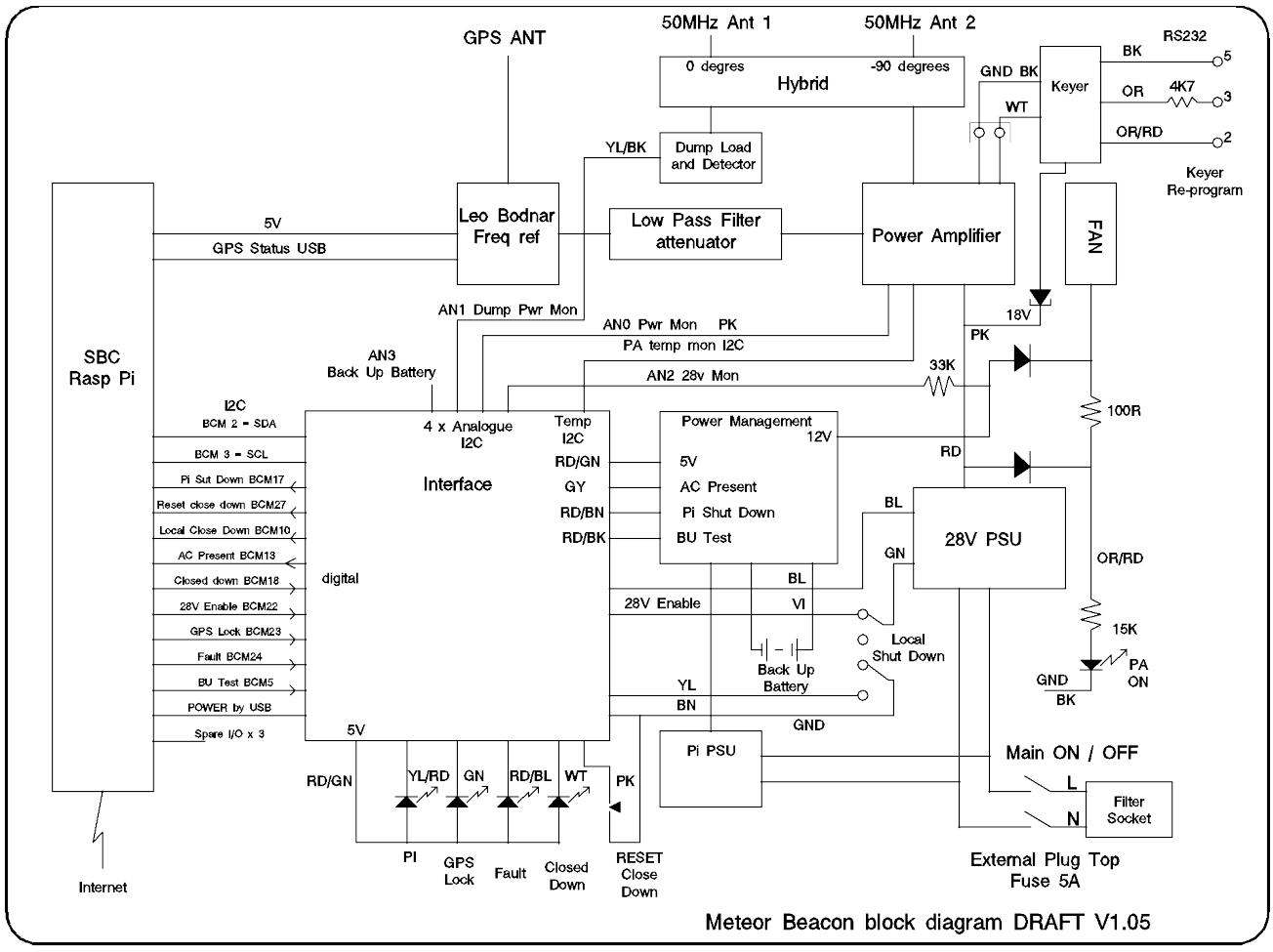

Figure 5 – Block diagram of the beacon transmitter.

[17] Leo Bodnar mini frequency reference: http://bit.ly/3UnTgw8

The beacon is monitored and controlled by a Raspberry Pi single-board computer, with interface circuits to monitor output power, dump power, PA voltage, PA temperature and back-up battery voltage. This battery ensures an orderly shut-down in the event of a power failure, but does not maintain beacon operation during a power cut. The Raspberry Pi also provides a web interface that can be viewed from the beacon website[18] (See *Figure 6*).

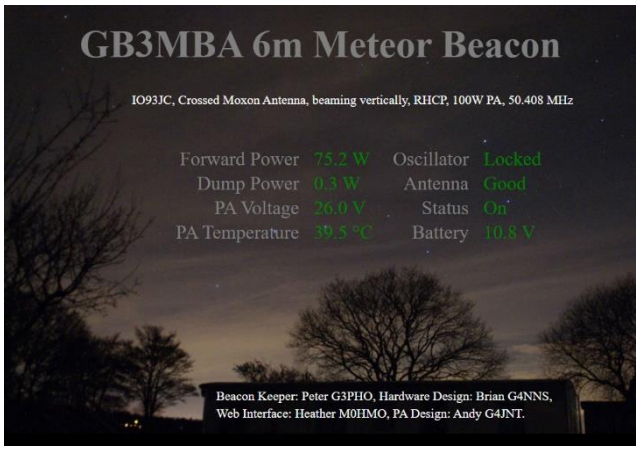

Figure 6 – The GB3MBA status page.

The beacon has been built by volunteers from the amateur radio community, including the author (call sign G4NNS), Andy Talbot (G4JNT) who built the PA, and Chris Bryant (G3WIE) who made the four-port hybrid. Monitor, control and web interface software has been written by Heather Nickalls (M0HMO).

4 The transmit antenna

Figure 7 – The beacon antenna.

The transmit antenna consists of two Moxon[19] antennas at right angles, fed with a 90-degree phase shift to generate right-hand circular polarization (*Figure 7*). The Moxon design was chosen as it is compact, with a very high front-to-back ratio and a broad beamwidth to illuminate the largest possible area above. Circular polarization is used as head echoes are linearly polarized and would sometimes be cross-polarized with a linear transmit antenna, resulting in little or no echo. It is not considered necessary to use circular polarization for receive, although this is an area that could benefit from further research.

5 Receivers

The best and most economical way of receiving and displaying radio echoes from meteors is to use a software-defined radio (SDR) connected to a PC. For my work so far, I use a FUNcube Dongle Pro Plus or RSP Duo together with SDR Console[20]; I recommend this kind of configuration as a starting point (see *Figures 2 and 3*).

For those who already have one, a conventional receiver covering 50.408MHz can be used with an audio spectrum display such as Spectran[3]. It is most convenient to display meteor echoes on a spectrum waterfall display.

To monitor GB3MBA, only a small bandwidth (e.g., ± 1.5kHz) centered on the transmit frequency of 50.408MHz is required. If you are thinking of establishing a receiver that can join the network proposed for Phase II of this project, you will need an SDR that can be locked to an external frequency reference, as precision Doppler measurements will be needed. The Phase II design team have yet to make a final decision on which SDR to use, but the RSPdx is under consideration at the time of writing.

6 Displaying meteor echoes

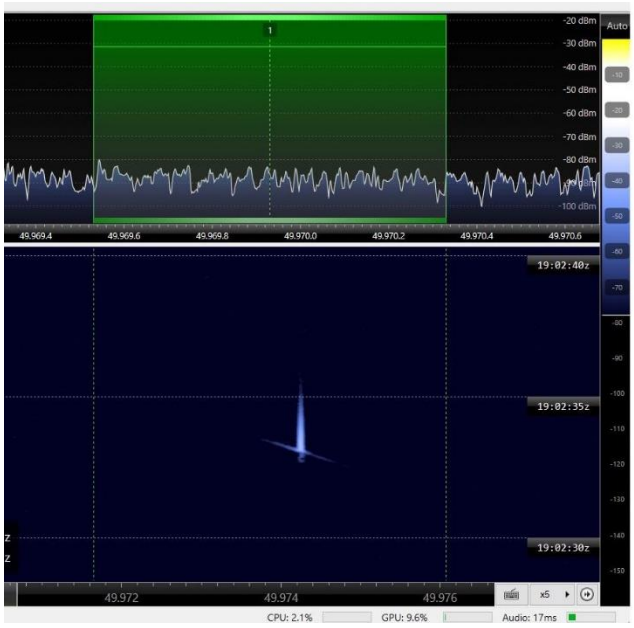

Figure 8 – A head and tail echo from BRAMS.

Figure 8 shows a meteor echo from BRAMS, as displayed by SDR Console. The upper portion of the display is a

[18] http://ukmeteorbeacon.org/Bstatus
[19] Moxon Design: http://bit.ly/3Sd4l1d
[20] SDR Console: http://bit.ly/3RUbvb5

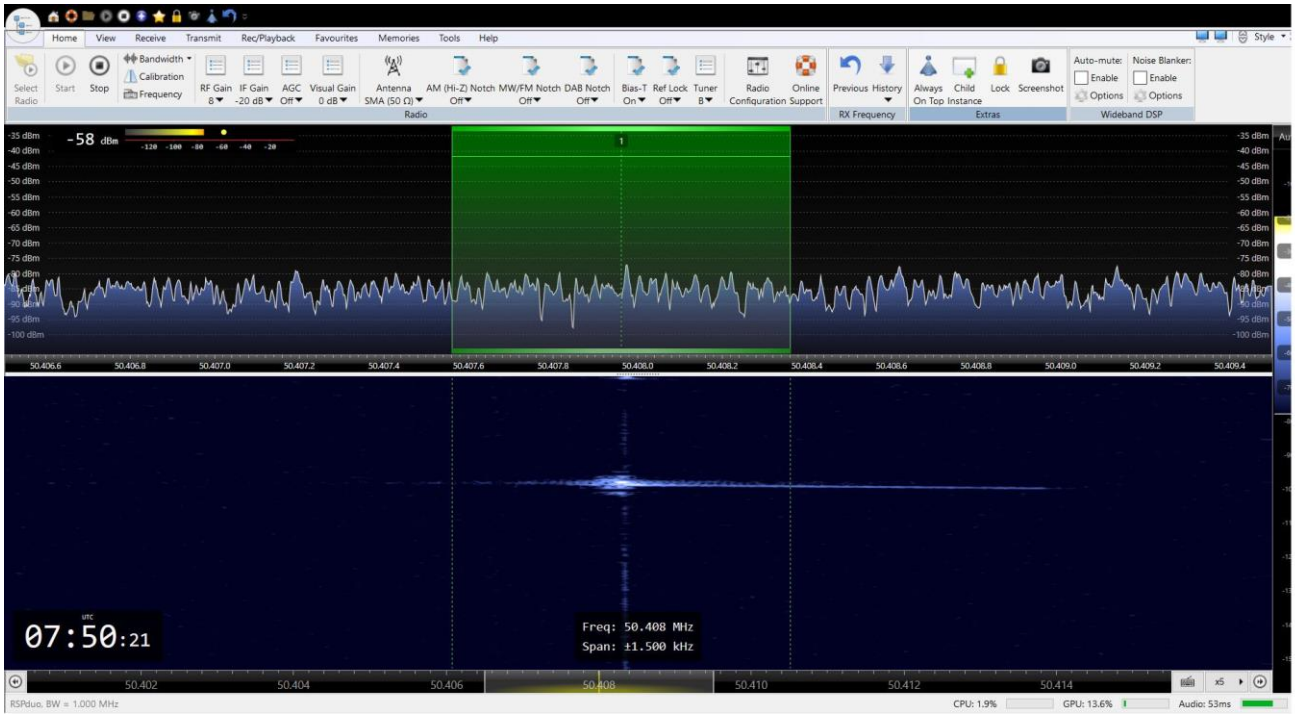

Figure 9 – A strong head echo, with a positive Doppler shift as the meteor approaches and then a negative shift as it recedes, before the trace disappears.

spectrogram showing amplitude vs. frequency; the wavy line represents the 'noise floor'. The lower portion is a waterfall display and shares the frequency scale with the spectrogram above. The amplitude of the echo is represented by brightness on the waterfall and time flows downwards.

The head echo is the thin slanting line at the bottom of the bright trace on the waterfall. It shows the characteristic, rapidly changing Doppler shift as the meteor decelerates. In this example, the distance from beacon to meteor to receiver is reducing, as shown by positive shift.

The thicker, vertical line is the tail echo; little shift forms as the meteor passes through a region that becomes ionized. In this case, the meteor continues and the path from beacon via meteor to receiver increases, giving rise to a negative shift until it is completely burnt up or has cooled below the point where ionization is sustained, and the head echo fades out. The region ionized by the passage of the meteor remains reflective to radio for a longer period of time. This is the tail echo.

Radio echoes from meteors come in all sorts of shapes and sizes when viewed with a waterfall display. *Figure 9* shows a particularly strong head echo, with a large positive Doppler shift as the meteor approaches and then a negative shift as it recedes.

It is the Doppler shift of events like this that we hope to use to calculate the location, trajectory and hence radiant (apparent origin) of meteors. The maximum shift observed, in this case, is almost 1000Hz, which means the path from the beacon to the meteor and on to the receiver was reducing at almost 6000m/s. The head echo ends with a negative shift of approximately 250Hz, so the path from the beacon via the meteor to the receiver was extending at about 1500m/s.

7 Receive antennas

An objective of the project is to enable observations without the need for elaborate and expensive equipment, so that individuals and schools can create exciting STEM-based projects. A low-cost SDR with a PC and a simple wire antenna will, in many cases, provide a satisfactory way of observing meteor echoes. For those within a few hundred kilometers of the beacon, a dipole made from wire would be a good starting point (*Figure 10*).

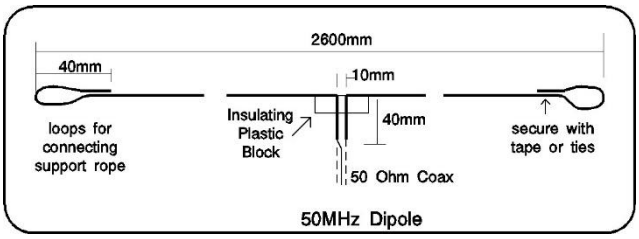

Figure 10 – A simple-to-make dipole for 50.408MHz.

At greater distances, an antenna with gain and directivity will be helpful. For best results, it should be pointed towards the point 100km above the beacon. A Moxon antenna is proving a popular choice, due to its compact size and good directivity. UKRAA have a stock of a suitable Moxon antennas available to buy. Alternatively, you can make your own from wire and plastic waste pipe, as per the design referenced[7].

8 Man-made noise

Man-made noise is the bane of radio astronomers everywhere, but particularly so in urban areas at 50MHz. So, it is well worth starting with a simple low-cost antenna such as a dipole to assess your local noise level, keeping the antenna in the clear and as far away from noise sources as possible.

A simple test to assess your local noise level is to measure the noise floor with the antenna connected and compare to when the antenna is replaced with a 50-ohm resistor. SDR Console shows the noise level at the upper left-hand side of the spectrum display (see *Figure 3*). If the noise floor increases by much more than 10dB when you connect the antenna, this indicates that you have a high local noise level and you may struggle to receive meteor echoes. First, try repositioning the antenna to find the quietest place for it. Even if you are close to the beacon, an antenna with directivity may help to null out local noise as you can point it upwards, away from the noise sources.

If your local noise level is too high to receive meteor echoes, all is not lost as in Phase II of this project is to deploy a number of receivers to radio-quiet locations and stream their data over the Internet, making them available to all via a central server.

9 Project phase II

After some successful proof-of-concept tests, work is now starting on developing web-based receivers that can stream I/Q data via the Internet to a central server. The receivers will incorporate precision timing and frequency control so that events can be correlated and Doppler measurements from different directions used, to calculate the location of the event and the trajectory of the meteor.

If you want any more information or would like to contribute relevant skills to the project, please do get in touch[21].

[21] https://ukmeteorbeacon.org/ContactAdd

Radio observations on the Perseids and some other showers in August and September 2022

Wilhelm Sicking

Augustin-Wibbelt-Straße 13 48712 Gescher Germany
wil.sicking@gmail.com

The Perseids 2022 were recorded between August 6th and 19th with two almost identical receiving systems, which differ only in the antennas. It's a cross Yagi and an omnidirectional antenna, a discone. Surprisingly, the discone gives the better Perseid results. The Perseid stream contained many very large echoes or particles, often appearing in bursts. There was no strong outburst like in 2021, but a small burst was detected at the same point, at solar longitude 141.5. There were no pronounced notches like those of the Arietids or the Geminids. Between August 28th and September 12th, the Northern iota Aquariids (NIA) were recorded. The September Perseids showed little activity in this time window. Surprisingly, the NIA instead provided interesting insights: a notch is clearly visible, allowing some details to be viewed.

1 Introduction

Notches in meteor histograms are known in the literature. According to Felix Verbelen (Verbelen, 2019), there are notches in all major streams. Kaufmann (Kaufmann 2020) postulates that head echoes produce a very large Doppler shift, so the signal is out of range of the receiver, which would result in a notch. In my first meteor paper (Sicking, 2022) I proposed a mechanism for how notches appear in GRAVES meteor data. The Perseids 2022 should now provide further insights. Eventually, only a small notch was observed, but there were a few other unexpected surprises.

2 Setup

The meteor echoes are recorded with two almost identical systems. They differ only in the antennas, which are a right-hand circularly polarized 4-element cross-Yagi and an omnidirectional antenna, a discone, with vertical polarization. The discone/cross Yagi combination is actually used to test my hypothesis about the notches and the in-line-effect. The antennas are mounted in the attic, so that the configuration can be easily changed. Low-noise preamplifiers with a frequency range of 140–150 MHz and a noise figure of 0.25 dB are connected directly to the antennas. The receivers are Icom IC-R8600. Spectrum-Lab (SL) serves as the recording software. SL generates plots every 20 seconds with the appropriate date and time in the file name, which are evaluated later with a self-written image processing software based on Python3 and OpenCV. The histograms in *Figures 1, 5 and 6* are smoothed with a variable Gaussian filter over up to 11 hours, while the histograms in *Figures 2 and 3* are smoothed with a fixed Gaussian like filter with the coefficients 0.31, 0.74, 1.0, 0.74 and 0.31. The feature of plotting different sizes in different traces allows insights into the streams that are not necessarily visible in the sum. After many tests I estimate the uncertainty on the rate to be < 5%. At the maximum of the streams, the error may be higher if the echoes are too close to each other. During the period examined, I saved Canadian Meteor Orbit Radar (CMOR) screenshots several times a day. This allows the peaks to be assigned to the currents. This is necessary because minor shower activity is not sustained by the method of single station meteor echo detection. The radiant heights were estimated using Stellarium Web for Dijon in France, located close to the GRAVES radar. Unless otherwise noted, data are shown from the right hand circularly polarized antenna.

3 Results and discussion

The histograms of the two receiving systems are shown in *Figures 1 and 2*. The scale is identical in each case. In *Figure 1*, the white lines with the letters a) and b) show that the X-Yagi delivers more echoes than the omnidirectional antenna on the days before and after the Perseids. This is because the directional antenna faces south toward GRAVES and thus collects more forward-scattered signals than the omnidirectional antenna.

However, the discone detects significantly more Perseid echoes than the directional antenna in relation to the baseline and also in absolute terms, as the comparison of the lines marked with a) and b) shows. In numbers: The Perseids grow out of the basic level by a factor of 1.99 for the discone and by a factor of 1.58 for the X-Yagi. This is because the Perseid radiant is farther north, so the directional antenna for the Perseids is pointing in the wrong direction. The southern showers, the Aquariids and the daytime xi-Orionids are better captured by the directional antenna. Details of the southern streams are discussed below.

The blue area in *Figure 2* shows the histograms in bins of ten minutes of the rate and the green area shows the rate weighted by the sizes. The long green spikes indicate that the Perseid shower contained many very large echoes/particles, often appearing in clusters. *Figure 3* shows a comparison of the Perseids with the Arietids: The rates don't differ that much, but the meteors are significantly larger in the Perseids when comparing the rates weighted with the sizes.

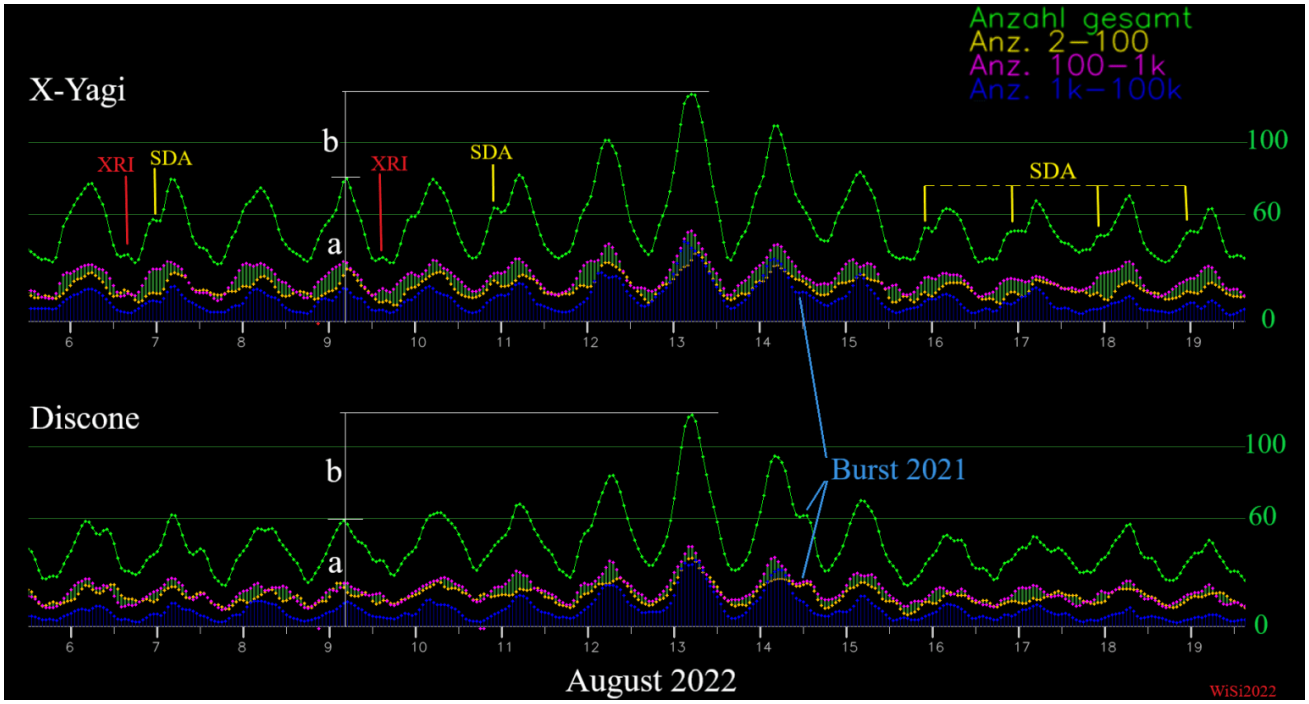

Figure 1 – Comparison of the X-Yagi and the Discone data of the Perseids 2022. The figure shows the meteor detection rate for different echo sizes. The blue lines represent the rate of large echoes (1k-100k pixels), the purple line shows the medium sized echos (100 to 1k) and the yellow line shows the small echoes (below 100 pixels). Finally, the green curve shows the rate of all sizes summed up.

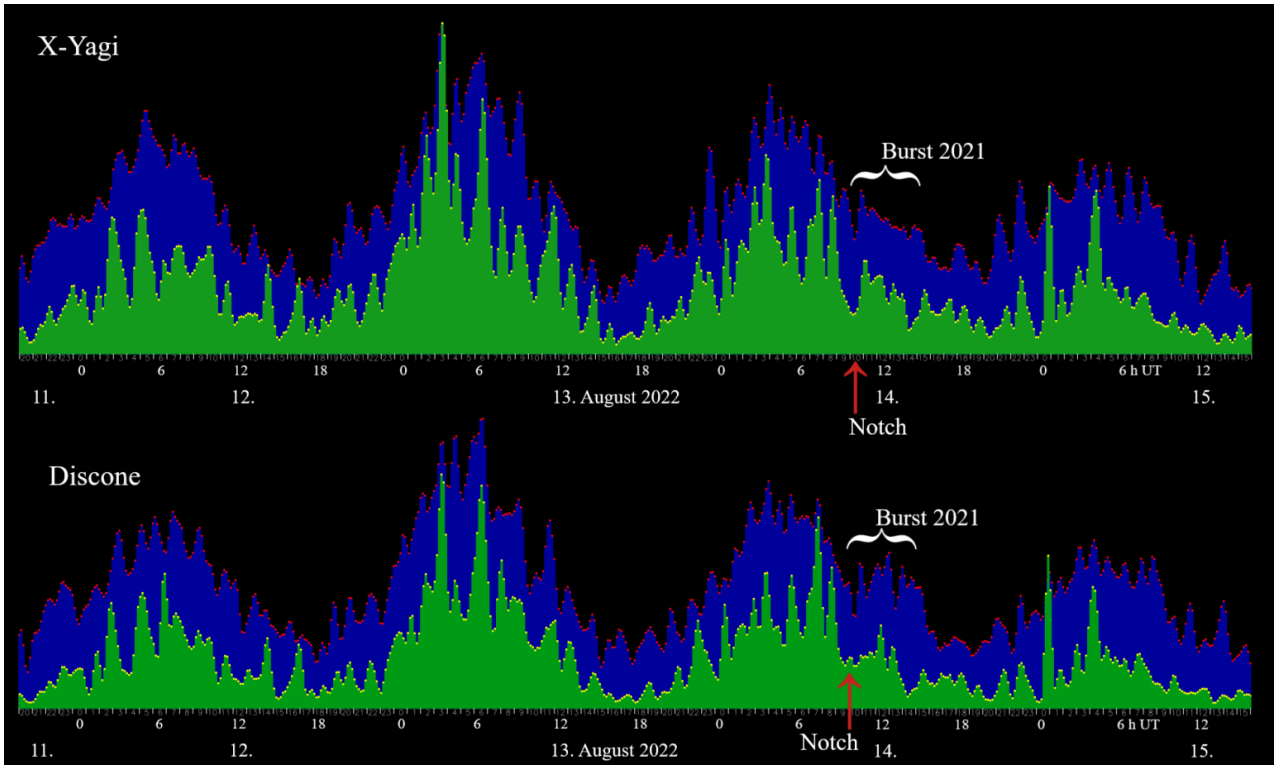

Figure 2 – Histograms of the rate (blue) and of the rate weighted by the sizes (green) in bins of ten minutes. Probably the plot shows a notch on August 14 at 10^h UT, see text. The small burst is clearly visible in the discone data.

4 Perseid outburst

The data show a mini-burst on August 14 between 10^h UT and 16^h UT, see *Figures 1 and 2*. At this point, solar longitude $\lambda_\odot = 141.489°$ on August 14, 8^h30^m UT, according to Miskotte et al. (2021) a very large outburst was observed in 2021. So, I labeled the point Burst 2021. This is probably the same burst, just smaller. At the maximum of the burst in 2021, the radiant height was 57°. On the other hand, in 2022 the solar longitude of 141.489 corresponds to 14^h30^m and a radiant height of only ~18°. Judging by the plots, the mini-burst 2022 seems to consist of small material. Presumably, the (normal-sized) particles are poorly visible because of the deep radiant and are simply registered as small echoes. The burst, like the main Perseid stream, is more visible with the discone than with the directional antenna and therefore cannot be one of the southern streams. The peak is also visible in the data from

RMOB observers, see for example entries by Ian Evans[22], Philip Norton[23], Philip Rourke[24] and Felix Verbelen[25] on August 14, 12^h–13^h UT.

5 To the notches

Figure 3 shows a comparison of the Perseids with the Arietids. The Perseids do not have a clear notch as in the Arietids, since the radiant does not pass southern of the GRAVES antenna. However, the signal dip on August 14 at 10^h UT could be a notch see *Figure 2*, the red arrows. At that time the radiant height was ~45°. The wider notch in the discone data and the small in-line peak at the lower red arrow suggest, that it is a real notch. Since the GRAVES transmitter radiates to the south, only a lower transmission power in side lobes and back lobes goes north. In the case of the Perseids, therefore, a large number of less intense echoes are detected. A weak signal along with a strong one, presumably a main lobe signal, is shown in *Figure 4*. Maybe next year I should record the Perseids with a third antenna pointing to north.

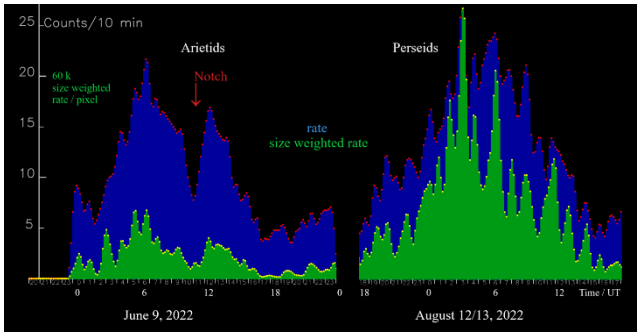

Figure 3 – Comparable histograms of the rate and of the rate weighted by the sizes of the Arietids and the Perseids. The rates don't differ that much, but the meteors are significantly larger in the Perseids when comparing the size-weighted rates.

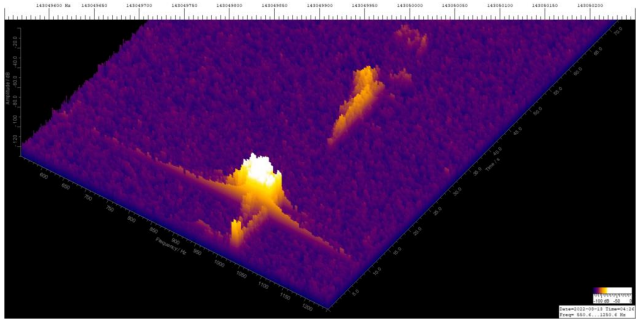

Figure 4 – Original Spectrum Lab output from 04^{h}26^m UT on 2022 August 13. Two echoes (above the threshold) are visible, a strong and a weak.

6 Daytime xi Orionids and Aquariids

Not only sporadic meteors and the Perseids, but also some other streams were active during the observed days. The main showers that occurred during the period are:

- XRI, Daytime xi Orionids,
- SDA, Southern delta Aquariids,
- NDA, Northern delta Aquariids,
- NIA, Northern iota Aquariids,
- PER, Perseids,
- SPE, September epsilon Perseids.

On August 7th and 9th, daytime xi Orionids (XRI) are marked in *Figure 1*. It must be XRI peaks, since according to CMOR no other radiant was active at that time and location. The Southern delta Aquariids (SDA) are also active throughout the period. Some peaks are marked too. The three Aquariid currents form a larger radiant field, so the peaks (and notches) are correspondingly wide. In *Figure 1* they are labeled "SDA" because SDA is the dominant stream. The maximum radiant height is about 2^h UT.

As with the Aquariids, the radiant field of XRI is very wide too. The radiant of XRI covered according to CMOR the entire constellation of Gemini and is not located at Orion. The maximum radiant height is at about 9–10^h. *Figure 5* shows the August 6 and 7 in more detail. The maximum of the radiant is indicated by an arrow. Like at the Arietids a notch in the XRI trace is generated, so that finally a local maximum at about 16^h UT instead of 10^h is visible in the green trace. The same happens with the SDA: the sum, the green trace, shows a local maximum in the wrong place at 23^h UT instead of 2^h UT. The next chapter shows an example that is perhaps a bit clearer.

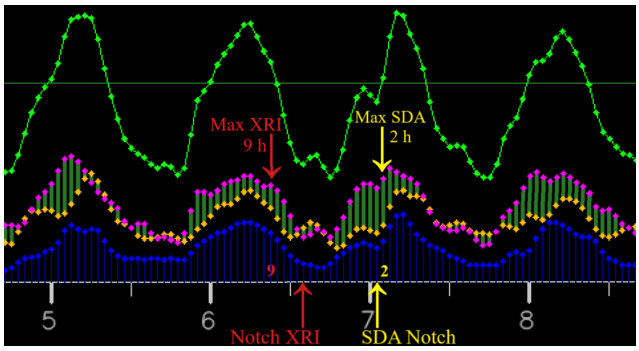

Figure 5 – The figure shows how the two peaks in the green trace on August 7 were formed by the superimposition of notches on the streams, see text. Admittedly, the effects are small, but the example shows that weak currents can be detected with simple means. The filter-width was chosen in a manner, that minima and maxima are shown a bit more clearly.

7 September Perseids and Northern iota Aquariids

Between August 28th and September 12th data were collected to prove the September Perseids which should peak on September 9th. However, the September Perseids are not visible as a maximum in the graphical representation, although the counts increase slightly, see *Figure 6*. According to a personal communication with Felix Verbelen, the Ieper (49.99 MHz) data clearly show increased activity from September 8th to 11th. Instead, the Northern iota Aquariids (NIA) are clearly visible with very

[22] https://www.rmob.org/visual/2022/evans_082022rmob.txt
[23] https://www.rmob.org/visual/2022/norton_082022rmob.txt
[24] https://www.rmob.org/visual/2022/rourke_082022rmob.txt
[25] https://www.rmob.org/visual/2022/verbelen_082022rmob.txt

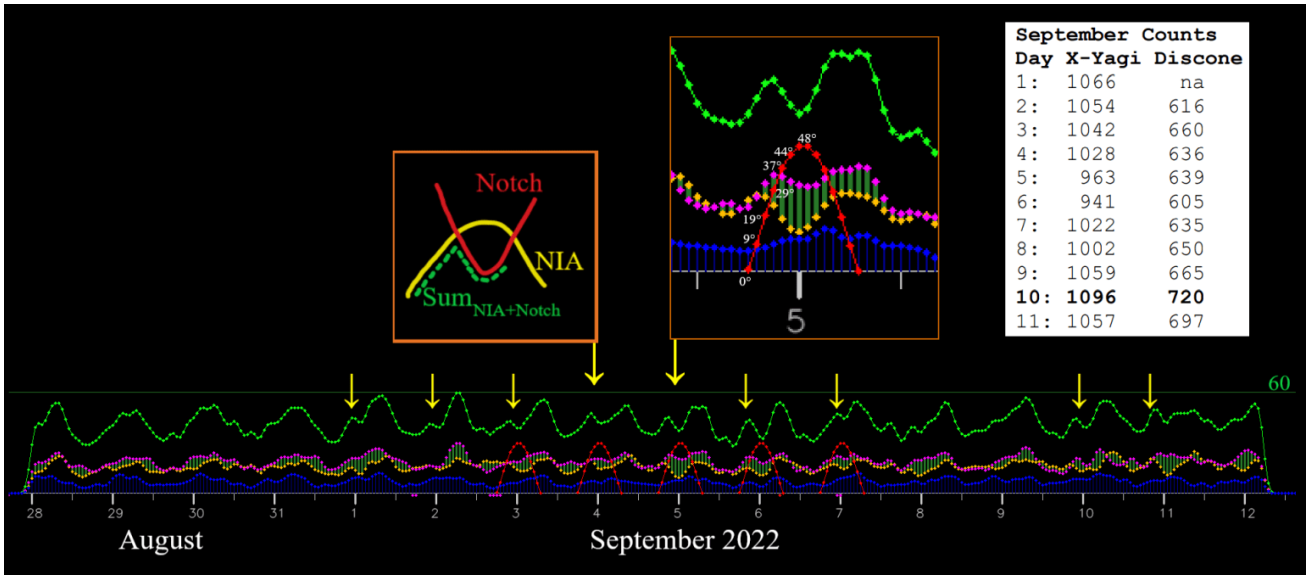

Figure 6 – Data between August 28th and September 12th. Instead of September Perseids, Northern iota Aquariids (NIA) are clearly visible, see the yellow arrows. The left inset shows how the green trace results from NIA + notch. The middle inset shows how the different sized echoes decay at different rates. The right inset shows the counts accumulated over one day. A slight maximum is seen on September 10th, but is not visible on the hourly charts of both antennas. Discone hourly data are not shown.

nice peaks one to two hours before midnight, although they had already reached their maximum on August 25th.

The red curves show the radiant height of the NIA. The maximum of the radiant height is 48°at 0h–1h UT. The sum, the green trace has local maxima around 21h–22h, which is about 2–3 hours too early for the NIA. This can only be caused by a notch that hide the echoes. This can be illustrated particularly well on September 4th: According to CMOR, only the NIA were active on September 4th. Therefore, the radiant field was small and the maximum, the result of the NIA and notch, is very sharp. The situation was made clear by a small drawing, see the left inset in *Figure 6*. However, I have to add caution: The NIA shower is not confirmed by video. The small particles are probably beyond the reach of most systems.

The middle-inset shows that the yellow trace, i.e., the small echoes, are mainly responsible for the dip. The purple trail, the medium-sized echoes break in less and the big blue break in barely. It was different with the Geminids and Arietids – the reason is still unknown. The angle from which the notch grips can be roughly estimated with 20°.

8 Conclusions

The data show a mini-burst on August 14 of the Perseids. A comparison with the Arietids shows that the rates do not differ that much, but the meteors in the Perseids are significantly larger and appear in clusters.

Weak showers like the XRI and SDA are covered in the normal daily cycle of the meteors, however they give themselves away through the notches as the notches are very narrow and sharp while the maxima are wide and flat. This fact was used, for example, for the minimum bearing.

The knowledge about notches is important. The sporadic meteors are also affected, but the effect is not visible because no dip is visible. Overall, the effects lead to an underestimation of the sporadic meteors and of the showers. Finally, observing notches is a nice feature to look for weak showers.

Acknowledgment

Many thanks to Felix Verbelen and Richard Kacerek for reading the article and for helpful comments according my interpretation of minor shower activity.

References

Kaufmann W. (2020). “Limitations of the observability of radio meteor head echoes in a forward scatter setup”. *WGN, Journal of the International Meteor Organization*, **48**, 12–16.

Miskotte K., Sugimoto H., Martin P. (2021). “The big surprise: a late Perseid outburst on August 14, 2021!”. *eMetN*, **6**, 517–525.

Sicking W. (2022). “A Notch in the Arietids Radio Data and a new so called In-Line-Effect”. *eMetN*, **7**, 331–335.

Verbelen F. (2019). “Meteor velocity derived from head echoes obtained by a single observer using forward scatter from a low powered beacon”. *WGN, Journal of the International Meteor Organization*, **47**, 49–54.

Radio meteors August 2022

Felix Verbelen

Vereniging voor Sterrenkunde & Volkssterrenwacht MIRA, Grimbergen, Belgium
felix.verbelen@skynet.be

An overview of the radio observations during August 2022 is given.

1 Introduction

The graphs show both the daily totals (*Figure 1 and 2*) and the hourly numbers (*Figure 3 and 4*) of "all" reflections counted automatically, and of manually counted "overdense" reflections, overdense reflections longer than 10 seconds and longer than 1 minute, as observed here at Kampenhout (BE) on the frequency of our VVS-beacon (49.99 MHz) during the month of August 2022.

The hourly numbers, for echoes shorter than 1 minute, are weighted averages derived from:

$$N(h) = \frac{n(h-1)}{4} + \frac{n(h)}{2} + \frac{n(h+1)}{4}$$

Local interference and unidentified noise remained moderate to low for most of the month. Lightning activity was observed on 7 days; the August 16 thunderstorm made observations quite difficult as it was temporarily active near our radio beacon.

Especially in the first half of the month there were several intense solar eruptions causing sometimes considerable noise (*Figure 5*). Oddly enough, there were only a few faint solar flares on radio waves in the last ten days of the month, notwithstanding the numerous sunspots, prominences, and other eruptions.

The eye-catchers of the month were of course the Perseids, with many long-lasting reflections. After an initial period of increasing activity in the first part of the month, the shower reached its maximum during the nights of 12–13 and 13–14 August. Longer overdense reflections, as usual, came a little later than the underdense.

After the shower's maximum, meteor activity declined rapidly and remained quite low during the second half of the month, with nonetheless some long reflections.

Over the entire month, 63 reflections longer than 1 minute were registered here. A selection of these and some other interesting reflections are included. (*Figures 6 to 25*). In addition to the usual graphs, you will also find the raw counts in cvs-format[26] from which the graphs are derived.

The table contains the following columns: day of the month, hour of the day, day + decimals, solar longitude (epoch J2000), counts of "all" reflections, overdense reflections, reflections longer than 10 seconds and reflections longer than 1 minute, the numbers being the observed reflections of the past hour.

[26] https://www.meteornews.net/wp-content/uploads/2022/09/202208_49990_FV_rawcounts.csv

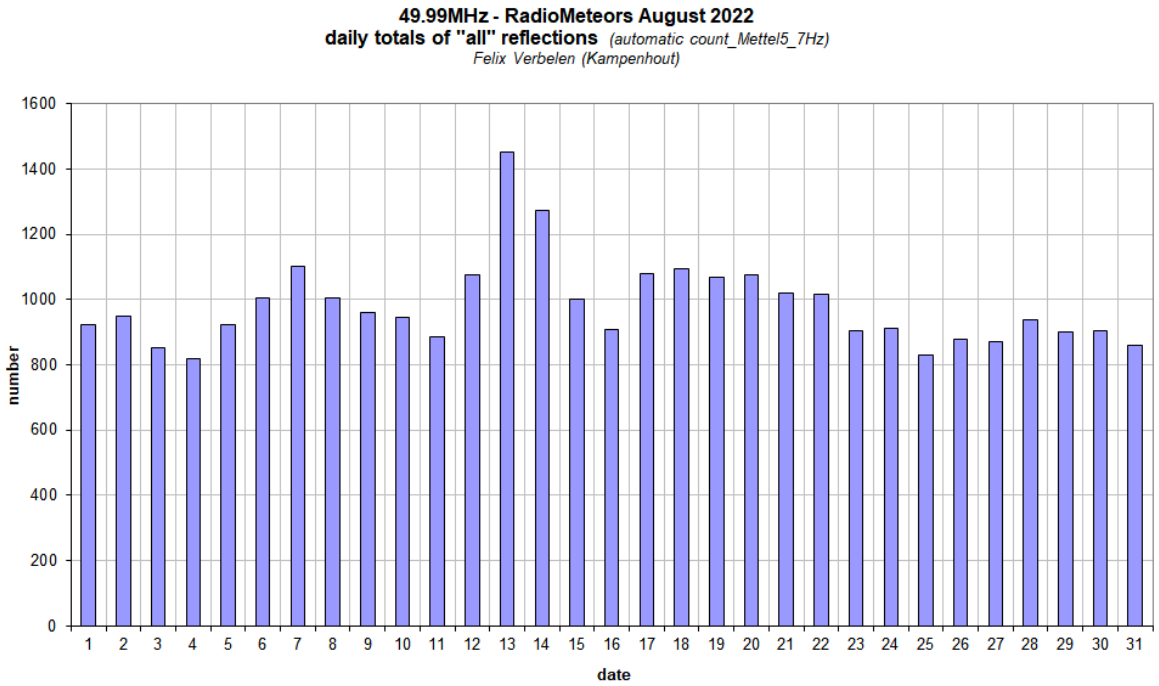

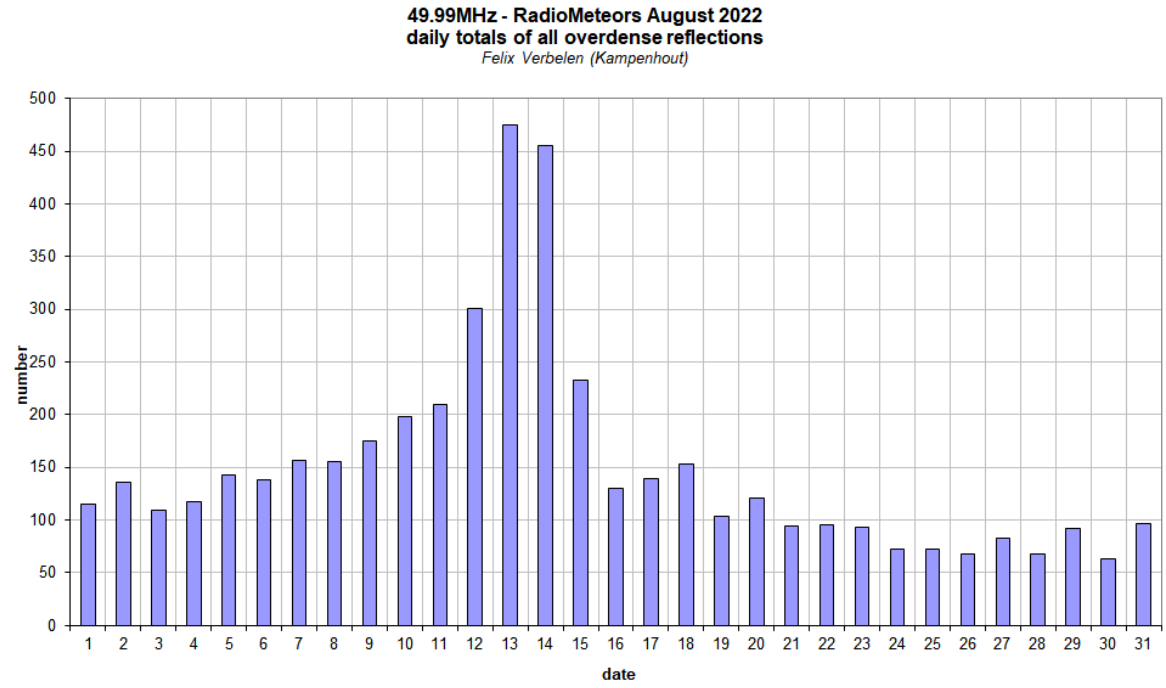

Figure 1 – The daily totals of "all" reflections counted automatically, and of manually counted "overdense" reflections, as observed here at Kampenhout (BE) on the frequency of our VVS-beacon (49.99 MHz) during August 2022.

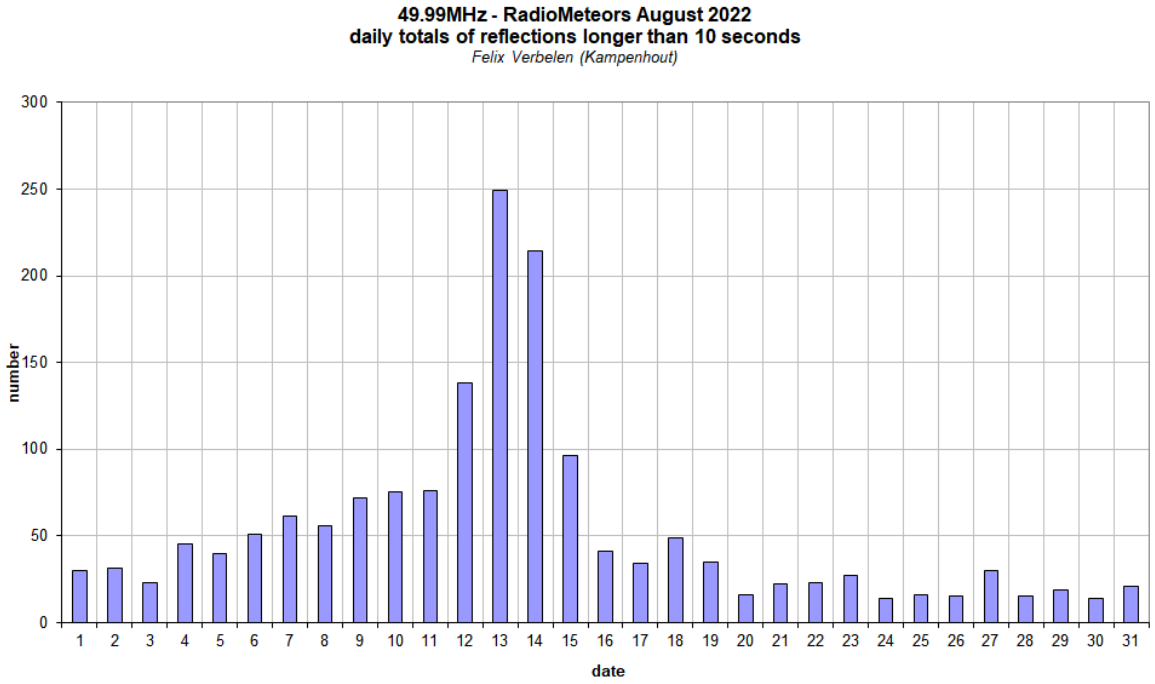

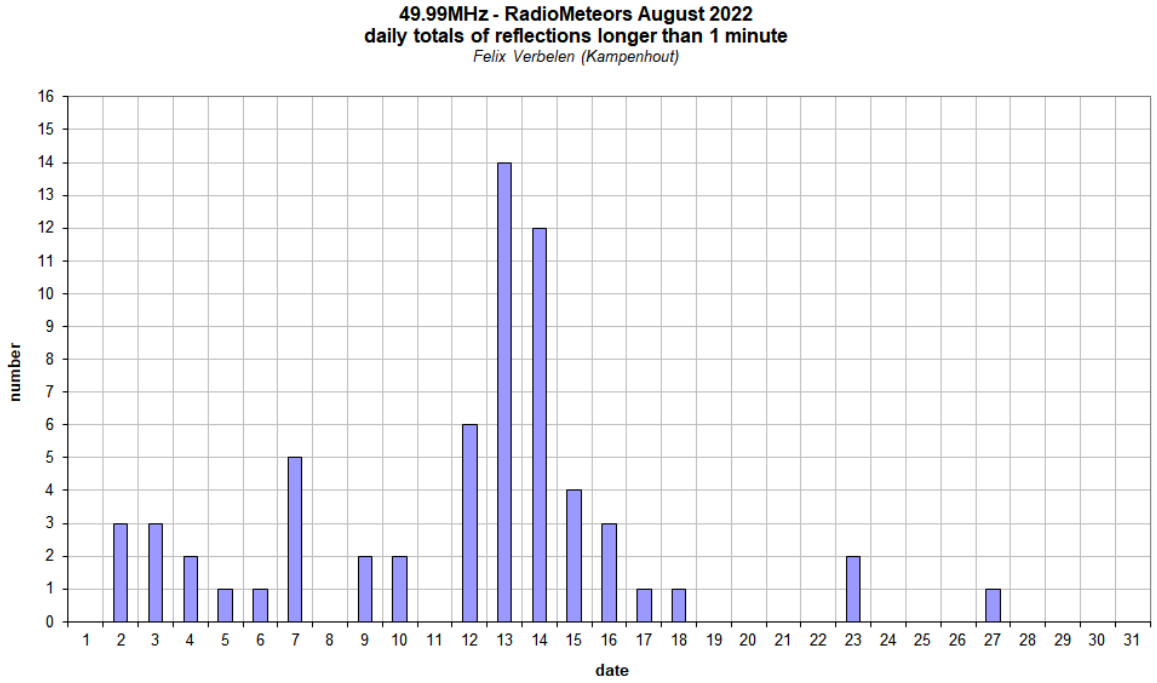

Figure 2 – The daily totals of overdense reflections longer than 10 seconds and longer than 1 minute, as observed here at Kampenhout (BE) on the frequency of our VVS-beacon (49.99 MHz) during August 2022.

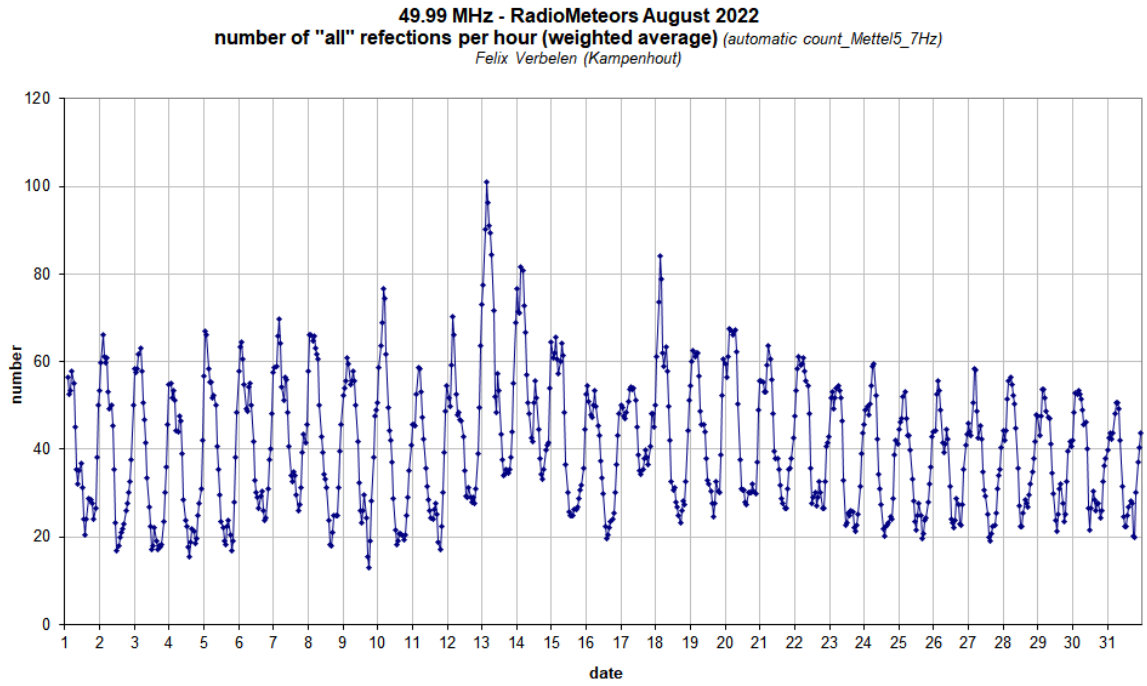

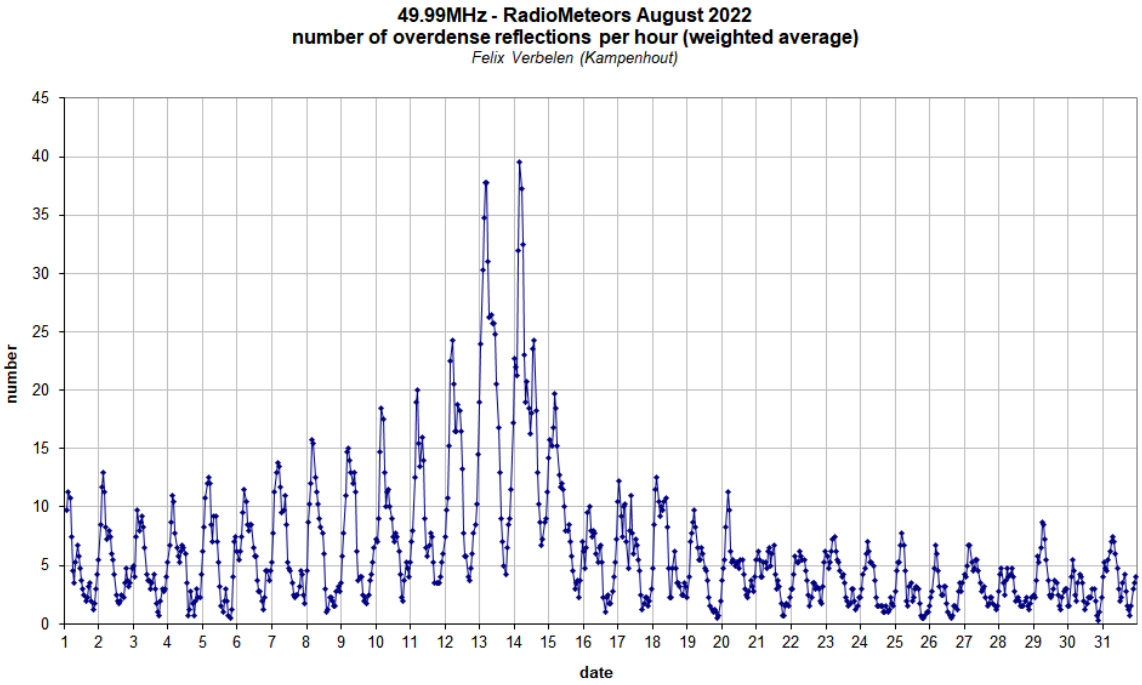

Figure 3 – The hourly numbers of "all" reflections counted automatically, and of manually counted "overdense" reflections, as observed here at Kampenhout (BE) on the frequency of our VVS-beacon (49.99 MHz) during August 2022.

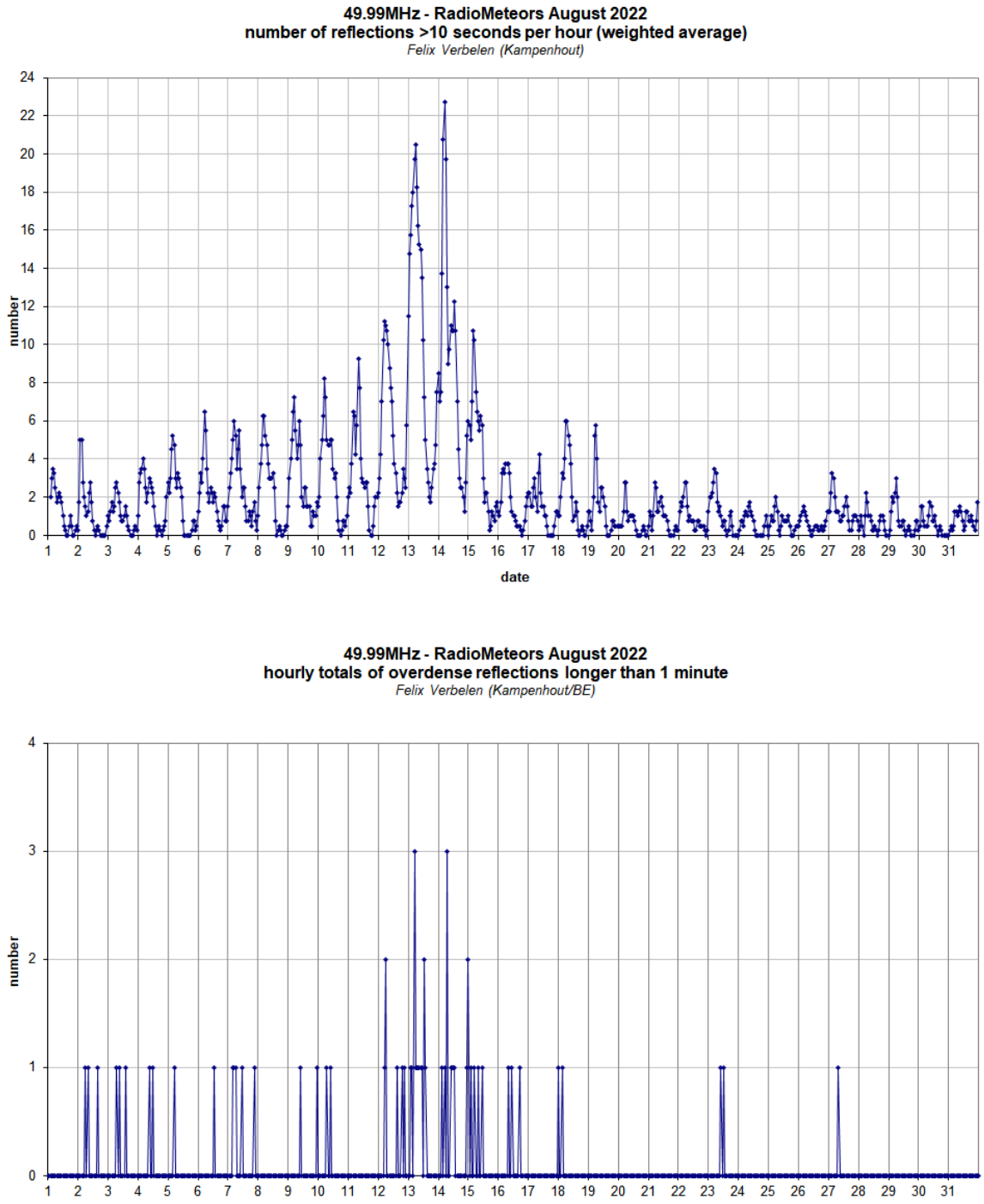

Figure 4 – The hourly numbers of overdense reflections longer than 10 seconds and longer than 1 minute, as observed here at Kampenhout (BE) on the frequency of our VVS-beacon (49.99 MHz) during August 2022.

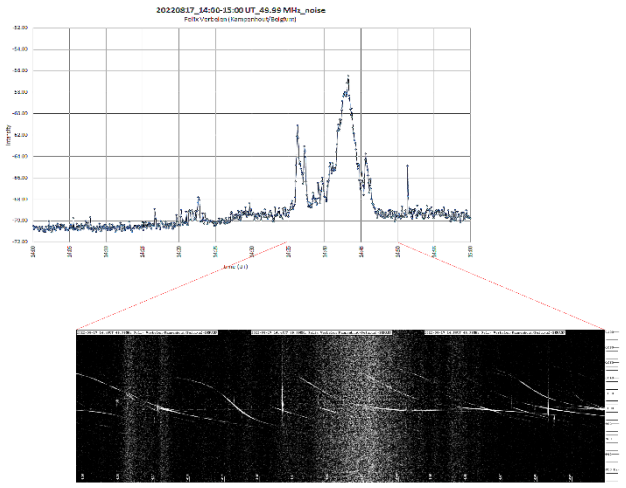

Figure 5 – Solar eruptions often caused considerable noise.

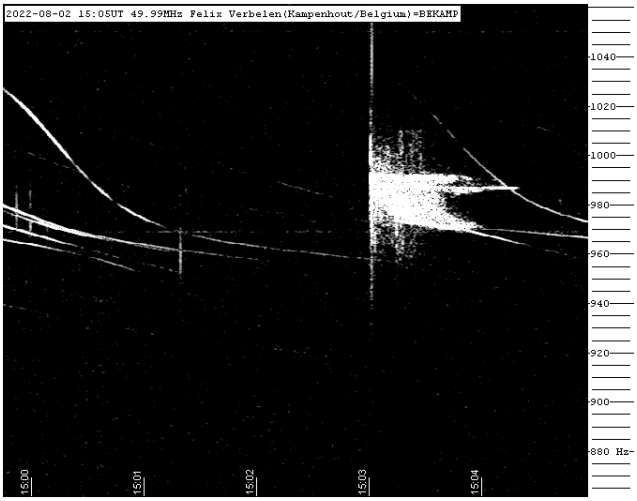

Figure 6 – Meteor reflection 2 August 2022, 15^h05^m UT.

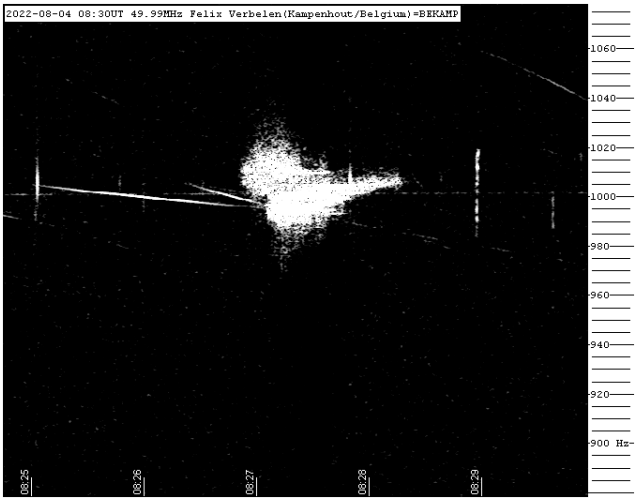

Figure 7 – Meteor reflection 4 August 2022, 08^h30^m UT.

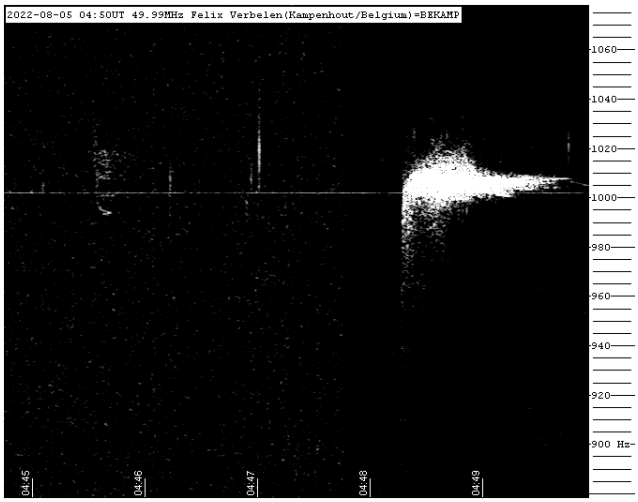

Figure 8 – Meteor reflection 5 August 2022, 04^h50^m UT.

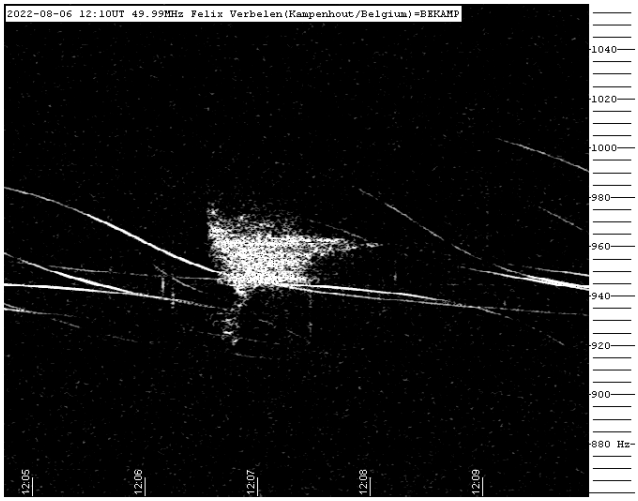

Figure 9 – Meteor reflection 6 August 2022, 12^h10^m UT.

Figure 10 – Meteor reflection 7 August 2022, 04^h30^m UT.

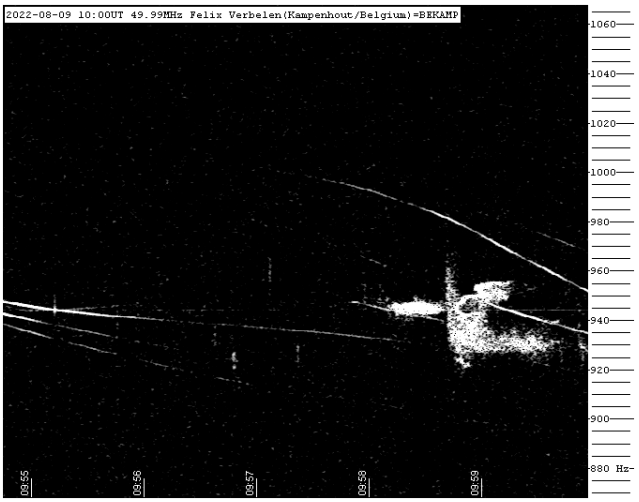

Figure 11 – Meteor reflection 9 August 2022, 10^h00^m UT.

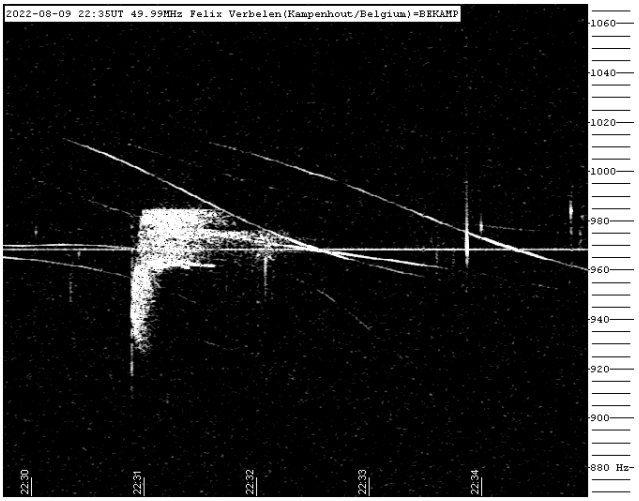

Figure 12 – Meteor reflection 9 August 2022, 22^h35^m UT.

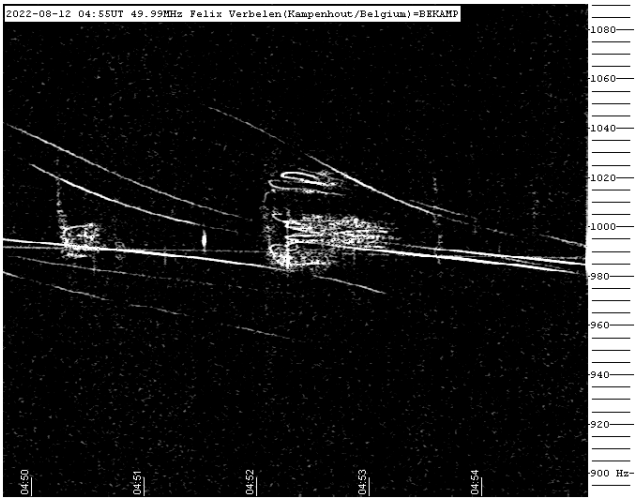

Figure 13 – Meteor reflection 12 August 2022, 04^h55^m UT.

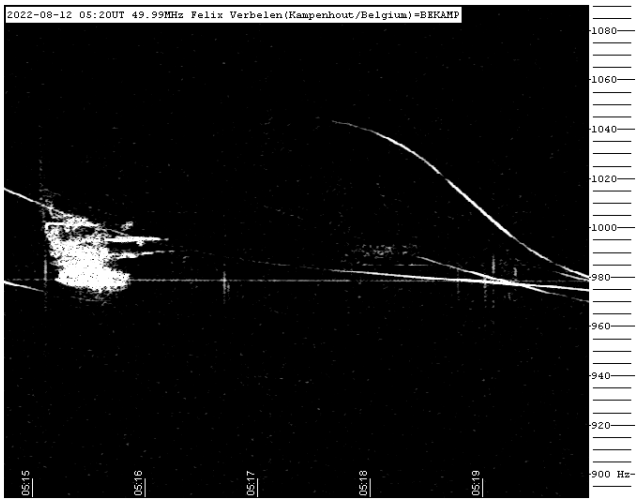

Figure 14 – Meteor reflection 12 August 2022, 05^h20^m UT.

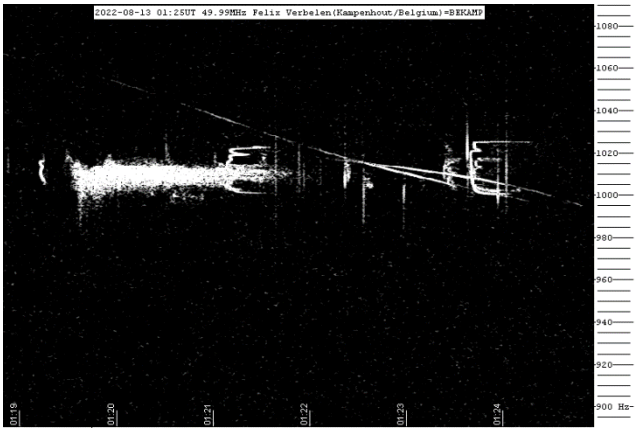

Figure 15 – Meteor reflection 13 August 2022, 01^h25^m UT.

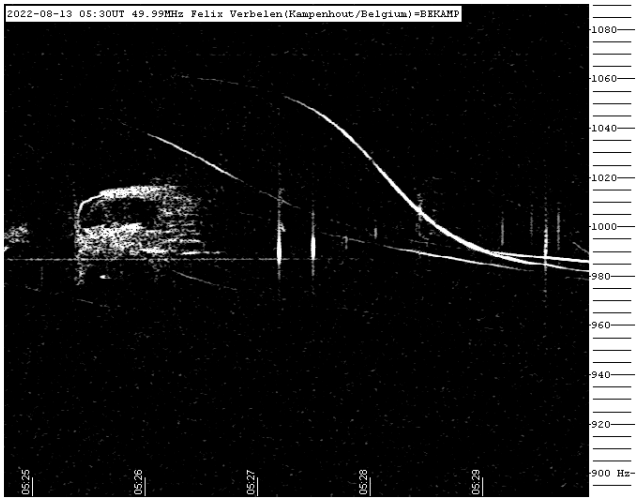

Figure 16 – Meteor reflection 13 August 2022, 05^h30^m UT.

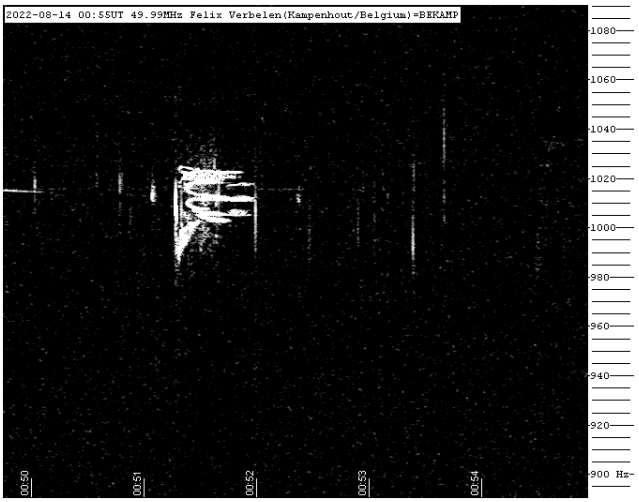

Figure 17 – Meteor reflection 14 August 2022, 00^h55^m UT.

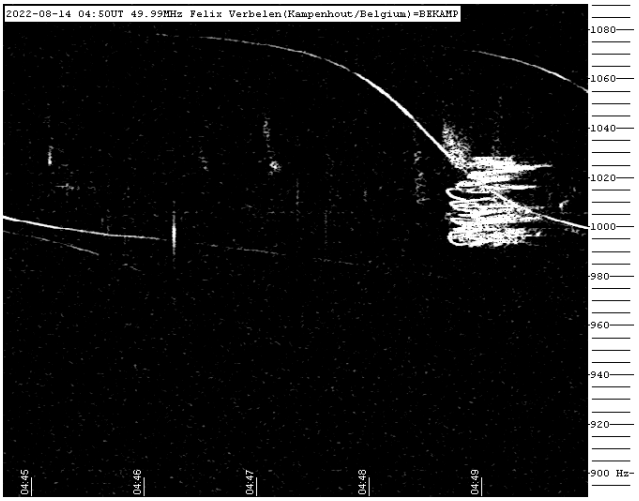

Figure 18 – Meteor reflection 14 August 2022, 04^h50^m UT.

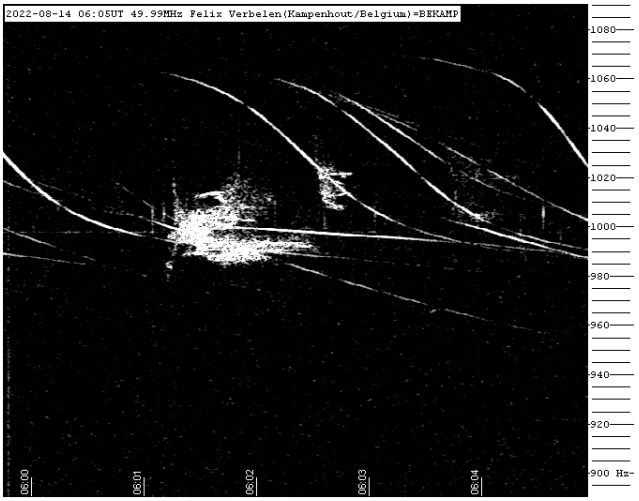

Figure 19 – Meteor reflection 14 August 2022, 06^h05^m UT.

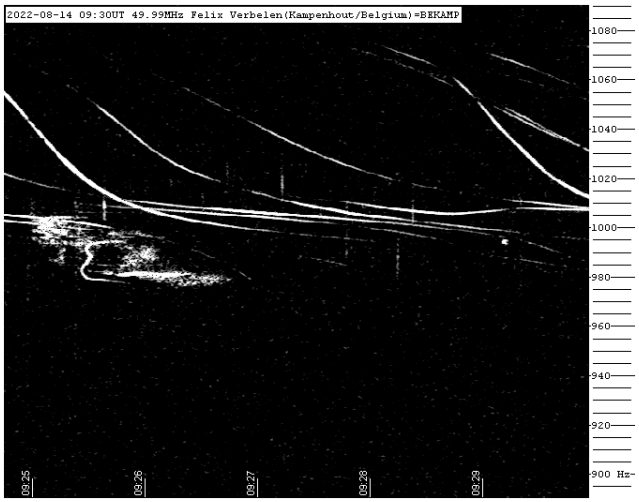

Figure 20 – Meteor reflection 14 August 2022, 09^h30^m UT.

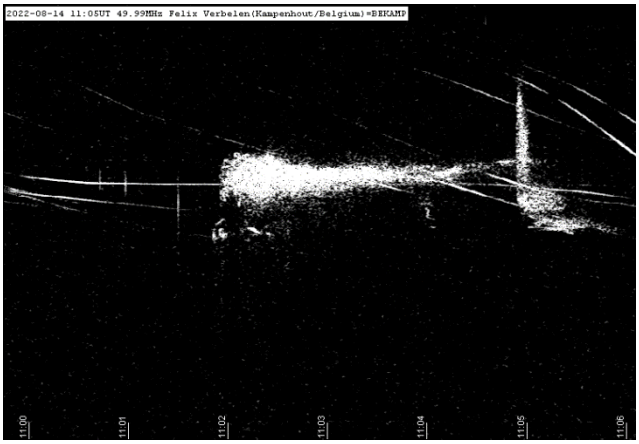

Figure 21 – Meteor reflection 14 August 2022, 11^h05^m UT.

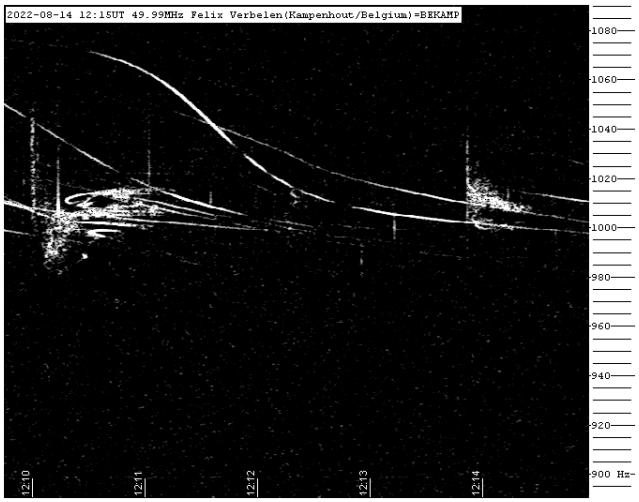

Figure 22 – Meteor reflection 14 August 2022, 12^h15^m UT.

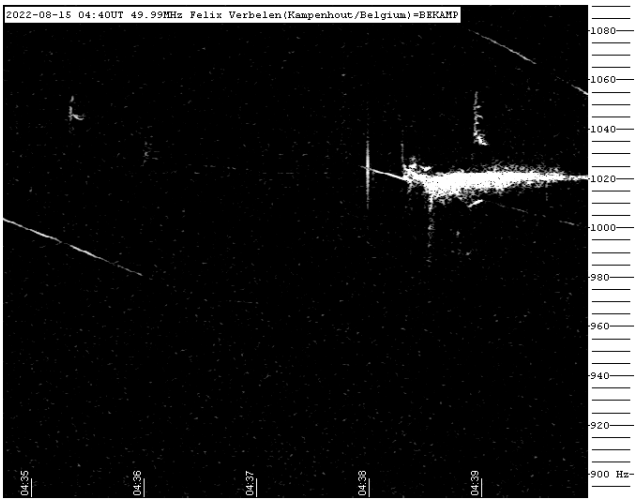

Figure 23 – Meteor reflection 15 August 2022, 04^h40^m UT.

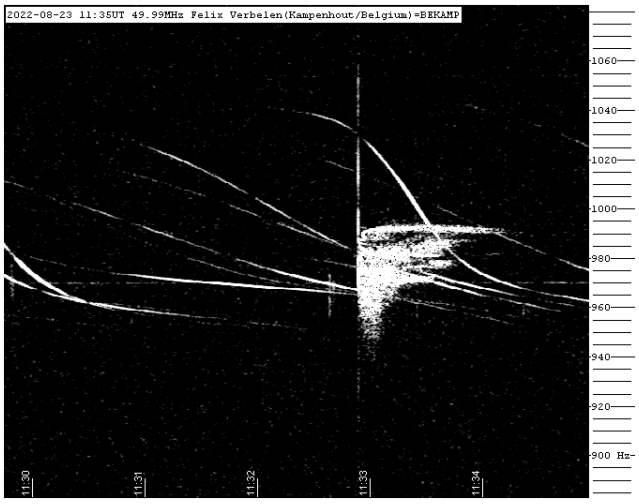

Figure 25 – Meteor reflection 23 August 2022, 11^h35^m UT.

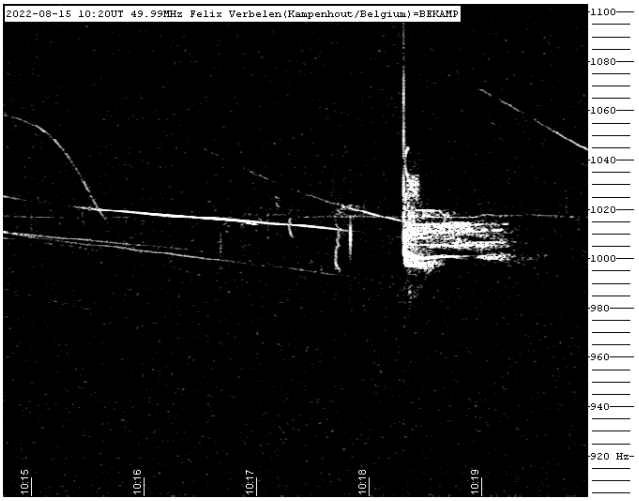

Figure 24 – Meteor reflection 15 August 2022, 10^h20^m UT.

Radio meteors September 2022

Felix Verbelen

Vereniging voor Sterrenkunde & Volkssterrenwacht MIRA, Grimbergen, Belgium
felix.verbelen@skynet.be

An overview of the radio observations during September 2022 is given.

1 Introduction

The graphs show both the daily totals (*Figure 1 and 2*) and the hourly numbers (*Figure 3 and 4*) of "all" reflections counted automatically, and of manually counted "overdense" reflections, overdense reflections longer than 10 seconds and longer than 1 minute, as observed here at Kampenhout (BE) on the frequency of our VVS-beacon (49.99 MHz) during the month of September 2022.

The hourly numbers, for echoes shorter than 1 minute, are weighted averages derived from:

$$N(h) = \frac{n(h-1)}{4} + \frac{n(h)}{2} + \frac{n(h+1)}{4}$$

On many days, especially during the evening and night, radio reception was disturbed by unidentified noise. In addition, sometimes intense lightning activity was recorded on 12 days and also solar eruptions caused strong noise on several occasions.

Manual counting of the reflections remained possible despite these disturbances, but the automatic counts were quite difficult and had to be corrected manually.

There were hardly any real eye-catchers this month, but around September 9, 18, 25 and 29 there were clearly structured increases of overdense reflections longer than 10 seconds, which is best seen in the daily totals.

Over the entire month, 15 reflections longer than 1 minute were registered here. attached are selections of long reflections (Figures 5 to 14) and of "epsilons" (Figures 15 to 30).

In addition to the usual graphs, you will also find the raw counts in cvs-format[27] from which the graphs are derived.

The table contains the following columns: day of the month, hour of the day, day + decimals, solar longitude (epoch J2000), counts of "all" reflections, overdense reflections, reflections longer than 10 seconds and reflections longer than 1 minute, the numbers being the observed reflections of the past hour.

[27] https://www.meteornews.net/wp-content/uploads/2022/10/202209_49990_FV_rawcounts.csv

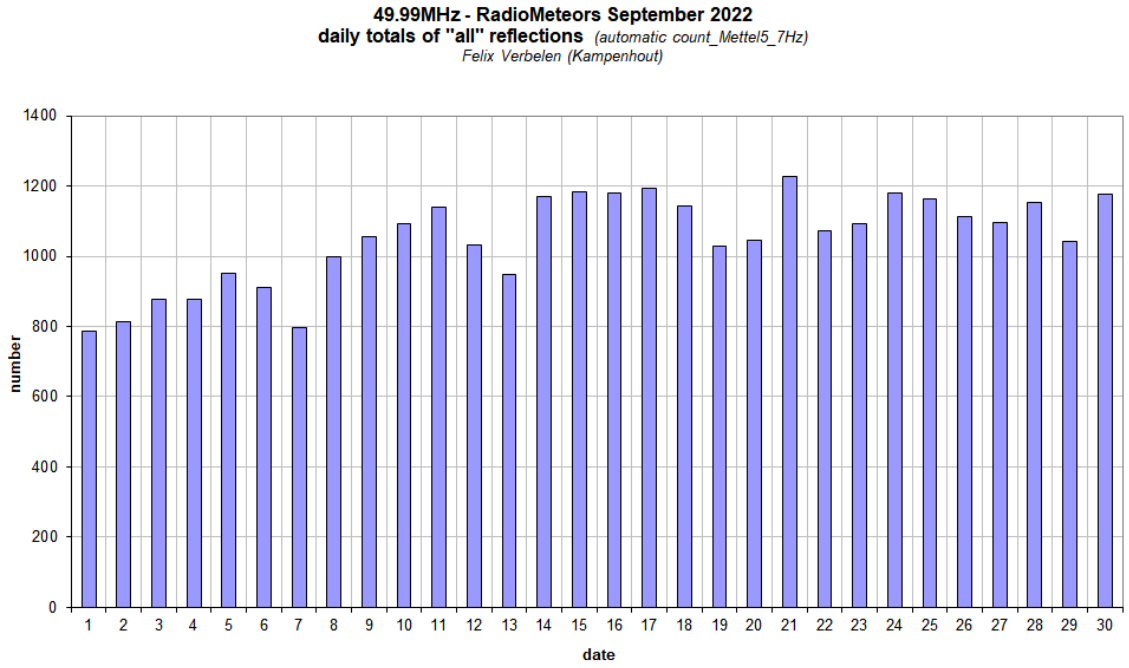

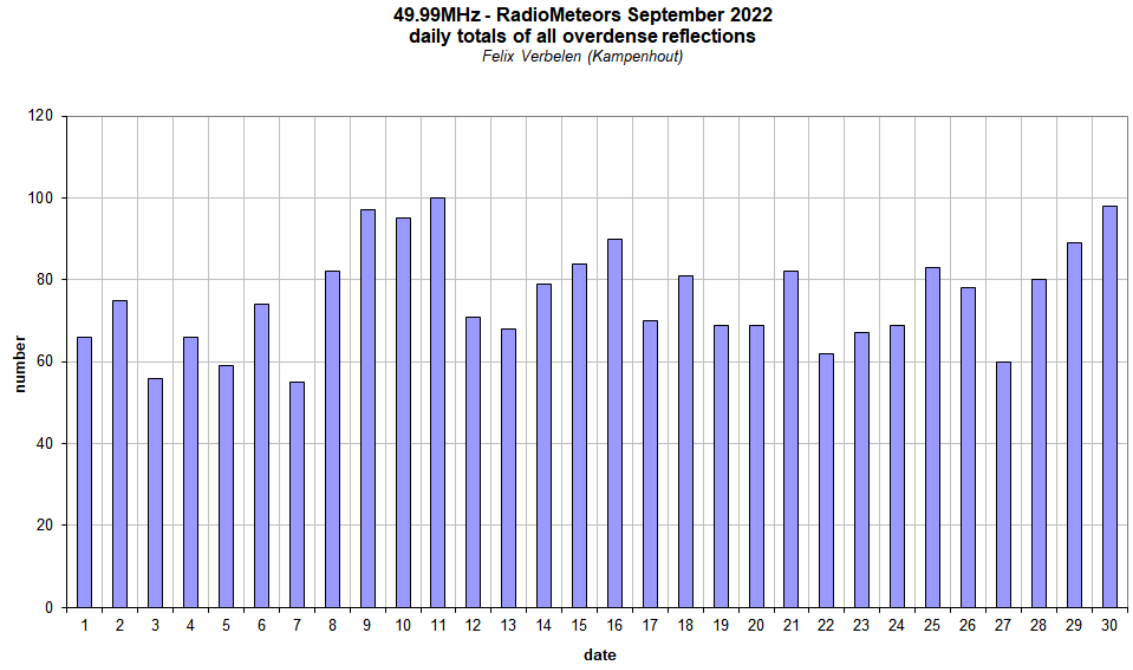

Figure 1 – The daily totals of "all" reflections counted automatically, and of manually counted "overdense" reflections, as observed here at Kampenhout (BE) on the frequency of our VVS-beacon (49.99 MHz) during September 2022.

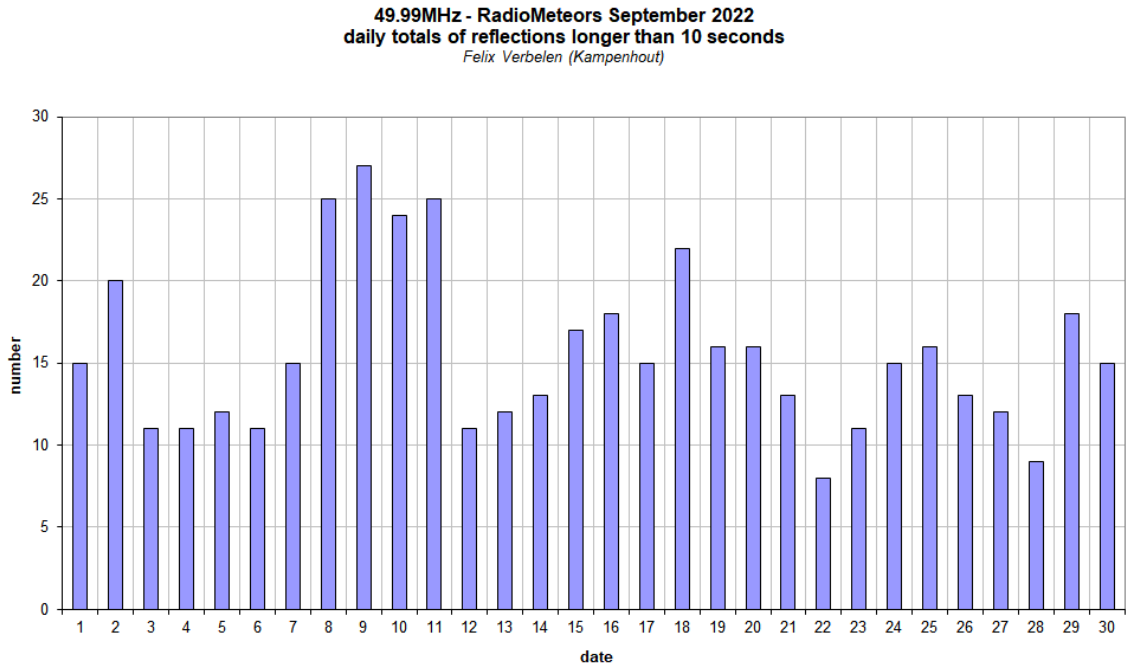

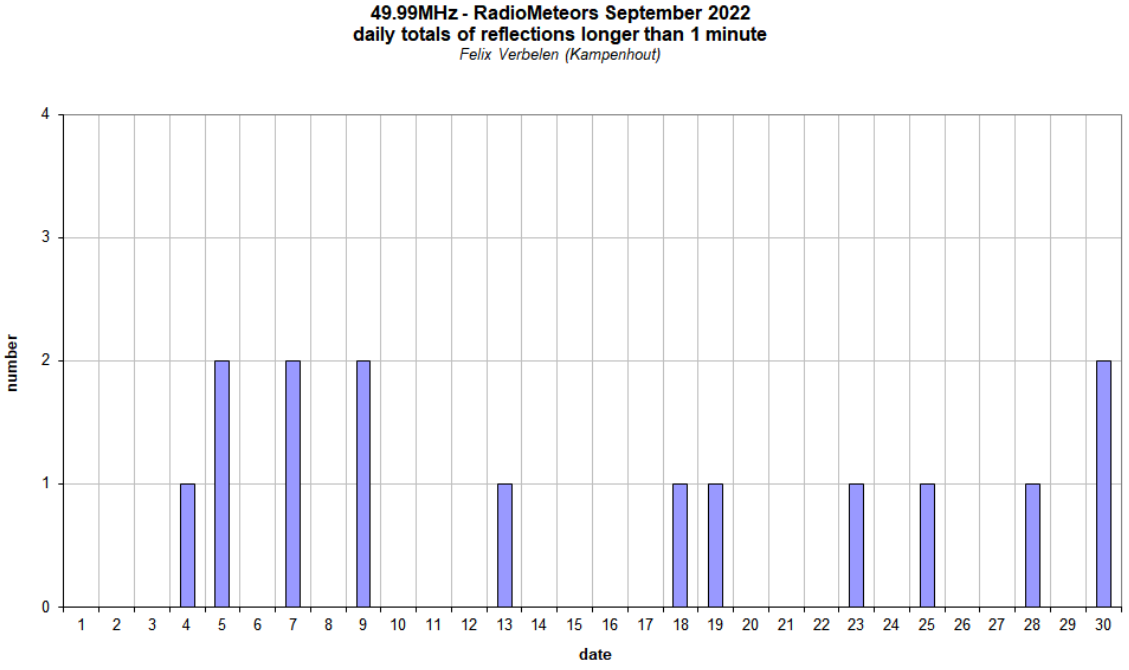

Figure 2 – The daily totals of overdense reflections longer than 10 seconds and longer than 1 minute, as observed here at Kampenhout (BE) on the frequency of our VVS-beacon (49.99 MHz) during September 2022.

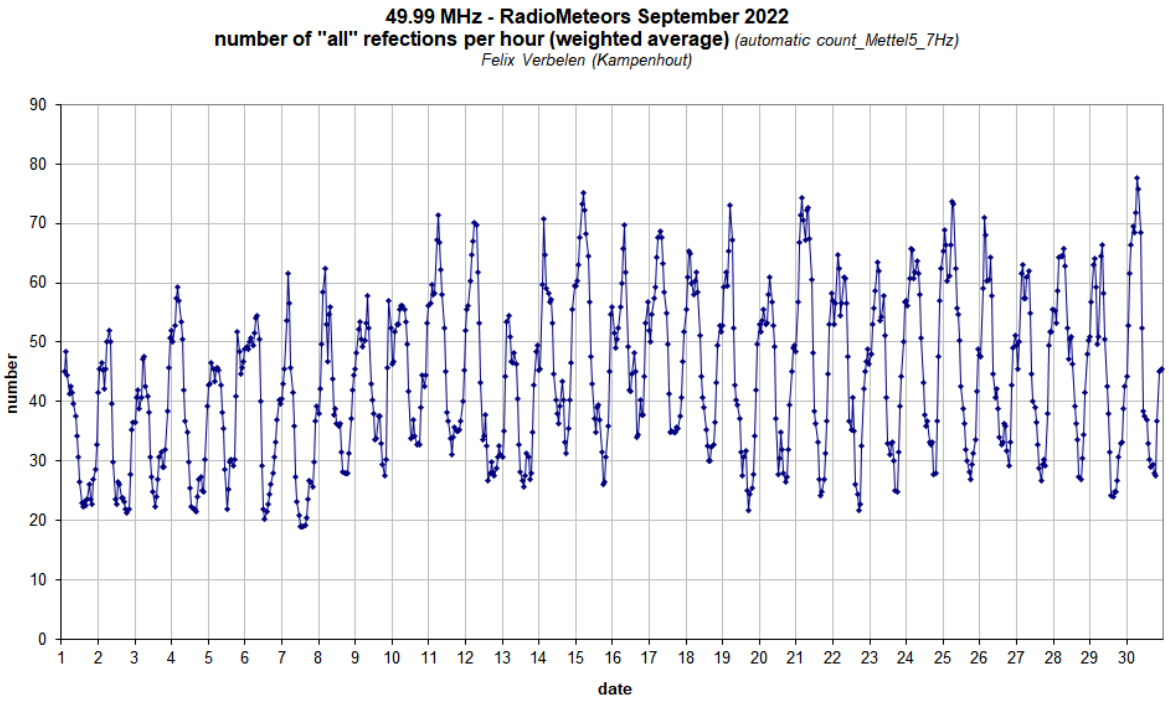

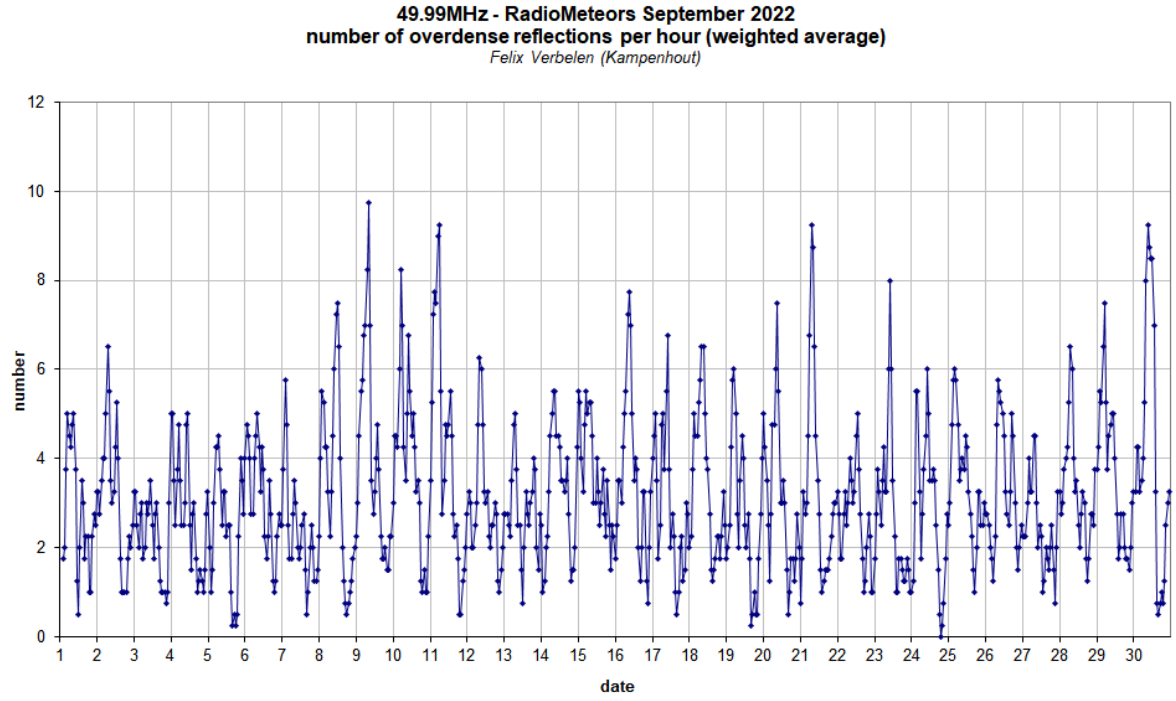

Figure 3 – The hourly numbers of "all" reflections counted automatically, and of manually counted "overdense" reflections, as observed here at Kampenhout (BE) on the frequency of our VVS-beacon (49.99 MHz) during September 2022.

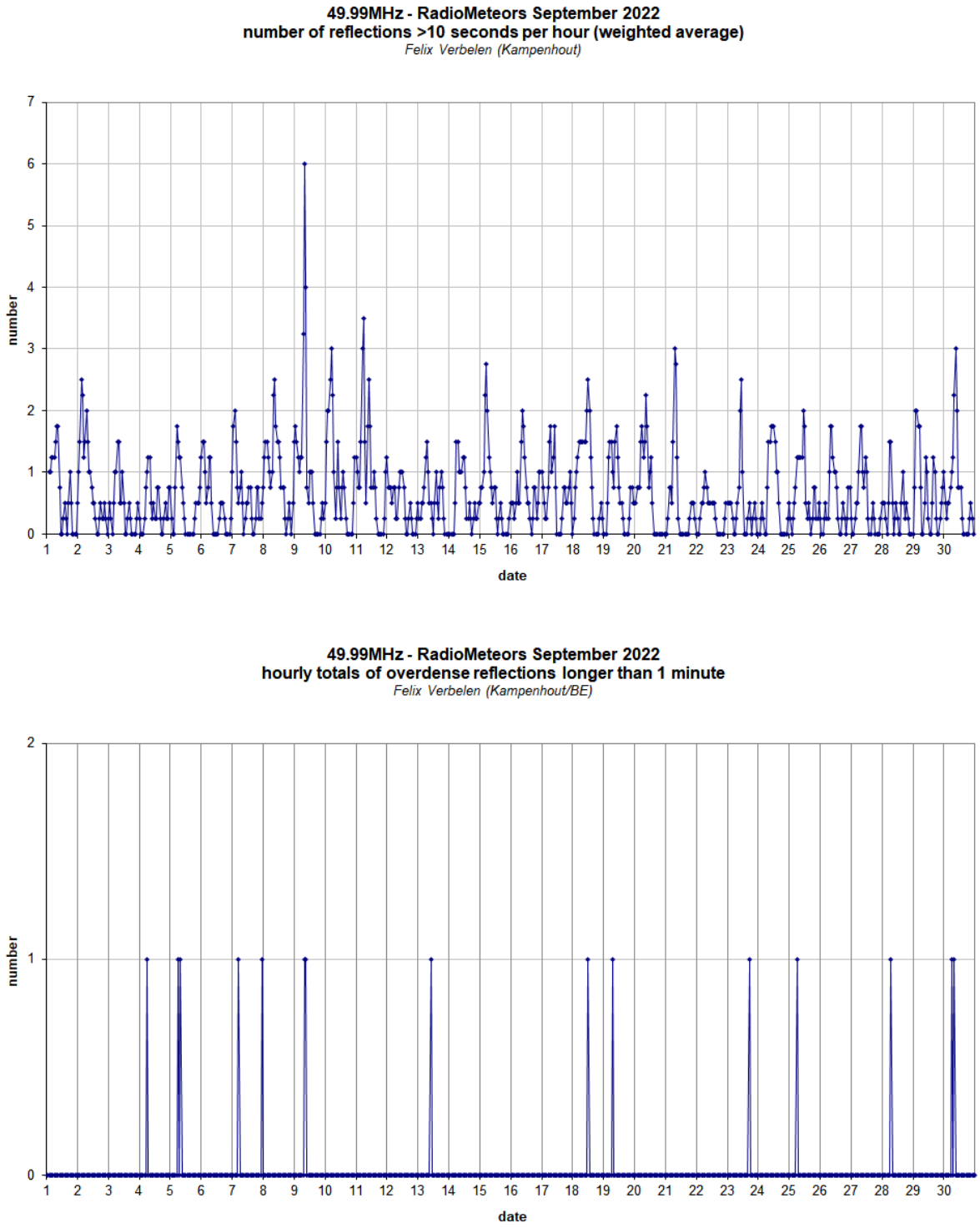

Figure 4 – The hourly numbers of overdense reflections longer than 10 seconds and longer than 1 minute, as observed here at Kampenhout (BE) on the frequency of our VVS-beacon (49.99 MHz) during September 2022.

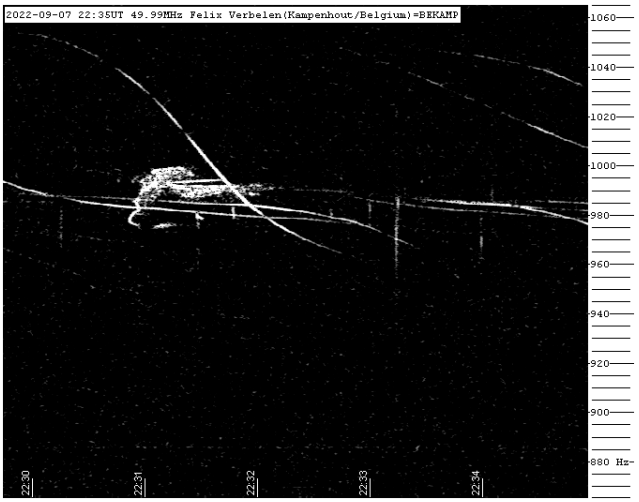

Figure 5 – Meteor reflection 7 September 2022, 22^h35^m UT.

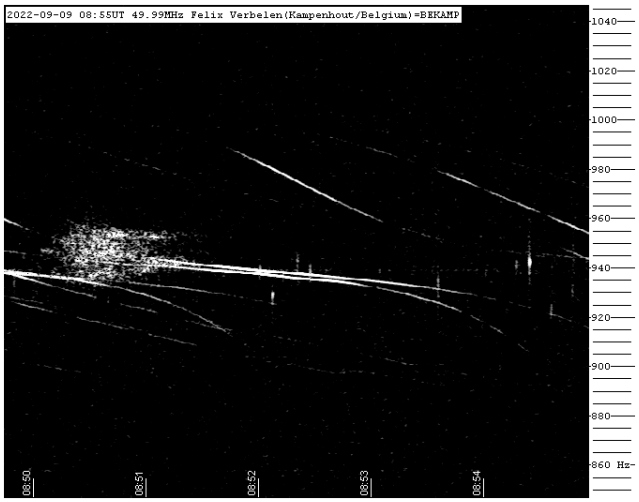

Figure 8 – Meteor reflection 9 September 2022, 08^h55^m UT.

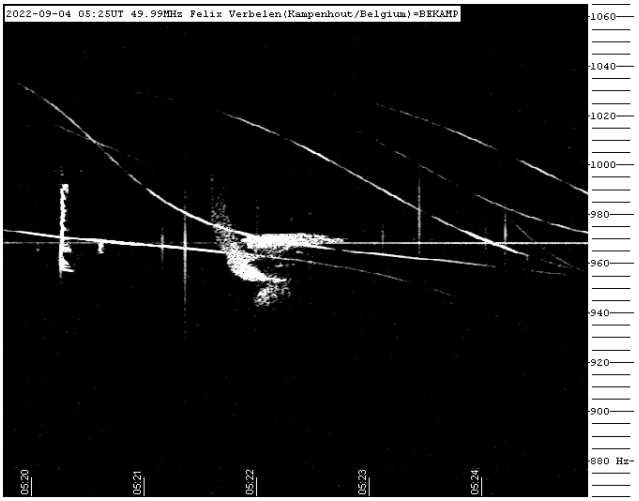

Figure 6 – Meteor reflection 4 September 2022, 05^h25^m UT.

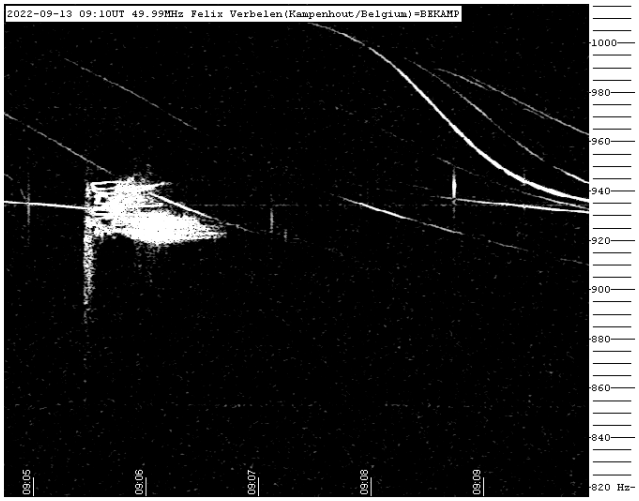

Figure 9 – Meteor reflection 13 September 2022, 09^h10^m UT.

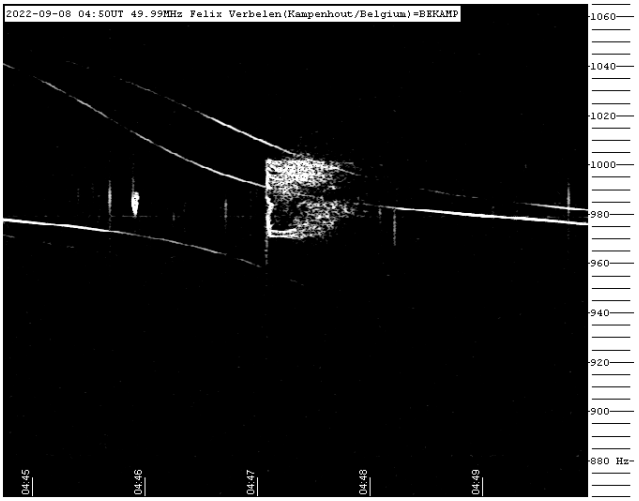

Figure 7 – Meteor reflection 8 September 2022, 04^h50^m UT.

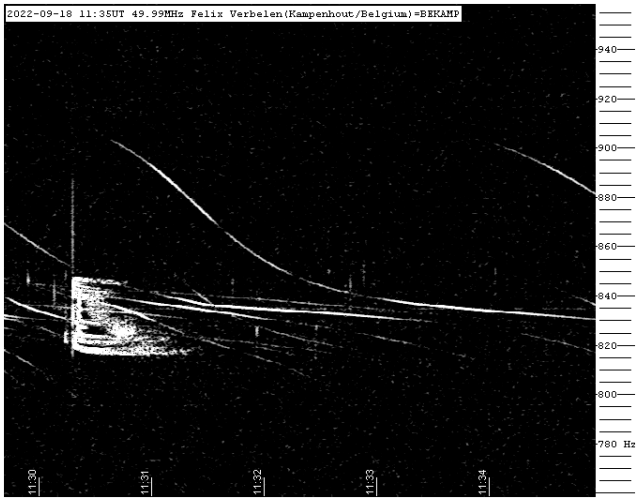

Figure 10 – Meteor reflection 18 September 2022, 11^h35^m UT.

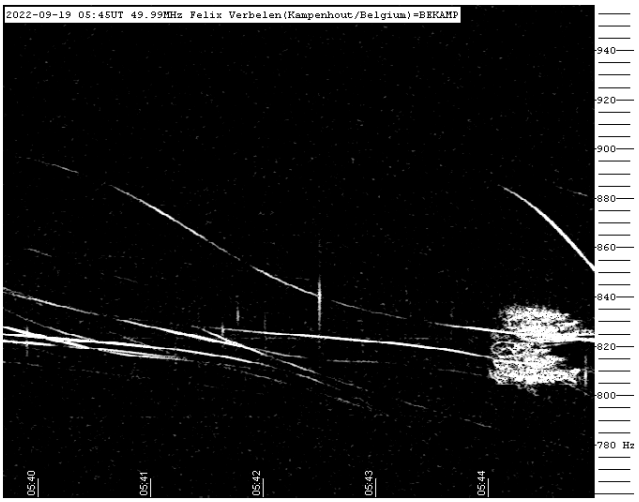

Figure 11 – Meteor reflection 19 September 2022, 05^h45^m UT.

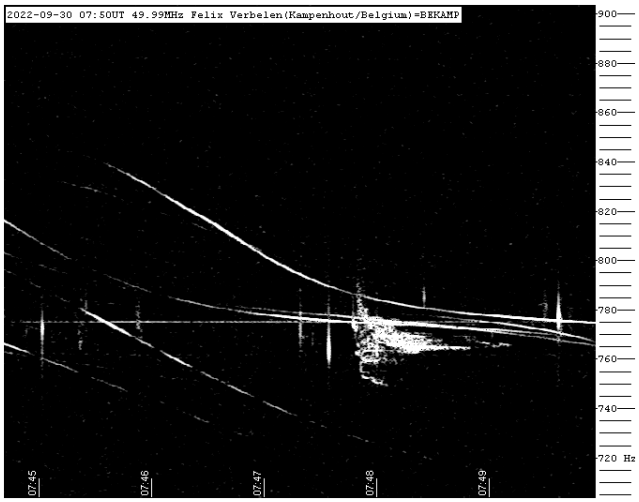

Figure 14 – Meteor reflection 30 September 2022, 07^h50^m UT.

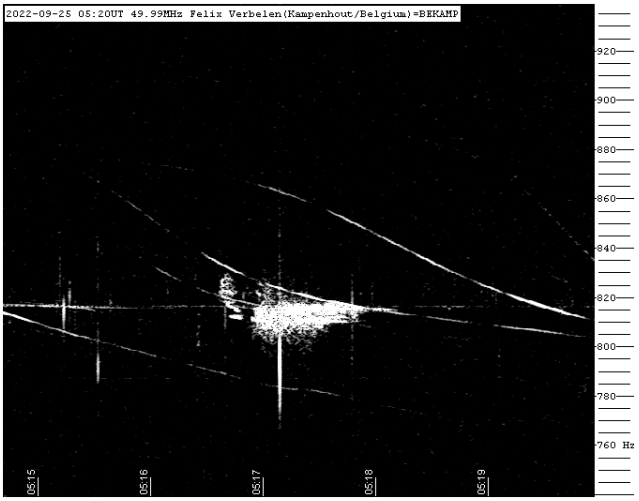

Figure 12 – Meteor reflection 25 September 2022, 05^h20^m UT.

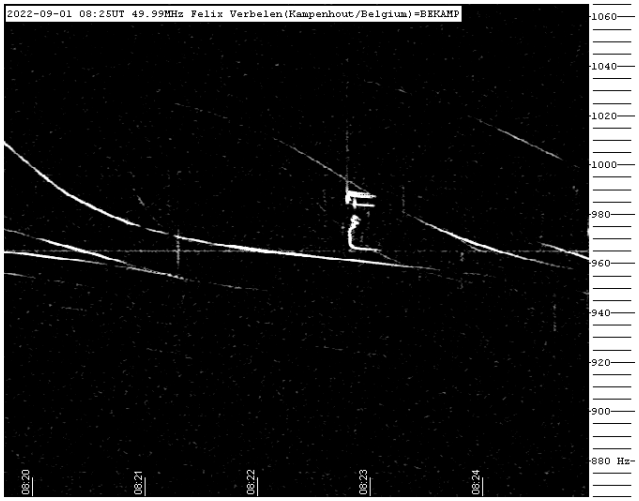

Figure 15 – "Epsilon" 1 September 2022, 08^h25^m UT.

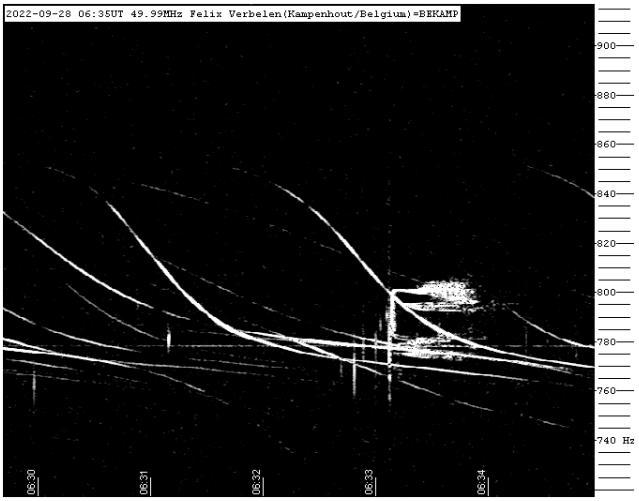

Figure 13 – Meteor reflection 29 September 2022, 06^h35^m UT.

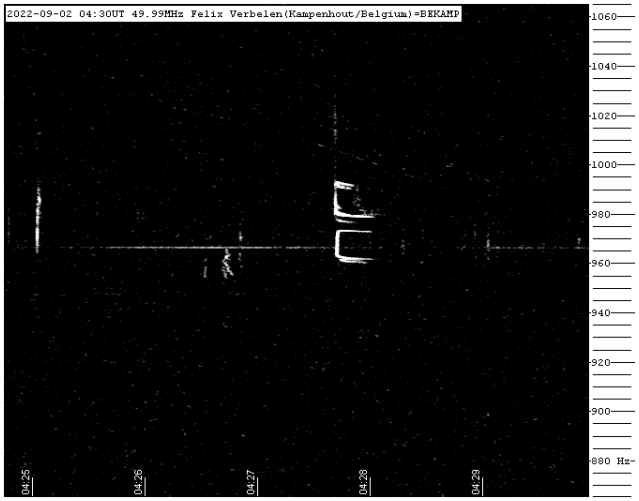

Figure 16 – "Epsilon" 2 September 2022, 04^h30^m UT.

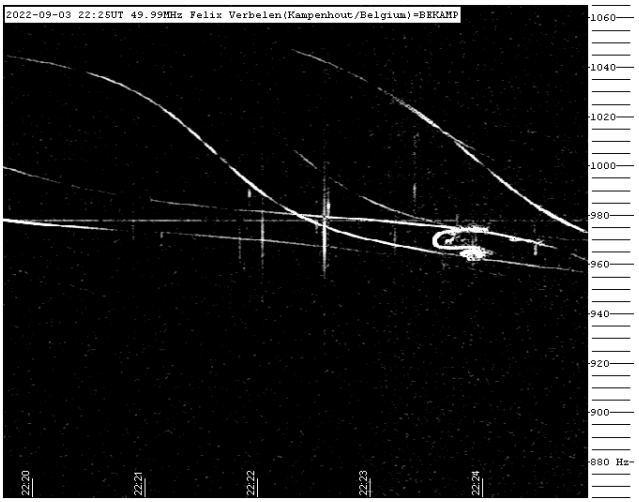

Figure 17 – "Epsilon" 3 September 2022, 22^h25^m UT.

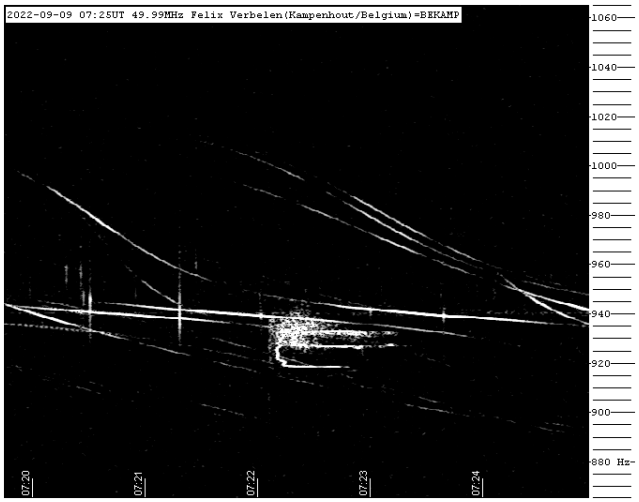

Figure 20 – "Epsilon" 9 September 2022, 07^h25^m UT.

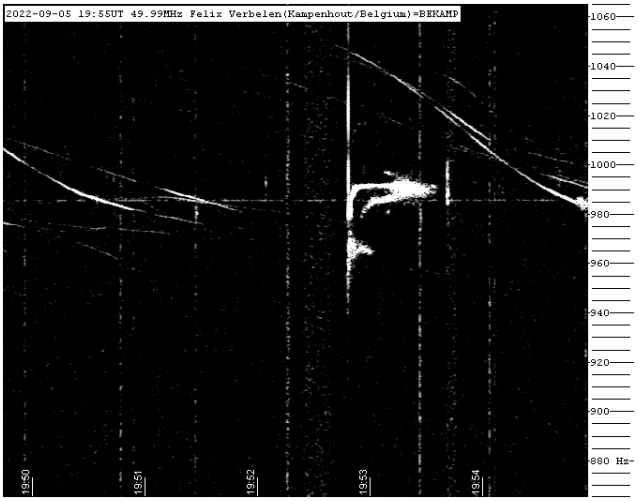

Figure 18 – "Epsilon" 5 September 2022, 19^h55^m UT.

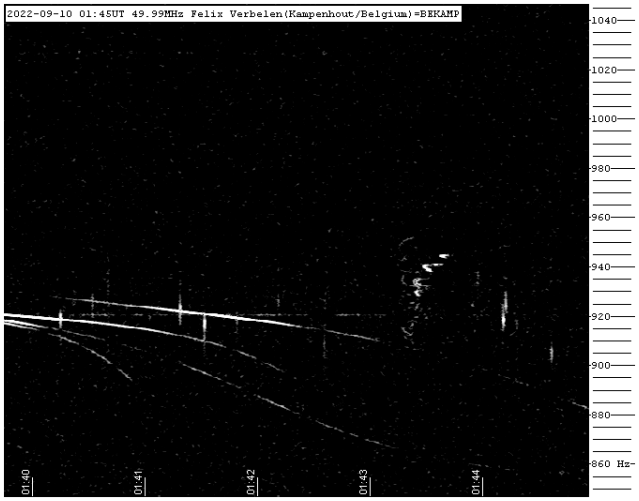

Figure 21 – "Epsilon" 10 September 2022, 01^h45^m UT.

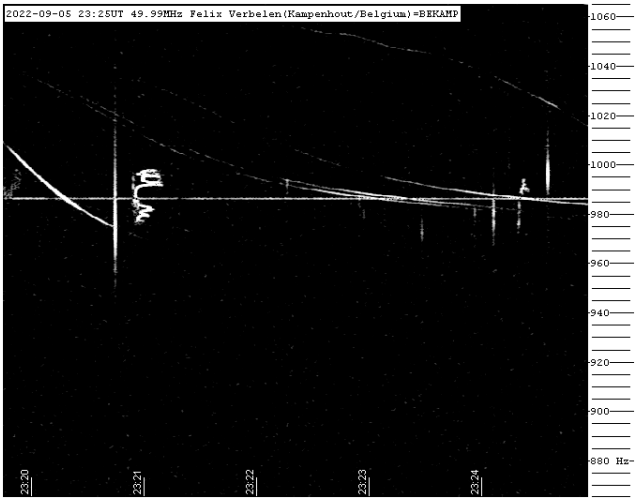

Figure 19 – "Epsilon" 5 September 2022, 23^h25^m UT.

Figure 22 – "Epsilon" 10 September 2022, 03^h30^m UT.

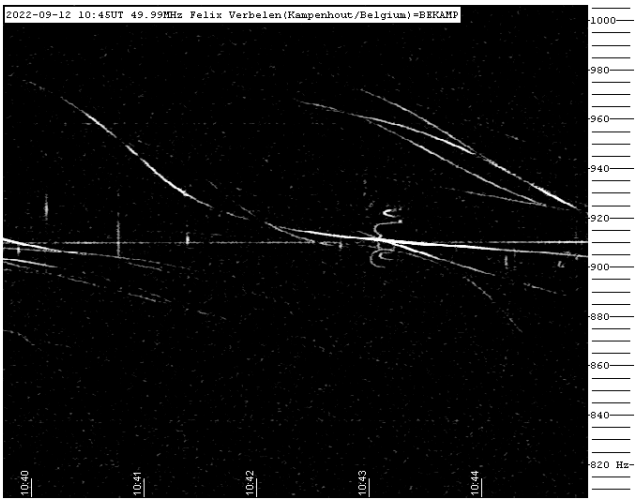

Figure 23 – "Epsilon" 12 September 2022, 10^h45^m UT.

Figure 24 – "Epsilon" 14 September 2022, 05^h05^m UT.

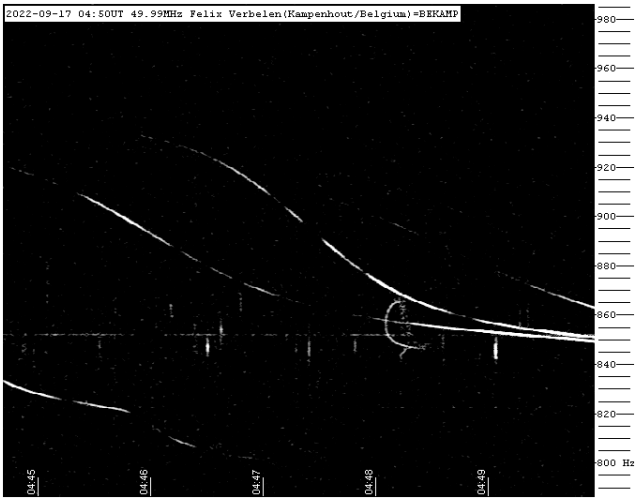

Figure 25 – "Epsilon" 17 September 2022, 04^h50^m UT.

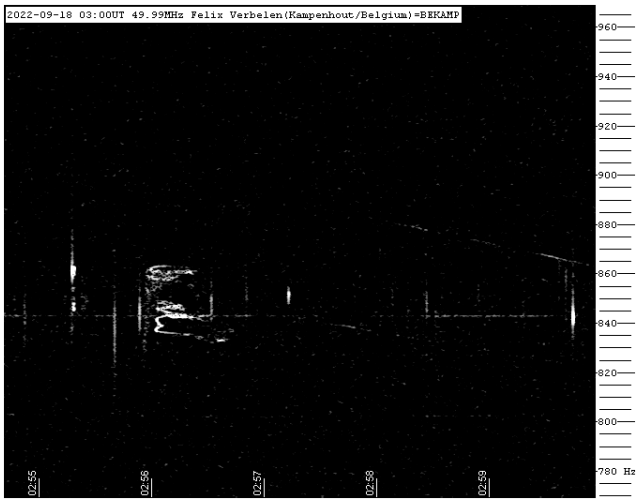

Figure 26 – "Epsilon" 18 September 2022, 03^h00^m UT.

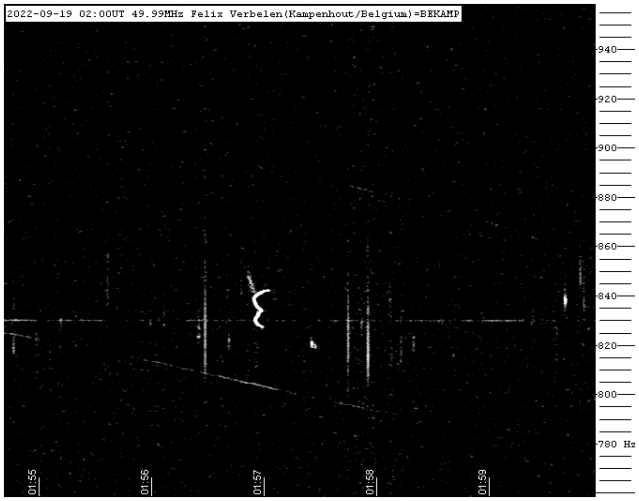

Figure 27 – "Epsilon" 19 September 2022, 02^h00^m UT.

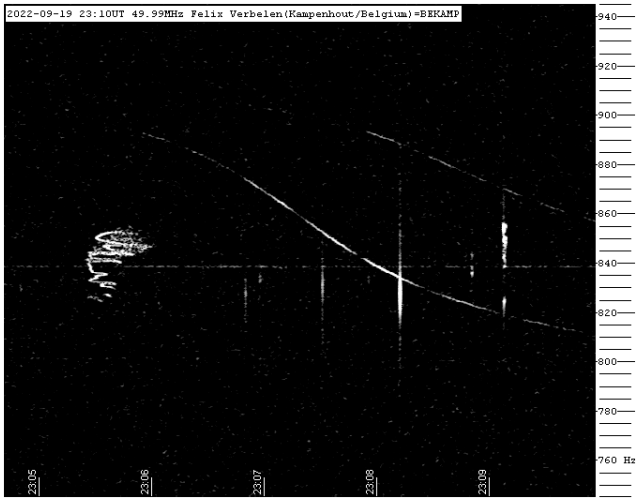

Figure 28 – "Epsilon" 19 September 2022, 23^h10^m UT.

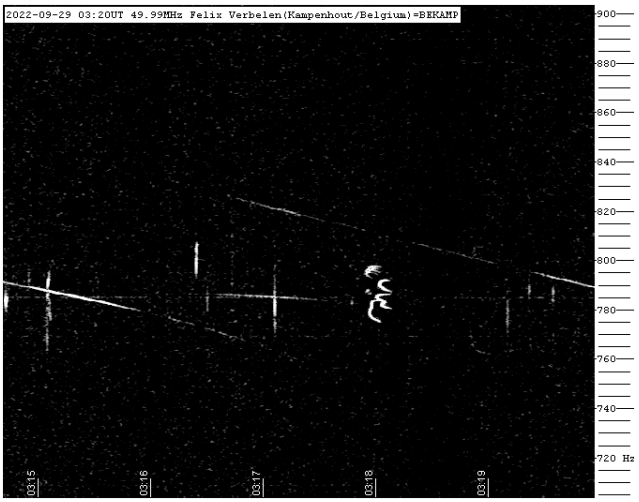

Figure 29 – "Epsilon" 29 September 2022, 03^h20^m UT.

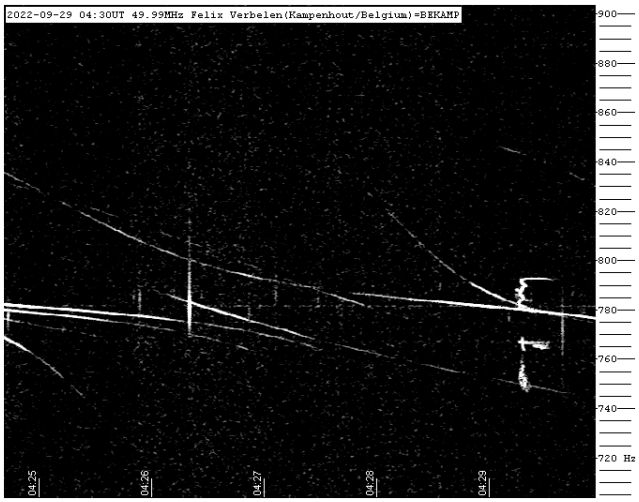

Figure 30 – "Epsilon" 29 September 2022, 04^h30^m UT.

August 2022 report CAMS BeNeLux

Carl Johannink

Am Ollenkamp 4, 48599 Gronau, Germany
c.johannink@t-online.de

A summary of the activity of the CAMS BeNeLux network during the month of August 2022 is presented. This month we collected a total of 57530 multi-station meteors resulting in 14807 orbits.

1 Introduction

August remains the favorite observing month for many amateurs. Especially around August 12 many observers try to observe one of the great showers on the northern hemisphere, the Perseids. Moon wise, the circumstances for meteor observing were bad: Full Moon coincidences nearly exact with the period of the greatest meteor activity. Another aspect that could hamper observations is off course the weather. But this year, that would not be a big problem.

2 August 2022 statistics

The weather in August 2022 was dominated by high pressure over western Europe. Cloudy and rainy weather was nearly absent. As a result, we could collect many meteors simultaneously in every night: in 27 nights the number of orbits was above 100. In 12 nights, the number of orbits exceeded 500 and in 2 nights even more than 1000 orbits were collected. In every night we obtained at least dozens of orbits. During the maximum activity of the Perseids on August 12–13 we could collect 1803 orbits, despite the Full Moon.

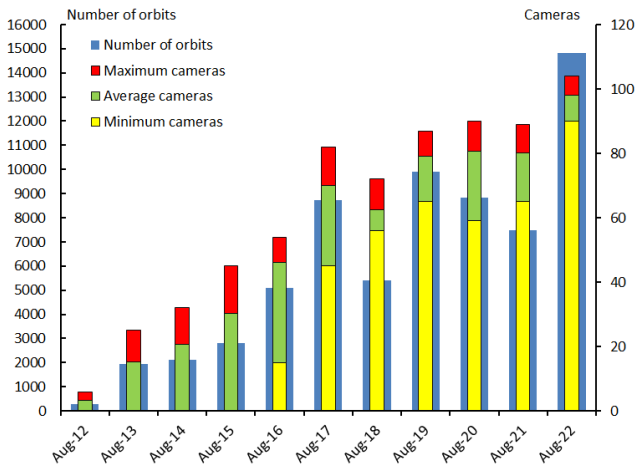

Figure 1 – Comparing August 2022 to previous months of August in the CAMS BeNeLux history. The blue bars represent the number of orbits, the red bars the maximum number of cameras capturing in a single night, the green bar the average number of cameras capturing per night and the yellow bar the minimum number.

The number of orbits this month reached 14807. Nearly 50% more than the highest August number up to then (*Figure 1* and *Table 1*). As said, the very stable weather made this result possible. But another aspect should be mentioned here. Most nights were clear for all stations, from northern France up to the North Sea. The normal decline in the number of clear nights we see in the climate data of our regions, when looking from the southern parts to the northern parts of the BeNeLux, remained absent.

As another aspect of the favorable conditions this month, we see that at least 90 cameras were active every night. This number can be compared with the highest number of active cameras in all previous years (*Table 2*). In this month a maximum of 104 cameras were active in one or more nights. The mean value of active cameras was 98.1 (*Figure 1*).

These high numbers are also a result of some new cameras that were added to our network (*Pierre-Yves Péchart* at Hagnicourt, northern France and *Jim Rowe* at Eastbourne, Great Brittan), and, fortunately, there were only very few technical problems at most stations.

Table 1 – August 2022 compared to previous months of August.

Year	Nights	Orbits	Stations	Max. Cams	Min. Cams	Mean Cams
2012	21	283	5	6	–	3.2
2013	27	1960	13	25	–	15.3
2014	28	2102	14	32	–	20.8
2015	25	2821	15	45	–	30.4
2016	30	5102	20	54	15	46.2
2017	28	8738	21	82	45	69.9
2018	30	5403	19	72	56	62.4
2019	29	9916	23	87	65	79.0
2020	31	8845	24	90	59	80.6
2021	29	7496	27	89	65	80.2
2022	31	14807	31	104	90	98.1
Total	309	67473				

3 A new meteor shower on August 16?

On August 16, 2022, the global CAMS low-light videocamera networks detected an outburst from a mean radiant in the anti-helion source. This new shower was called the 18-Aquariids (Jenniskens, 2022a). The shower was detected first mainly by the networks in the USA and Chile, but when all data was available from our stations, we could add 17 members of this shower which turned out to

be the August delta Capricornids stream (#199 ADC) (Jenniskens, 2022b).

According to Jenniskens there were two peaks in activity. The first peak at August 16 ~08^h40^m UT, not visible for our network. A second peak, a bit stronger, appeared at August 16 ~22^h00^m UT (Jenniskens, 2022b). It was during this peak that our network collected 17 members of this meteoroid stream on August 16, 20^h00^m–23^h45^m UT. The radiant of these meteors was very compact. The spread in right ascension in our data was ~1.5 degree (lowest value for α = 324.2 deg; highest value for α = 325.8 deg). The spread in declination in our data was ~ 1 degree (lowest value for δ = –11.7 deg; highest value for δ = –10.6 deg). For the mean values of the geocentric radiant and the orbital elements of these 17 meteors, see *Table 2*. These results are in good agreement with values found by Jenniskens and Roggemans (Jenniskens, 2022c; 2022d; Roggemans et al., 2022).

Table 2 – Geocentric radiant and orbital elements of 17 August delta Capricornids (ADC#199).

	CAMS BeNeLux	GMN
α (°)	325.3	325.3 ± 0.4
δ (°)	–11.34	–11.5 ± 0.4
v_g (km/s)	24.07	23.9 ± 0.3
H_b (km)	97.2	98.1 ± 2.6
H_e (km)	86.0	84.0 ± 4.2
λ–$\lambda_\odot$ (°)	180.1	180.04 ± 0.35
β (°)	+2.39	+2.28 ± 0.45
a (AU)	3.02	2.91 ± 0.15
q (AU)	0.549	0.551 ± 0.005
e	0.817	0.811 ± 0.01
i (°)	1.96	1.81 ± 0.36
ω (°)	270.9	270.9 ± 0.7
Ω (°)	143.80	143.75 ± 0.18
Π (°)	54.7	54.6 ± 0.7
N	17	123

4 Conclusion

Results in August 2022 are by far the best during 11 years of the CAMS BeNeLux project.

Acknowledgment

Many thanks to all operators of cameras in the CAMS BeNeLux network for their work and quick delivery of data. During this month the CAMS BeNeLux network kept active by the following volunteers:

Hans Betlem (Woold, Netherlands, CAMS 3071, 3072 and 3073), *Jean-Marie Biets* (Wilderen, Belgium, CAMS 379, 380, 381 and 382), *Ludger Boergerding* (Holdorf, Germany, RMS 3801), *Günther Boerjan* (Assenede, Belgium, RMS 3823), Martin Breukers (Hengelo, Netherlands, CAMS 320, 321, 322, 323, 324, 325, 326 and 327, RMS 319, 328 and 329), *Seppe Canonaco* (Genk, RMS 3818 and 3819), *Pierre de Ponthiere* (Lesve, Belgium, RMS 3816 and 3826), *Bart Dessoy* (Zoersel, Belgium, CAMS 397, 398, 804, 805, 806, 3888 and RMS 3827), *Tammo Jan Dijkema* (Dwingeloo, Netherlands, RMS 3199), *Isabelle Ansseau, Jean-Paul Dumoulin, Dominique Guiot* and *Christian Walin* (Grapfontaine, Belgium, CAMS 814 and 815, RMS 3814 and 3817), *Uwe Glässner* (Langenfeld, Germany, RMS 3800), *Luc Gobin* (Mechelen, Belgium, CAMS 3890, 3891, 3892 and 3893), *Tioga Gulon* (Nancy, France, CAMS 3900 and 3901), *Robert Haas* (Alphen aan de Rijn, Netherlands, CAMS 3160, 3161, 3162, 3163, 3164, 3165, 3166 and 3167), *Robert Haas* (Burlage, Germany, RMS 3803 and 3804), *Robert Haas* (Texel, Netherlands, CAMS 810, 811, 812 and 813), *Kees Habraken* (Kattendijke, Netherlands, RMS 378), *Klaas Jobse* (Oostkapelle, Netherlands, CAMS 3030, 3031, 3032, 3033, 3034, 3035, 3036 and 3037), *Carl Johannink* (Gronau, Germany, CAMS 3100, 3101, 3102, 3103, 3104 and 3105), *Reinhard Kühn* (Flatzby, Germany, RMS 3802), *Hervé Lamy* (Dourbes, Belgium, CAMS 394 and 395, RMS 3825), *Hervé Lamy* (Humain, Belgium, CAMS 816, RMS 3821), *Hervé Lamy* (Ukkel, Belgium, CAMS 393), *Koen Miskotte* (Ermelo, Netherlands, CAMS 3051, 3052, 3053 and 3054), *Jos Nijland* (Terschelling, Netherlands, CAMS 841, 842 and 844), *Pierre-Yves Péchart* (Hagnicourt, France, RMS 3902 and 3903), *Tim Polfliet* (Gent, Belgium, CAMS 396, RMS 3820), *Steve Rau* (Oostende, Belgium, RMS 3822), *Steve Rau* (Zillebeke, Belgium, CAMS 3850 and 3852, RMS 3851 and 3853), *Paul and Adriana Roggemans* (Mechelen, Belgium, RMS 3830 and 3831, CAMS 3832, 3833, 3834, 3835, 3836 and 3837), *Jim Rowe* (Eastbourne, Great Britain, RMS 3829), *Hans Schremmer* (Niederkruechten, Germany, CAMS 803), *Erwin van Ballegoij* (Heesh, Netherlands CAMS 3148 and 3149).

References

Jenniskens P. (2022a). "18-Aquariid meteor shower 2022". CBET 5159, published 2022, August 17. Ed.: D. W.E. Green. Cambridge: Central Bureau for Astronomical Telegrams.

Jenniskens P. (2022b). "August delta Capricornids meteor shower". CBET 5161, published 2022, August 26. Ed.: D. W. E. Green. Cambridge: Central Bureau for Astronomical Telegrams.

Jenniskens P. (2022c). "Ongoing outburst from a new radiant on Aquarius/Capricorn border". *eMetN*, **7**, 304–305.

Jenniskens P. (2022d). "August delta Capricornids meteor shower 2022". *eMetN*, **7**, 306.

Roggemans P., Šegon D., Vida D., Greaves J., Sekiguchi S., Angelsky A. and Davydov A. (2022). "Near anti-helion meteor shower outburst recorded by Global Meteor Network". *eMetN*, **7**, 293–301.

September 2022 report CAMS BeNeLux

Carl Johannink

Am Ollenkamp 4, 48599 Gronau, Germany
c.johannink@t-online.de

A summary of the activity of the CAMS BeNeLux network during the month of September 2022 is presented. This month we collected a total of 18236 multi-station meteors resulting in 5446 orbits.

1 Introduction

Although no major meteoroid streams are active in September, meteor activity in general this month is high due to higher sporadic activity. Nights are getting longer, so the effective observing time is increasing significantly in this month. That makes this month very interesting for observing.

2 September 2022 statistics

September 2022 alternated complete clear nights with more or less variable nights. Remarkable is the difference in temperature between the first half (very warm) and the second half of this month (cold). The number of complete clear nights wasn't as high as in August, but on the other side, there was not one night completely clouded out. As a result, CAMS BeNeLux registered a total of 18236 multi-station meteors, resulting in 5446 orbits. See *Figure 1* and *Table 1*.

Especially during September 3–4, 4–5, 20–21, 21–22, 28–29 and 29–30 a large number of orbits (400–500) could be collected. 666 meteors were captured by more than two stations, that is approximately 12% of the total number of orbits.

That number is significantly lower than last month, as a result of the more variable weather: some places did have clear conditions, other places were clouded out at the same time. The mean number of active cameras was ~83. At least 66 cameras were active every night, see *Table 1*. These numbers are also lower than last month. The main reasons were again technical problems, not only with WATECS, but also with some RMS-cameras during this month.

Private reasons caused less results for Alphen and Texel, but in October these stations will be active again.

3 Conclusion

Results for September 2022 are nearly compatible with the results in September 2018. But the results for September 2020 and 2021 were much better.

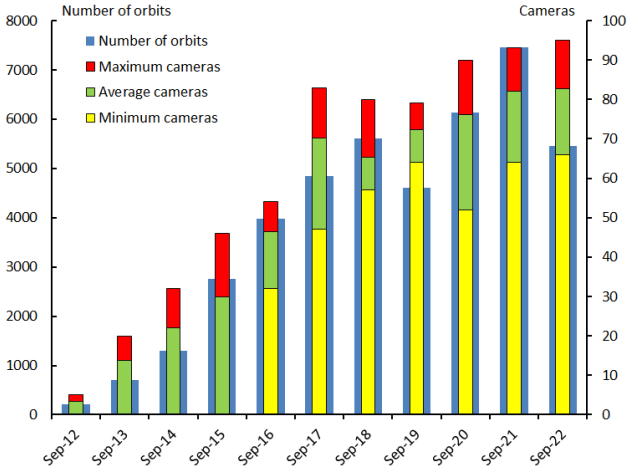

Figure 1 – Comparing September 2022 to previous months of September in the CAMS BeNeLux history. The blue bars represent the number of orbits, the red bars the maximum number of cameras capturing in a single night, the green bar the average number of cameras capturing per night and the yellow bar the minimum number.

Table 1 – September 2022 compared to previous months of September.

Year	Nights	Orbits	Stations	Max. Cams	Min. Cams	Mean Cams
2012	18	209	5	5	–	3.4
2013	19	712	9	20	–	13.7
2014	27	1293	14	32	–	22.0
2015	29	2763	15	46	–	30.0
2016	30	3982	19	54	32	46.5
2017	29	4839	22	83	47	70.2
2018	28	5606	20	80	57	65.4
2019	29	4609	20	79	64	72.3
2020	26	6132	24	90	52	76.2
2021	30	7457	26	93	64	82.0
2022	30	5446	30	95	66	82.8
Total	295	43048				

Acknowledgment

Many thanks to all operators of our cameras in the CAMS BeNeLux network for their efforts and everlasting delivery of data.

In September 2022 the CAMS BeNeLux network was operated by the following volunteers:

Hans Betlem (Woold, Netherlands, CAMS 3071, 3072 and 3073), *Jean-Marie Biets* (Wilderen, Belgium, CAMS 379, 380, 381 and 382), *Ludger Boergerding* (Holdorf, Germany, RMS 3801), *Günther Boerjan* (Assenede, Belgium, RMS 3823), Martin Breukers (Hengelo, Netherlands, CAMS 320, 321, 322, 323, 324, 325, 326 and 327, RMS 319, 328 and 329), *Seppe Canonaco* (Genk, RMS 3818 and 3819), *Pierre de Ponthiere* (Lesve, Belgium, RMS 3816 and 3826), *Bart Dessoy* (Zoersel, Belgium, CAMS 397, 398, 804, 805, 806, 3888 and RMS 3827), *Tammo Jan Dijkema* (Dwingeloo, Netherlands, RMS 3199), *Isabelle Ansseau*, *Jean-Paul Dumoulin*, *Dominique Guiot* and *Christian Walin* (Grapfontaine, Belgium, CAMS 814 and 815, RMS 3814 and 3817), *Uwe Glässner* (Langenfeld, Germany, RMS 3800), *Luc Gobin* (Mechelen, Belgium, CAMS 3890, 3891, 3892 and 3893), *Tioga Gulon* (Nancy, France, CAMS 3900 and 3901), *Robert Haas* (Alphen aan de Rijn, Netherlands, CAMS 3160, 3161, 3162, 3163, 3164, 3165, 3166 and 3167), *Robert Haas* (Texel, Netherlands, CAMS 810, 811, 812 and 813), *Kees Habraken* (Kattendijke, Netherlands, RMS 3780 and 3781), *Klaas Jobse* (Oostkapelle, Netherlands, CAMS 3030, 3031, 3032, 3033, 3034, 3035, 3036 and 3037), *Carl Johannink* (Gronau, Germany, CAMS 3100, 3101, 3102, 3103, 3104 and 3105), *Reinhard Kühn* (Flatzby, Germany, RMS 3802), *Hervé Lamy* (Dourbes, Belgium, CAMS 394 and 395, RMS 3825), *Hervé Lamy* (Humain, Belgium, RMS 3821), *Hervé Lamy* (Ukkel, Belgium, CAMS 393), *Koen Miskotte* (Ermelo, Netherlands, CAMS 3051, 3052, 3053 and 3054), *Pierre-Yves Péchart* (Hagnicourt, France, RMS 3902 and 3903), *Tim Polfliet* (Gent, Belgium, CAMS 396, RMS 3820), *Steve Rau* (Oostende, Belgium, RMS 3822), *Steve Rau* (Zillebeke, Belgium, CAMS 3850 and 3852, RMS 3851 and 3853), *Paul and Adriana Roggemans* (Mechelen, Belgium, RMS 3830 and 3831, CAMS 3832, 3833, 3834, 3835, 3836 and 3837), *Jim Rowe* (Eastbourne, Great Britain, RMS 3829), *Hans Schremmer* (Niederkruechten, Germany, CAMS 803), *Erwin van Ballegoij* (Heesh, Netherlands CAMS 3148 and 3149).

Remarkable fireballs spotted in the framework of the Southwestern Europe Meteor Network along August and September 2022

J. M. Madiedo[1], J. L. Ortiz[1], J. Izquierdo[2], P. Santos-Sanz[1], J. Aceituno[3], E. de Guindos[3], P. Yanguas[4], J. Palacián[4], A. San Segundo[5], D. Ávila[6], B. Tosar[7], A. Gómez-Hernández[8], Juan Gómez-Martínez[8], Antonio García[9], and A.I. Aimee[10]

[1] **Departamento de Sistema Solar, Instituto de Astrofísica de Andalucía (IAA-CSIC), 18080 Granada, Spain**
madiedo@cica.es, ortiz@iaa.es, psantos@iaa.es

[2] **Departamento de Física de la Tierra y Astrofísica, Universidad Complutense de Madrid, 28040 Madrid, Spain**
jizquierdo9@gmail.com

[3] **Observatorio Astronómico de Calar Alto (CAHA), E-04004, Almería, Spain**
aceitun@caha.es, guindos@caha.es

[4] **Departamento de Estadística, Informática y Matemáticas e Institute for Advanced Materials and Mathematics, Universidad Pública de Navarra, 31006 Pamplona, Navarra, Spain**
yanguas@unavarra.es, palacian@unavarra.es

[5] **Observatorio El Guijo (MPC J27), Galapagar, Madrid, Spain**
mpcj27@outlook.es

[6] **Estación de Meteoros de Ayora, Ayora, Valencia, Spain**
David_ayora007@hotmail.com

[7] **Casa das Ciencias. Museos Científicos Coruñeses. A Coruña, Spain**
borjatosar@gmail.com

[8] **Estación de Registro La Lloma, Olocau, Valencia, Spain**
curso88@gmail.com

[9] **Estación de Meteoros de Cullera (Faro de Cullera), Valencia, Spain**
antonio.garcia88@joseantoniogarcia.com

[10] **Southwestern Europe Meteor Network, 41012 Sevilla, Spain**
swemn.server@gmail.com

Some of the bright bolides observed in the framework of the Southwestern Europe Meteor Network between August and September 2022 are described in this work. These have been spotted from the Iberian Peninsula. Their maximum luminosity ranges from mag. –7 to mag. –12. One of these bolides gave rise to a meteorite.

1 Introduction

Our meteor network performs a systematic monitoring of meteor activity in the framework of the SMART project (Spectroscopy of Meteoroids by means of Robotic Technologies), which started operation in 2006 to analyze the properties of meteoroids ablating in our planet's atmosphere. This includes chemical data derived from the emission spectra of meteors generated by these particles of interplanetary matter. This survey, which is being conducted in the framework of the Southwestern Europe Meteor Network (SWEMN), employs an array of automated spectrographs deployed at meteor-observing stations in Spain (Madiedo, 2014; Madiedo, 2017). This allows to derive the luminous path of meteors and the orbit of their progenitor meteoroids, and also to study the evolution of meteor plasmas from the emission spectrum produced by these events (Madiedo, 2015a,b). SMART also provides important information for our MIDAS project, which is being conducted by the Institute of Astrophysics of Andalusia (IAA-CSIC) to study lunar impact flashes produced when large meteoroids impact the Moon (Madiedo et al., 2015; Madiedo et al., 2018; Madiedo et al. 2019; Ortiz et al., 2015).

In this work we focus on the preliminary analysis of seven fireballs recorded by the SWEMN network between August and September 2022. One of them was a meteorite-producing bolide that overflew the Mediterranean Sea. This work has been fully written by AIMIE (acronym for Artificial Intelligence with Meteoroid Environment Expertise) from the records included in the SWEMN fireball database (Madiedo et al., 2021; Madiedo et al., 2022).

2 Equipment and methods

To record the events presented in this work we have used Watec 902H2 and Watec 902 Ultimate CCD cameras. Their field of view ranges from around 62 × 50 degrees to about 14 × 11 degrees. We have also employed digital CMOS color cameras (models Sony A7S and A7SII) operating in HD video mode (1920 × 1080 pixels). These cover a field of view of around 70 × 40 degrees. A detailed description of this hardware and the way it operates was given in previous works (Madiedo, 2017). Besides digital CMOS cameras manufactured by ZWO, model ASI185MC were used. The atmospheric paths of the events were triangulated by employing the SAMIA software, developed by J. M. Madiedo. This program employs the planes-intersection method (Ceplecha, 1987).

Figure 1 – Stacked image of the SWEMN20220803_001420 meteor as recorded from Calar Alto.

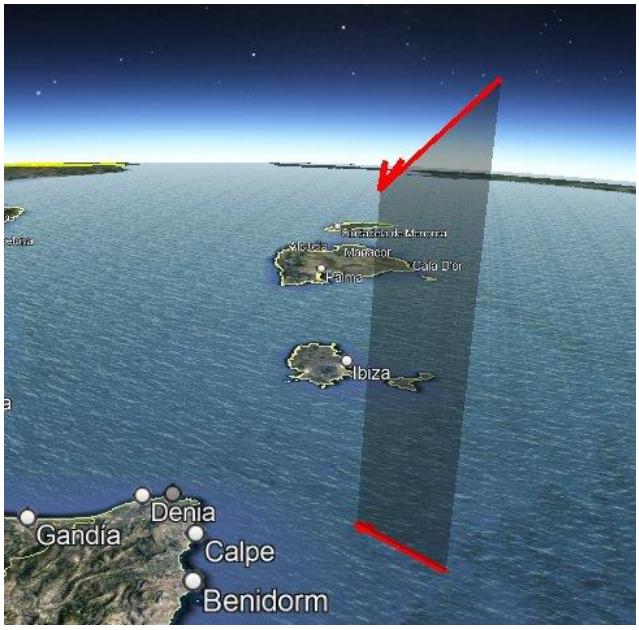

Figure 2 – Atmospheric path of the SWEMN20220803_001420 fireball, and its projection on the ground.

3 The 2022 August 3 event

We spotted this bright bolide from the meteor-observing stations located at Ayora, Huelva, La Hita, CAHA, OSN, La Sagra, and Sevilla. The bright meteor was captured on 2022 August 3, at $0^h14^m20.0 \pm 0.1^s$ UT. The peak brightness the event, which exhibited a bright flare at the final phase of its atmospheric trajectory, was equivalent to an absolute magnitude of –9.0 ± 1.0 (*Figure 1*). This flare occurred as a consequence of the sudden break-up of the meteoroid. It was added to the SWEMN meteor database with the code SWEMN20220803_001420. A video about this bolide was uploaded to YouTube[28].

Atmospheric trajectory, radiant and orbit

It was concluded according to the analysis of the atmospheric path of the meteor that this bolide overflew the Mediterranean Sea. Its initial altitude was $H_b = 106.7 \pm 0.5$ km. The fireball penetrated the atmosphere till a final height $H_e = 81.1 \pm 0.5$ km. The equatorial coordinates found for the apparent radiant are $\alpha = 307.82º$, $\delta = –7.43º$. The entry velocity in the atmosphere obtained for the parent meteoroid was $v_\infty = 24.2 \pm 0.3$ km/s. *Figure 2* shows the obtained projection on the ground of the trajectory in our atmosphere of the event. *Figure 3* shows the orbit in the Solar System of its progenitor meteoroid.

Table 1 – Orbital data (J2000) of the progenitor meteoroid before its encounter with our planet.

a (AU)	2.8 ± 0.1	ω (º)	261.29 ± 00.03
e	0.77 ± 0.01	Ω (º)	130.348137 ± 10^{-5}
q (AU)	0.638 ± 0.003	i (º)	6.0 ± 0.1

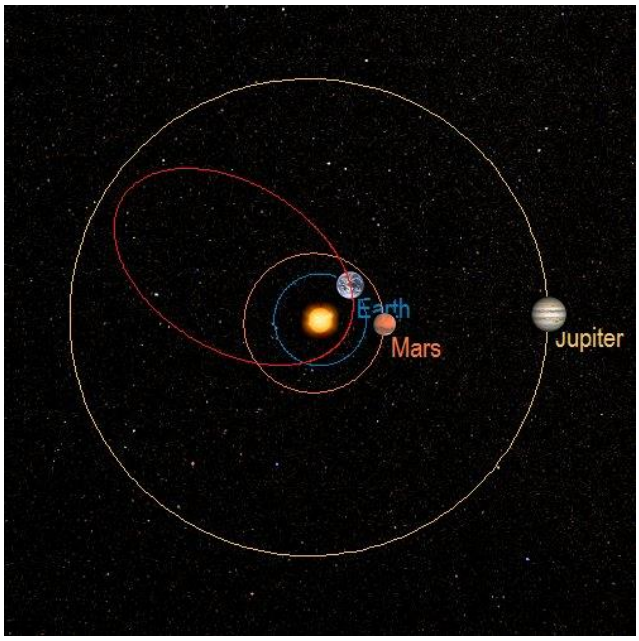

Figure 3 – Projection on the ecliptic plane of the orbit of the SWEMN20220803_001420 fireball.

The parameters of the orbit of the progenitor meteoroid

[28] https://youtu.be/5gNGIOsfUDI

before its encounter with our planet have been included in *Table 1*, and the geocentric velocity yields v_g = 21.6 ± 0.3 km/s. The value found for the Tisserand parameter referred to Jupiter (T_J = 2.75) indicates that the meteoroid followed a cometary (JFC) orbit before entering our atmosphere. These values and the derived radiant confirm that the fireball was linked to the α-Capricornids (IAU meteor shower code CAP#0001). The proposed progenitor body of this shower, which peaks around August 1, is Comet 169P/NEAT (= 2002 EX12) (Jenniskens et al., 2016).

Figure 4 – Stacked image of the SWEMN20220805_002528 event as recorded from Calar Alto.

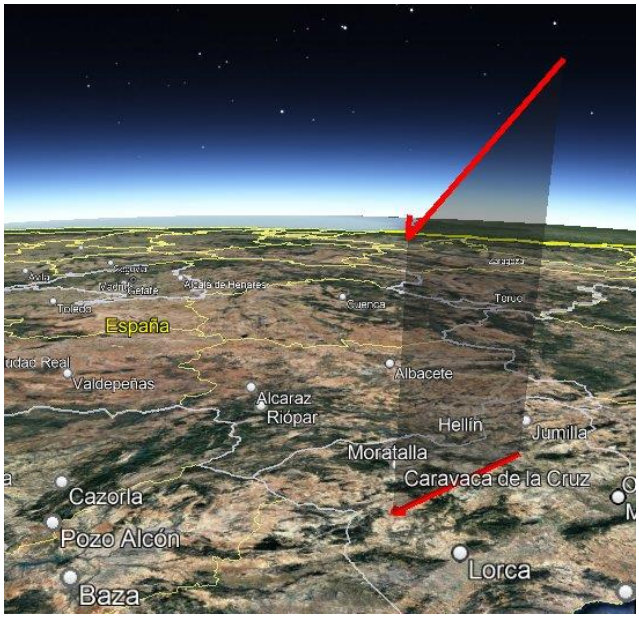

Figure 5 – Atmospheric path of the SWEMN20220805_002528 event, and its projection on the ground.

4 Description of the 2022 August 5 meteor

This gorgeous event was spotted on 2022 August 5 at $0^h25^m28.0 \pm 0.1^s$ UT from the meteor-observing stations located at La Hita, CAHA, OSN, La Sagra, and Sevilla. The bolide, which presented a bright flare at the terminal stage of its atmospheric path, had a peak absolute magnitude of –11.0 ± 1.0 (*Figure 4*). This flare arose as a consequence of the sudden disruption of the meteoroid. It was included in the SWEMN meteor database with the code SWEMN20220805_002528.

Atmospheric path, radiant and orbit

The calculation of the atmospheric path of the fireball allowed to conclude that this event overflew Murcia (Spain). The luminous event began at an altitude H_b = 124.3 ± 0.5 km. The bolide penetrated the atmosphere till a final height H_e = 79.6 ± 0.5 km. The equatorial coordinates of the apparent radiant yield α = 38.72º, δ = +54.76º. Besides, we concluded that the meteoroid impacted the atmosphere with a velocity v_∞ = 60.9 ± 0.5 km/s. The obtained luminous path of the fireball is shown in *Figure 5*. The heliocentric orbit of the meteoroid is drawn in *Figure 6*.

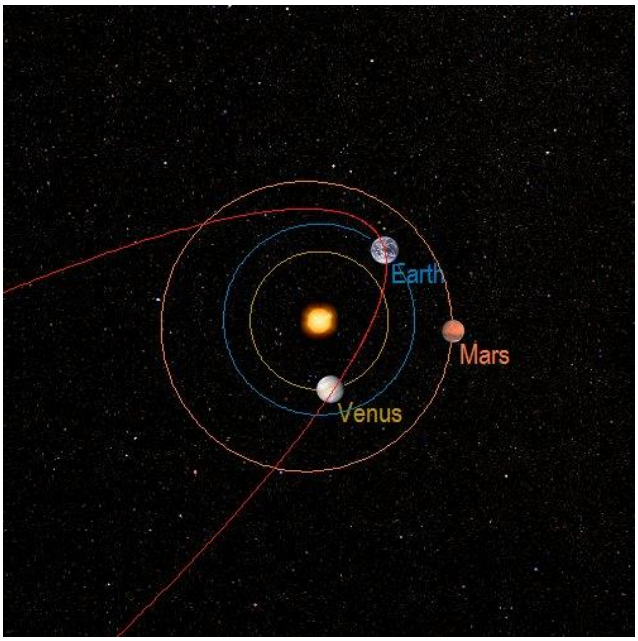

Figure 6 – Projection on the ecliptic plane of the orbit of the SWEMN20220805_002528 bolide.

This event was named “Don Gonzalo”, because the bright meteor overflew this locality during its final phase. The parameters of the orbit of the progenitor meteoroid before its encounter with our planet are included in *Table 2*. The geocentric velocity obtained for the particle yields v_g = 59.7 ± 0.5 km/s. The value derived for the Tisserand parameter with respect to Jupiter (T_J = –0.24) indicates that before hitting our planet’s atmosphere the particle was moving on a cometary (HTC) orbit. By taking into account this orbit and the radiant position, the fireball was produced by the Perseid meteoroid stream (IAU code PER#0007), whose parent is Comet 109P/Swift-Tuttle (Jenniskens et al., 2016).

Table 2 – Orbital data (J2000) of the progenitor meteoroid before its encounter with our planet.

a (AU)	20.2 ± 17.	ω (º)	148.9 ± 00.7
e	0.95 ± 0.03	Ω (º)	132.292253 ± 10-5
q (AU)	0.943 ± 0.001	i (º)	114.9 ± 0.3

5 The 2022 August 11 meteor

This bright fireball was recorded by the systems operated by the SWEMN network at $4^h08^m35.0 \pm 0.1^s$ UT on 2022 August 11. The event, which exhibited a bright flare at the final phase of its path in the atmosphere, had a peak absolute magnitude of –9.0 ± 1.0 (*Figure 7*). This flare appeared as a consequence of the sudden disruption of the meteoroid. Its code in the SWEMN meteor database is SWEMN20220811_040835. The bright meteor can be viewed on this YouTube video[29].

Figure 7 – Stacked image of the SWEMN20220811_040835 meteor as recorded from Sierra Nevada.

Atmospheric path, radiant and orbit

This fireball overflew Jaén and Córdoba (Spain). Its initial altitude was H_b = 113.3 ± 0.5 km. The bolide penetrated the atmosphere till a final height H_e = 74.9 ± 0.5 km. The apparent radiant was located at the equatorial coordinates α = 48.63º, δ = +56.28º. The meteoroid hit the atmosphere with an initial velocity v_∞ = 60.8 ± 0.4 km/s. *Figure 8* shows the obtained path in the atmosphere of the bright meteor. The heliocentric orbit of the meteoroid is drawn in *Figure 9*.

The name given to the fireball was "Los Noguerones", since the bolide passed near the zenith of this locality during its initial phase. The orbital parameters of the parent meteoroid before its encounter with our planet have been listed in *Table 3*. The geocentric velocity of the meteoroid was v_g = 59.7 ± 0.4 km/s. From the value derived for the Tisserand parameter referred to Jupiter (T_J = –0.22), we found that the meteoroid followed a cometary (HTC) orbit before entering the atmosphere. These values and the derived radiant confirm that this bolide was also linked to the Perseids (IAU code PER#0007). The proposed progenitor body of this shower is Comet 109P/Swift-Tuttle (Jenniskens et al., 2016).

Figure 8 – Atmospheric path of the SWEMN20220811_040835 bolide, and its projection on the ground.

Table 3 – Orbital data (J2000) of the progenitor meteoroid before its encounter with our planet.

a (AU)	18.3 ± 11.	ω (º)	147.0 ± 00.6
e	0.94 ± 0.03	Ω (º)	138.190897 ± 10-5
q (AU)	0.934 ± 0.001	i (º)	115.0 ± 0.2

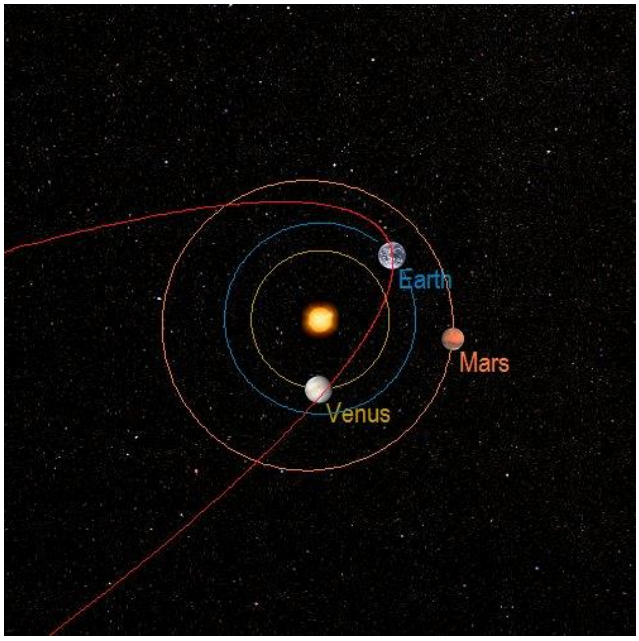

Figure 9 – Projection on the ecliptic plane of the orbit of the SWEMN20220811_040835 event.

[29] https://youtu.be/h79yEPYIB1k

6 Description of the 2022 August 17 meteor

This bright event was captured by the systems operated by the SWEMN network at $21^h18^m55.0 \pm 0.1^s$ UT on 2022 August 17 (*Figure 10*). It had a peak absolute magnitude of –9.0 ± 0.5. The code assigned to the event in the SWEMN meteor database is SWEMN20220817_211855. A video about this fireball can be viewed on YouTube[30]. Casual observers saw the bolide crossing the sky and reported the event on social networks.

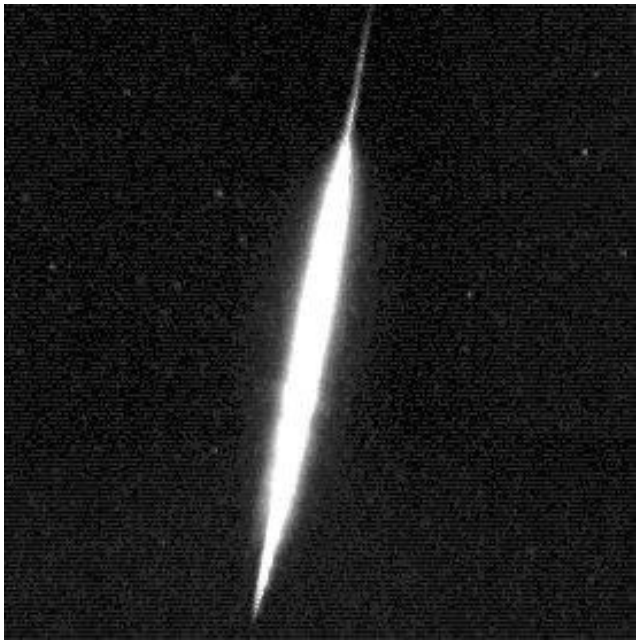

Figure 10 – Stacked image of the SWEMN20220817_211855 bolide.

Figure 11 – Atmospheric path of the SWEMN20220817_211855 event, and its projection on the ground.

Atmospheric path, radiant and orbit

The calculation of the atmospheric path of the fireball led to the conclusion that this bolide overflew the Mediterranean Sea. The luminous event began at an altitude $H_b = 82.3 \pm 0.5$ km. The event penetrated the atmosphere till a final height $H_e = 23.4 \pm 0.5$ km. The equatorial coordinates obtained for the apparent radiant are $\alpha = 256.37^o$, $\delta = +27.68^o$. The meteoroid hit the atmosphere with an initial velocity $v_\infty = 15.1 \pm 0.3$ km/s. *Figure 11* shows the calculated trajectory in the atmosphere of the fireball.

Figure 12 shows the orbit in the Solar System of the parent meteoroid, and *Table 4* shows the corresponding orbital parameters. The geocentric velocity of the meteoroid was $v_g = 10.5 \pm 0.4$ km/s. The Tisserand parameter referred to Jupiter ($T_J = 3.14$) suggests that before colliding with our atmosphere the particle was moving on an asteroidal orbit. These values and the calculated radiant confirm the sporadic nature of the bolide.

From the calculation of the trajectory in our atmosphere it was inferred that the meteoroid was not completely ablated in the atmosphere. Thus, a part of it survived and reached the ground as a meteorite. The full circumstances of this fall are still under analysis.

Table 4 – Orbital data (J2000) of the progenitor meteoroid before its encounter with our planet.

a (AU)	2.5 ± 0.1	ω (º)	185.0 ± 00.1
e	0.60 ± 0.02	Ω (º)	144.631242 ± 10-5
q (AU)	1.0109 ± 0.0001	i (º)	11.6 ± 0.4

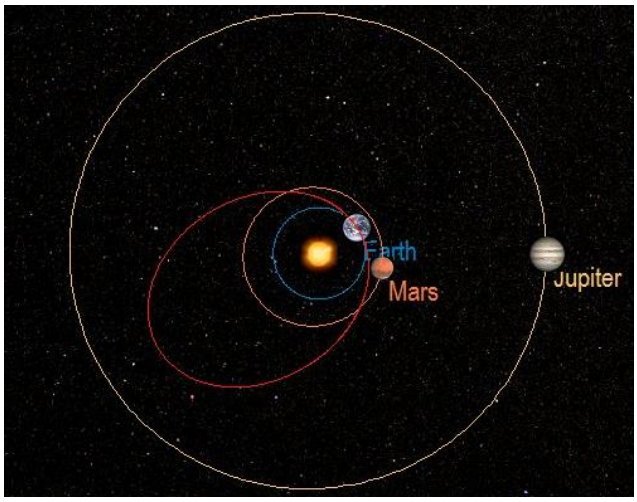

Figure 12 – Projection on the ecliptic plane of the orbit of the SWEMN20220817_211855 meteor.

Figure 13 – Stacked image of the SWEMN20220817_214643 event.

[30] https://youtu.be/IiFAVbL5sdw

7 The 2022 August 17 event

This bright fireball was recorded on 2022 August 17, at $21^h46^m43.0 \pm 0.1^s$ UT (*Figure 13*). The maximum luminosity the bright meteor, that showed a series of flares along its atmospheric trajectory, was equivalent to an absolute magnitude of –10.0 ± 1.0. These flares appeared as a consequence of the sudden disruption of the meteoroid. The code given to the fireball in the SWEMN meteor database is SWEMN20220817_214643. A video about this bright meteor was uploaded to YouTube[31]. The event could also be observed by a wide number of causal eyewitnesses. that reported the event on social networks.

Figure 14 – Atmospheric path of the SWEMN20220817_214643 fireball, and its projection on the ground.

Atmospheric path, radiant and orbit

This event overflew Spain and the Mediterranean Sea. Its initial altitude was $H_b = 103.7 \pm 0.5$ km. The fireball penetrated the atmosphere till a final height $H_e = 68.2 \pm 0.5$ km. From the analysis of the atmospheric path, we also inferred that the apparent radiant was located at the position $\alpha = 316.96^o$, $\delta = -10.70^o$. Besides, we obtained that the meteoroid impacted the atmosphere with a velocity $v_\infty = 24.2 \pm 0.3$ km/s. The calculated atmospheric trajectory of the bright meteor is shown in *Figure 14*. The orbit in the Solar System of the meteoroid is shown in *Figure 15*.

Table 5 – Orbital data (J2000) of the progenitor meteoroid before its encounter with our planet.

a (AU)	4.2 ± 0.3	ω (º)	253.34 ± 00.03
e	0.83 ± 0.01	Ω (º)	144.597323 ± 10-5
q (AU)	0.683 ± 0.002	i (º)	1.61 ± 0.08

The name given to the bright meteor was “Las Matanzas”, since the event was located over this locality during its final phase. The orbital parameters of the parent meteoroid before its encounter with our planet are listed in *Table 5*. The geocentric velocity of the meteoroid was $v_g = 21.4 \pm 0.3$ km/s. The value obtained for the Tisserand parameter with respect to Jupiter ($T_J = 2.20$) shows that before colliding with our planet’s atmosphere the meteoroid was moving on a cometary (JFC) orbit. These parameters and the calculated radiant confirm that the event was associated with the August ν-Aquariids (IAU code ANA#0467). The proposed progenitor body of this shower, which peaks around August 12, is Comet 72P/Denning-Fujikawa (Kornos et al., 2014).

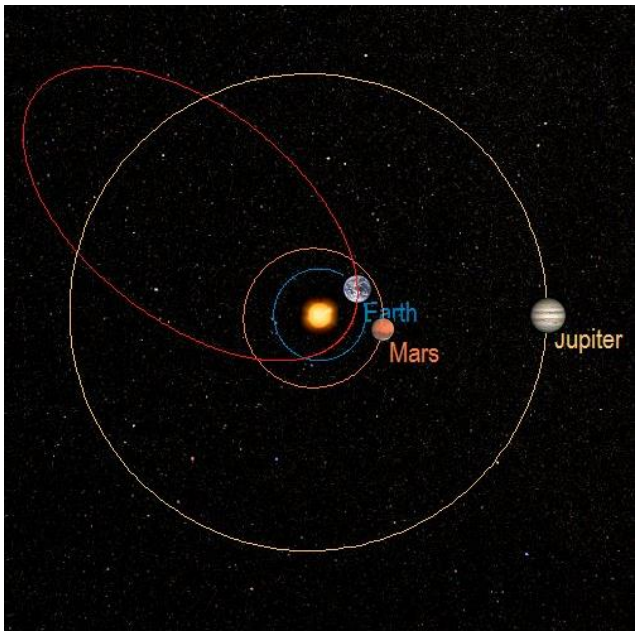

Figure 15 – Projection on the ecliptic plane of the orbit of the SWEMN20220817_214643 fireball.

8 Description of the 2022 September 3 event

Figure 16 – Stacked image of the SWEMN20220903_033415 event.

This notable bolide was spotted on 2022 September 3, at $3^h34^m15.0 \pm 0.1^s$ UT (*Figure 16*). The maximum luminosity the fireball, that presented various flares along its trajectory in the atmosphere, was equivalent to an absolute magnitude of –12.0 ± 1.0. These flares took place as a consequence of the sudden disruption of the meteoroid. Its code in the

[31] https://youtu.be/e_AjJItElUA

SWEMN meteor database is SWEMN20220903_033415. A video about this fireball can be viewed on YouTube[32].

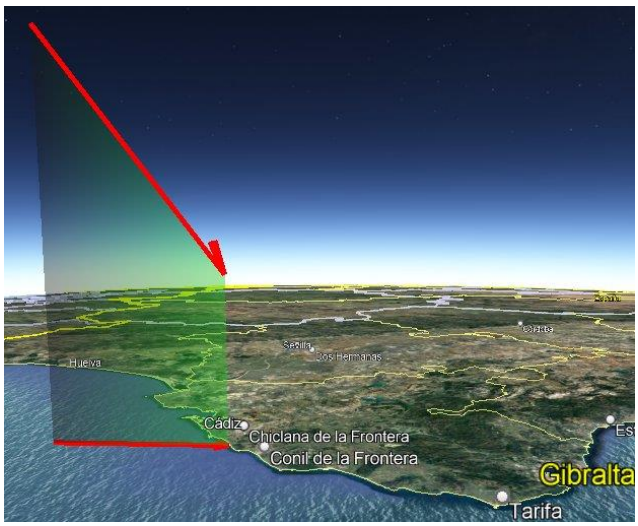

Figure 17 – Atmospheric path of the SWEMN20220903_033415 event, and its projection on the ground.

Atmospheric path, radiant and orbit

By calculating the trajectory in our atmosphere of the bolide it was concluded that this event overflew the Gulf of Cádiz. Its initial altitude was $H_b = 93.3 \pm 0.5$ km. The bright meteor penetrated the atmosphere till a final height $H_e = 38.5 \pm 0.5$ km. The equatorial coordinates of the apparent radiant yield $\alpha = 325.84^o$, $\delta = +51.18^o$. The meteoroid stroke the atmosphere with an initial velocity $v_\infty = 15.7 \pm 0.3$ km/s. The calculated luminous path of the event is shown in *Figure 17*. The orbit in the Solar System of the meteoroid is shown in *Figure 18*.

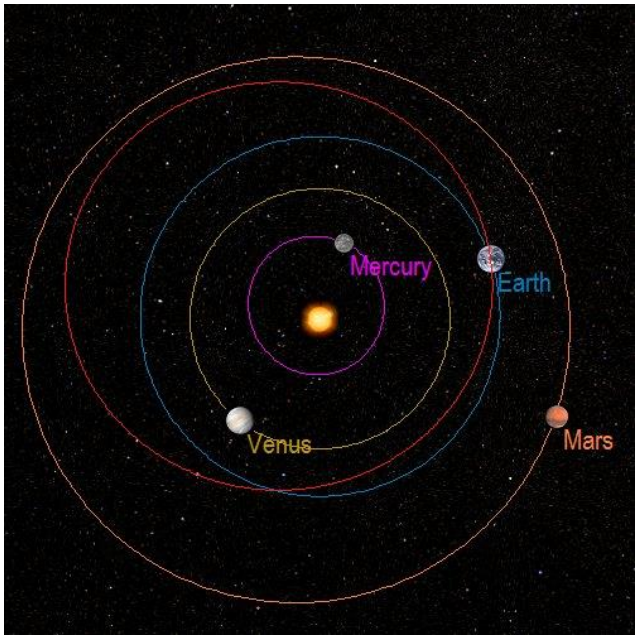

Figure 18 – Projection on the ecliptic plane of the orbit of the SWEMN20220903_033415 fireball.

Table 6 shows the orbital parameters of the parent meteoroid before its encounter with our planet., and the geocentric velocity yields $v_g = 11.4 \pm 0.4$ km/s. The value obtained for the Tisserand parameter referred to Jupiter ($T_J = 5.18$) reveals that the meteoroid was moving on an asteroidal orbit before colliding with our planet's atmosphere. By taking into account these orbital data and the radiant position, it was inferred that the fireball was generated by a sporadic meteoroid.

Table 6 – Orbital data (J2000) of the progenitor meteoroid before its encounter with our planet.

a (AU)	1.211 ± 0.007	ω (º)	240.0 ± 00.5
e	0.250 ± 0.007	Ω (º)	160.324857 ± 10-5
q (AU)	0.907 ± 0.004	i (º)	18.3 ± 0.6

Figure 19 – Stacked image of the SWEMN20220926_004442 event.

9 Analysis of the 2022 September 26 bolide

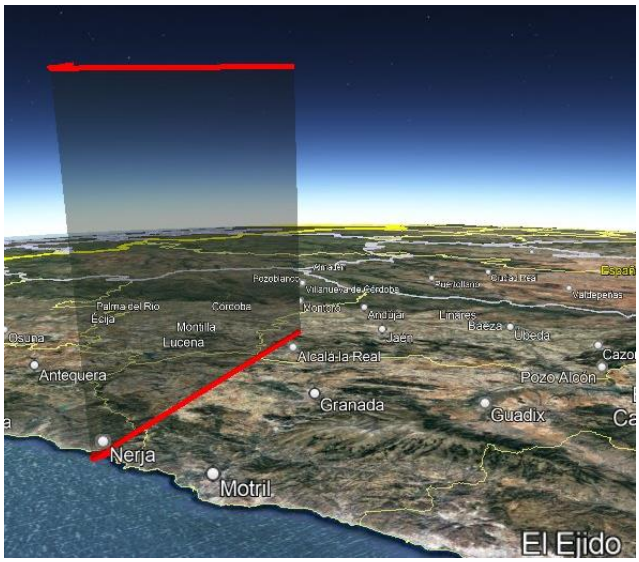

Figure 20 – Atmospheric path of the SWEMN20220926_004442 meteor, and its projection on the ground.

This bright event was captured on 2022 September 26 at $0^h44^m42.6 \pm 0.1^s$ UT from the SWEMN meteor-observing stations located at Huelva, La Hita, CAHA, OSN, La Sagra,

[32] https://youtu.be/HpgANm_vT_w

and Sevilla. The fireball was an Earth-grazer that had a peak absolute magnitude of –7.0 ± 0.5 (*Figure 19*). The code given to the bright meteor in the SWEMN meteor database is SWEMN20220926_004442. A video with images of the fireball and its trajectory in our atmosphere was uploaded to YouTube[33].

Atmospheric path, radiant and orbit

This bolide overflew the provinces of Jaén and Granada (south of Spain). The luminous event began at an altitude H_b = 88.1 ± 0.5 km. The bright meteor penetrated the atmosphere till a final height H_e = 78.8 ± 0.5 km. The equatorial coordinates of the apparent radiant yield α = 211.93º, δ = +55.77º. Besides, we concluded that the meteoroid collided with the atmosphere with a velocity v_∞ = 16.5 ± 0.2 km/s. *Figure 20* shows the calculated atmospheric trajectory of the fireball. The orbit in the Solar System of the meteoroid is shown in *Figure 21*.

Table 7 – Orbital data (J2000) of the progenitor meteoroid before its encounter with our planet.

a (AU)	1.277 ± 0.008	ω (º)	118.1 ± 00.1
e	0.314 ± 0.005	Ω (º)	182.616433 ± 10-5
q (AU)	0.876 ± 0.001	i (º)	16.5 ± 0.4

The bolide was named "Tocón", because the event was located over this locality during its final phase. *Table 7* shows the orbital parameters of the progenitor meteoroid before its encounter with our planet., and the geocentric velocity derived in this case was v_g = 12.3 ± 0.3 km/s. From the value derived for the Tisserand parameter with respect to Jupiter (T_J = 4.98), we found that the particle followed an asteroidal orbit before entering the atmosphere. By taking into account this orbit and the radiant position, the bright meteor was linked to the sporadic background.

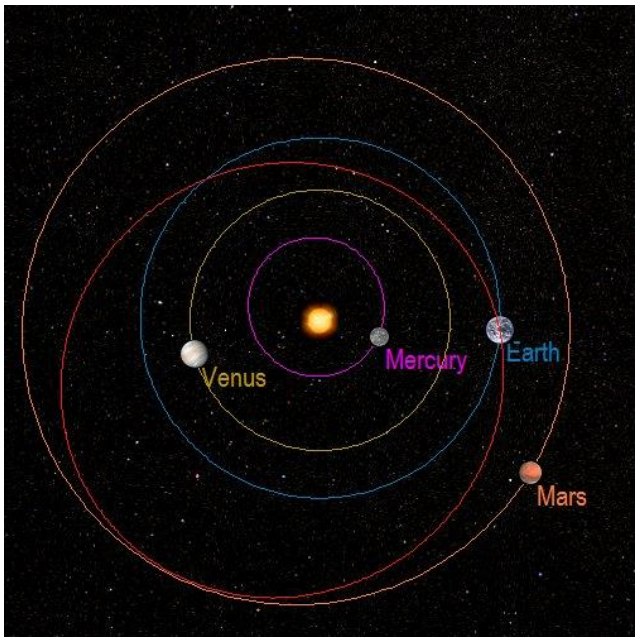

Figure 21 – Projection on the ecliptic plane of the orbit of the SWEMN20220926_004442 fireball.

10 Conclusions

We have analyzed in this work some of the most remarkable meteors recorded by our meteor-observing stations from August to September 2022. Their peak absolute brightness ranges from mag. –7 to mag. –12.

The first bolide described in this paper was recorded on August 3. It reached a peak absolute magnitude of –9.0, and was associated with the α-Capricornids (CAP#0001). This meteor overflew the Mediterranean Sea. The particle was moving on a cometary (JFC) orbit before hitting our atmosphere and exhibited the typical final flare of bright members of this shower.

The second fireball analyzed here was the "Don Gonzalo" event, which was recorded on August 5. Its peak magnitude was –11.0. The bolide was produced by a Perseid meteoroid and overflew Murcia (Spain). The progenitor body of this meteoroid stream is Comet 109P/Swift-Tuttle.

The next bright meteor described here was the "Los Noguerones" bolide. This was recorded on August 11. It also belonged to the Perseids (PER#0007). Its peak magnitude was –9.0 and overflew the provinces of Jaén and Córdoba (south of Spain).

The fourth fireball analyzed here was a bolide recorded on August 17. It was associated with the sporadic component. Its peak absolute magnitude was –9.0 and overflew the Mediterranean Sea. The meteoroid followed an asteroidal orbit before impacting our atmosphere. The ending altitude of this deep-penetrating meteor event was of about 23 km. From the analysis of the ending point of the luminous path of the event we concluded that this bolide was a meteorite-producer.

Next, we have analyzed the "Las Matanzas" event, which was recorded on August 17. It belonged to the August ν-Aquariids (ANA#0467). Its peak magnitude was –10.0 and it overflew Spain and the Mediterranean Sea. The meteoroid was moving on a cometary (JFC) orbit before colliding with our planet's atmosphere.

The next event analyzed here was a bolide recorded on September 3. The peak magnitude of this sporadic, which overflew the Gulf of Cádiz, was –12.0. The meteoroid was moving on an asteroidal orbit before striking our planet's atmosphere. The terminal altitude of this deep-penetrating meteor event was of about 38 km.

And the last fireball presented here was the "Tocón" fireball, which was recorded on September 26. This Earth-grazer was generated by a meteoroid belonging to the sporadic background. Its peak magnitude was –7.0 and it overflew the provinces of Jaén and Granada (south of Spain). Before hitting our planet's atmosphere the meteoroid was moving on an asteroidal orbit.

[33] https://youtu.be/HRGpknv-YVU

Acknowledgment

We acknowledge support from the Spanish Ministry of Science and Innovation (project PID2019-105797GB-I00). We also acknowledge financial support from the State Agency for Research of the Spanish MCIU through the "Center of Excellence Severo Ochoa" award to the Instituto de Astrofísica de Andalucía (SEV-2017-0709). P.S-S. acknowledges financial support by the Spanish grant AYA - RTI2018 – 098657 -J- I00 "LEO-SBNAF" (MCIU / AEI / FEDER, UE). The first author is very grateful to Casa das Ciencias (Museos Científicos Coruñeses) for their helpful support in the setup and operation of the automated meteor-observing station located at their facilities in A Coruña.

References

Ceplecha Z. (1987). "Geometric, dynamic, orbital and photometric data on meteoroids from photographic fireball networks". *Bull. Astron. Inst. Cz.*, **38**, 222–234.

Jenniskens P., Nénon Q., Albers J., Gural P. S., Haberman B., Holman D., Morales R., Grigsby B. J., Samuels D. and Johannink C. (2016). "The established meteor showers as observed by CAMS". *Icarus*, **266**, 331–354.

Kornos L., Marlovic P., Rudawska R., Toth J., Hajdukova M., Koukal Jr, Piffl R. (2014). "Confirmation and characterisation of IAU temporary meteor showers in EDMON database". *Meteoroids 2013, Proceedings of the Astronomical Conference*, held at A.M. University, Poznan, Poland, Aug. 26-30, 2013, eds Jopek T.J., Rietmeijer F.J.M., Watanabe J., Williams I.P., Adam Mickiewicz University Press in Poznan, pp 225–233.

Madiedo J. M. (2014). "Robotic systems for the determination of the composition of solar system materials by means of fireball spectroscopy". *Earth, Planets & Space*, **66**, 70.

Madiedo J. M. (2017). "Automated systems for the analysis of meteor spectra: The SMART Project". *Planetary and Space Science*, **143**, 238–244.

Madiedo J. M. (2015a). "Spectroscopy of a κ-Cygnid fireball afterglow". *Planetary and Space Science*, **118**, 90–94.

Madiedo J. M. (2015b). "The ρ-Geminid meteoroid stream: orbits, spectroscopic data and implications for its parent body". *Monthly Notices of the Royal Astronomical Society*, **448**, 2135–2140.

Madiedo J. M., Ortiz J. L., Organero F., Ana-Hernández L., Fonseca F., Morales N. and Cabrera-Caño J. (2015). "Analysis of Moon impact flashes detected during the 2012 and 2013 Perseids". *A&A*, **577**, A118.

Madiedo J. M., Ortiz J. L. and Morales N. (2018). "The first observations to determine the temperature of a lunar impact flash and its evolution". *Monthly Notices of the Royal Astronomical Society*, **480**, 5010–5016.

Madiedo J. M., Ortiz J. L., Morales N. and Santos-Sanz P. (2019a). "Multiwavelength observations of a bright impact flash during the 2019 January total lunar eclipse". *Monthly Notices of the Royal Astronomical Society*, **486**, 3380-3387.

Madiedo J. M., Ortiz J. L., Izquierdo J., Santos-Sanz P., Aceituno J., de Guindos E., Yanguas P., Palacian J., San Segundo A., and Avila D. (2021). "The Southwestern Europe Meteor Network: recent advances and analysis of bright fireballs recorded along April 2021". *eMetN*, **6**, 397–406.

Madiedo J. M., Ortiz J. L., Izquierdo J., Santos-Sanz P., Aceituno J., de Guindos E., Yanguas P., Palacian J., San Segundo A., Avila D., Tosar B., Gómez-Hernández A., Gómez-Martínez J., and García A. (2022). "The Southwestern Europe Meteor Network: development of new artificial intelligence tools and remarkable fireballs observed from January to February 2022". *eMetN*, **7**, 199–208.

Ortiz J. L., Madiedo J. M., Morales N., Santos-Sanz P. and Aceituno F. J. (2015). "Lunar impact flashes from Geminids: analysis of luminous efficiencies and the flux of large meteoroids on Earth". *Monthly Notices of the Royal Astronomical Society*, **454**, 344–352.

The mission of MeteorNews is to offer fast meteor news to a global audience, a swift exchange of information in all fields of active amateur meteor work without editing constraints. MeteorNews is freely available without any fees. To receive a notification: https://www.meteornews.net/newsletter-signup/.

You are welcome to contribute to MeteorNews on a regular or casual basis, if you wish to. Anyone can become an author or editor, send an email to us. For more info read: https://meteornews.net/writing-content-for-emeteornews/

MeteorNews account manager: Richard Kacerek rickzkm@gmail.com.

The running costs for website hosting are covered by a team of sponsors. We want to thank the 2022-2023 sponsors: Anonymous (3x), Mikhail Bidnichenko, Gaetano Brando, Trevor C, Nigel Cunnington, Kevin Heider, Paul Hyde, K. Jamrogowicx, Dave Jones, Richard Kacerek, Richard Lancaster, Joseph Lemaire, Mark McIntyre, Hiroshi Ogawa, Paul Mohan, Stan Nelson, Lubos Neslusan, BillR, Whitham D. Reeve, John Schlin, Ann Schroyens and Denis Vida.

Financial support is still needed and welcome: https://www.justgiving.com/crowdfunding/meteor-news?utm_term=JJBjmJpzV

Contributing to this issue:

- Aceituno J.
- Aimee A.I.
- Ávila D.
- Berman J.
- de Guindos E.
- Gaarder K.
- García A.
- Gómez-Hernández A.
- Gómez-Martínez J.
- Greaves J.
- Izquierdo J.
- Johannink C.
- Kacerek R.
- Koseki M.
- Kurenya I.
- Madiedo J.M.
- Miskotte K
- Ortiz J.L.
- Palacián J.
- Roggemans P.
- San Segundo A.
- Santos-Sanz P.
- Sicking W.
- Terentjeva A.
- Tosar B.
- Verbelen F.
- Yanguas P.

ISSN 2570-4745 Online publication https://meteornews.net

Listed and archived with ADS Abstract Service: https://ui.adsabs.harvard.edu/search/q=eMetN

MeteorNews Publisher:

Valašské Meziříčí Observatory, Vsetínská 78, 75701 Valašské Meziříčí, Czech Republic